



UNIVERSITÀ DEGLI STUDI DI PADOVA  
DIPARTIMENTO DI INGEGNERIA DELL'INFORMAZIONE  
TESI DI LAUREA MAGISTRALE

STUDIO, PROGETTAZIONE E  
SVILUPPO DI UN SISTEMA  
ELETTRONICO PER LA MISURA DI  
SEGNALI BIOMETRICI DELLA  
MANO FINALIZZATO AD  
APPLICAZIONI RIABILITATIVE.

RELATORE: Ch.mo Prof. Alessandro Paccagnella  
CORRELATORE: Dr. Matteo Scaramuzza  
LAUREANDO: *Federica Spada*

CORSO DI LAUREA MAGISTRALE IN BIOINGEGNERIA

Padova, 22 Ottobre 2012

---

Dedicated to all my family.

---

---

# Contents

<b>Introduction</b>	<b>1</b>
<b>1 The hand</b>	<b>3</b>
1.1 Anatomical concepts . . . . .	3
1.1.1 Force generation in hands . . . . .	5
1.2 Pathophysiology . . . . .	7
1.2.1 Stroke . . . . .	7
1.2.2 Spinal cord injury and other neurological disorders . . . . .	8
1.3 State of the art . . . . .	10
1.3.1 Therapeutic devices . . . . .	10
1.3.2 Assistive devices . . . . .	14
1.4 Open issues . . . . .	17
<b>2 Application of the system to hand functional rehabilitation</b>	<b>19</b>
2.1 Hand functionality . . . . .	19
2.1.1 Hand strength in Scientific Literature . . . . .	20
2.1.2 Weakness . . . . .	25
2.1.3 Muscular factors . . . . .	27
2.1.4 Neural factors . . . . .	28
2.2 Rehabilitation techniques . . . . .	28
2.2.1 Clinical classification of hand functions . . . . .	29
2.2.2 Ability and performance measurements . . . . .	31
2.2.3 Evaluation and validation . . . . .	32
2.2.4 Rehabilitation protocols . . . . .	33
2.3 Sollerman functional protocols . . . . .	33
2.4 Prehension patterns . . . . .	37
2.4.1 Types of grips . . . . .	37

## CONTENTS

---

2.4.2	Static grip evaluation method . . . . .	38
2.4.3	Tests for contact area definition . . . . .	42
<b>3</b>	<b>Software description</b>	<b>46</b>
3.1	System graphic interface . . . . .	46
3.1.1	Implemented functional rehabilitation protocol . . . . .	46
3.1.2	Main interface . . . . .	47
3.1.3	Report of a performed exercise . . . . .	50
3.1.4	Analysis interface . . . . .	51
3.2	Data record format . . . . .	54
3.2.1	Maximum identification . . . . .	56
3.3	Future developments . . . . .	56
<b>4</b>	<b>The prototype</b>	<b>59</b>
4.1	Prototype components . . . . .	59
4.2	Glove . . . . .	60
4.2.1	Sensors behaviour and features . . . . .	61
4.3	Driving electronic interface . . . . .	66
4.3.1	Sensing circuit fixed resistance . . . . .	68
4.3.2	DAQ . . . . .	71
4.4	Future improvements . . . . .	71
<b>5</b>	<b>Application of the prototype</b>	<b>73</b>
5.1	Glove wearing features . . . . .	73
5.2	Grips executions . . . . .	76
5.2.1	Example of a dynamic grip execution . . . . .	78
	<b>Conclusions</b>	<b>83</b>
<b>A</b>	<b>System electronic interface schematics and boards</b>	<b>85</b>
<b>B</b>	<b>Sollerman Table 84 (functional balance)</b>	<b>89</b>
<b>C</b>	<b>Example of recorded data</b>	<b>91</b>
<b>D</b>	<b>Sensors data sheets</b>	<b>95</b>
<b>E</b>	<b>Data acquisition device data sheets</b>	<b>101</b>



# List of Figures

1.1	Motor Homunculus from [34] . . . . .	4
1.2	Sensory innervation areas ( <i>on the left</i> ) are defined by dermatomes, and motor innervation areas ( <i>on the right</i> ) are defined by myotomes. . . . .	6
1.3	HandTutor of MediTouch . . . . .	11
1.4	Modular system for occupational therapy developed by TecnoBody. . . . .	12
1.5	<i>MIT-MANUS</i> . . . . .	12
1.6	<i>HandCARE3</i> system. Cables attached to the fingertips can pull the digits open. . . . .	13
1.7	<i>Hand Mentor</i> exoskeleton system produced by <i>Kinetic Muscle</i> . . . . .	14
1.8	Example of a rehabilitation exercise with a virtual piano player. A) CyberGrasp haptic device worn over a CyberGlove instrumented glove. B) Depiction of virtual key press. C) Piano trainer simulation. . . . .	15
1.9	An assistive workstation example. In detail the <i>Handy 1</i> workstation, intended to help users with eating, drinking, and grooming. First developed by Mike Topping at Staffordshire University [10]. . . . .	16
1.10	<i>KARES</i> workstation is intended to help users in tasks such as grasping objects and turning off and on light switches. . . . .	17
1.11	Orthotic exoskeleton system that allows basic pinching motion using natural sequence of muscle activation. Pinching motion between the index finger and the thumb provides the ability to perform a wide range of ADL. . . . .	18
2.1	Scheme of hand bones and phalanges structure. . . . .	20
2.2	Possible thumb movements. A) Flexion; B) extension; C) abduction; D) adduction; E) opposition; F) rotation. . . . .	21
2.3	Eight main hand-grips individuated by Sollerman [42]. . . . .	34



---

2.4	Two types of prehensile pattern of a right handed subject, in a everyday living task [30]. a) Power grip posture. b) Precision grip posture. . . . .	39
2.5	An example of a sequence for Tip prehension taken in a Kamakura test [20]. . . . .	40
2.6	An example of a sequence for Lateral Grip taken in a Kamakura test [20]. . . . .	41
2.7	Objects used to execute grips chosen from <i>Sollerman Table 84</i> (see appendix B). . . . .	42
2.8	Picture taken in collaboration with San Bortolo hospital equipe. A) The grip performed was the Index and Thumb pinch (or Pulp pinch) similar to Tip Grip of Kamakura test 2.5. B) The grip performed was the Lateral one similar to Kamakura test 2.6. . . .	43
2.9	Hand diagram of the contact areas results. . . . .	44
2.10	Pictures taken in collaboration with San Bortolo hospital equipe. . . . .	45
3.1	System main graphic interface . . . . .	48
3.2	Option panel. 1) Patient's name and surname box; 2) grip type box; 3) free note box. . . . .	48
3.3	Command panel. 1) Left or right hand option; 2) "Start" button; 3) "Pause" button; 4) "Stop" button; 5) "Analysis" button. . . .	49
3.4	Histogram panel. 1) Hand contact-area names and in green is shown their selection LEDs; 2) sensor histograms. . . . .	49
3.5	Hand schematic representation. 1) Hand color map scheme; 2) color map legend. . . . .	50
3.6	Resume after exercise execution page . . . . .	51
3.7	Analysis interface . . . . .	52
3.8	Analysis selection panel. 1) Field for the selection of the patient; 2) box for grip choice; 3) exercise selection areas. . . . .	53
3.9	Analysis visualization panel. 1) Schematical hand color map representation that visualizes exercises results; 2) color map that reports typical non-pathological hand results; 3) color legend; 4) "Close" button to exit the analysis session. . . . .	54
3.10	Record file template. . . . .	55

---

3.11	Example of <i>LabVIEW</i> software implementation of the function that converts and organizes the maximum values and corresponding time in data to be stored. . . . .	57
4.1	Biofeedback loop including patient. . . . .	60
4.2	Sensor typical force curve, reported in FSR 408 Data Sheet (see appendix D) . . . . .	64
4.3	Mounted sensor force curve. . . . .	66
4.4	Typical schematic of a single sensor (see appendix D) . . . . .	67
4.5	Typical curves measured for different values of resistances. Red lines indicates the mean resistance for a correctly worn glove (see <b>Chapter 5</b> ). . . . .	70
5.1	Glove wearing phases for fingers. . . . .	74
5.2	Glove wearing phases for fingers and palm. . . . .	75
5.3	Lateral pinch (see Figure 2.7) executed using the prototype. . . .	80
5.4	Transverse grip type 1 (see Figure 2.7) executed using the prototype.	81
5.5	Tripod (or tridigit) grip (see Figure 2.7) executed using the prototype. . . . .	82
A.1	Electronic schematic. . . . .	86
A.2	Board schematic top side. . . . .	87
A.3	Board schematic bottom side. . . . .	88
E.1	NI USB-6008 Block Diagram. . . . .	108

## List of Tables

2.1	Summary of strength and variability in each finger couplings and for simple grip across 100 subjects tested by Astin [2]. . . . .	24
-----	---	----

---

2.2	Summary of average finger strength and comparison with results of other studies [38]. . . . .	25
2.3	Evaluation of grip force in normal subject (control subjects) and after-stroke patients (stroke subject) [4]. . . . .	26
2.4	The percentage use of the eight most common hand-grips in ADL according to [41] . . . . .	35
2.5	Guidelines for scoring of subtests according to [41] . . . . .	36
4.1	$R_M$ fixed resistance values used in the calibration curves 4.5. . . .	68
4.2	$R_{FSR}$ resistance values used to represent sensor variable resistance in the calibration curves 4.5. . . . .	69

## CONTENTS

---

# Introduction

The rate of technological evolution is constantly increasing thanks to the great amount of knowledge available to researchers. Among the different technological improvements that aims to facilitate human life, one of the most outstanding is that applied to both clinical techniques and medical instruments development.

In particular, the impairment of hands can adversely affect quality of life: these limbs have great importance in many activities of our lives and are our primary mean of interaction with the external environment. Their fundamental role is reflected also on the disproportionately large regions of motor cortex and of corticospinal pathways devoted to hand muscles [34].

For this reason neurological injuries, resulting for example from stroke or degenerative diseases, often leads to hand impairment. These pathologies are widely spread and in the past 20 years robotic and mechatronic technologies have been developed to restore and alleviate functional losses.

The functional devices developed up to now can be divided into two main categories based on their final use: assistive devices, that are intended to perform tasks previously executed by hands, and therapeutic devices that focus on enhance recovery till devices are no longer needed.

As a growing number of people affected by stroke and spinal cord injury results in incomplete tetraplegia, development of therapeutic devices for retraining hand movements in these individuals has a growing importance[10]. The steps of the procedure needed to achieve any recovery would include rehabilitation and a quantitative evaluation of the improvements. Actual rehabilitation protocols are affected by subjectivity and rely on physiotherapist ability and experience, without any objective measurements nor guidelines.

Therefore the development of devices able to facilitate the correct process of rehabilitation is crucial both for patients and for physiotherapists.

### Main Goals

The goals of this Thesis are the study and implementation of a transduction system which permits both the collection of quantitative data and the corresponding functional analysis, in order to enable an impartial assessment of rehabilitation protocols efficacy.

This project has been developed in collaboration with *Wetware Concepts*, a University of Padova spin off, which has supported and promoted the activity of this Thesis.

Moreover a possible clinical application has been investigated by the *BioDevices Laboratory of the Department of Information Engineering of Padova University* in collaboration with the equipe of severe spinal/brain injured of *Vicenza San Bortolo Hospital* headed by Dr. Giannettore Bertagnoni. The purpose of the investigation was to identify functional exercises to train pathological hands.

### Overview of Thesis structure

**Chapter 1** outlines a brief description of hands and the implication of a reduced mobility due to different pathologies. The end of this Chapter consists of an overview of the devices already presented in Scientific Literature.

**Chapter 2** outlines the application of electrical transduction technologies to hand functional rehabilitation.

**Chapter 3** explains the computer interface for the training exercises implemented in the system.

**Chapter 4** describes the hardware section of the system and contains also some theoretical concepts about force measurement using piezoresistive polymeric sensors, in order to present in detail the first prototype built.

**Chapter 5** reports some preliminary measurements that have been carried out to test the feasibility of the system to a possible clinical application.

The **Conclusions** summarize the work done in the Thesis and provide general hints for future developments.

Further information can be found in the **Appendix**, which describes in greater detail some fundamental concepts presented throughout the Thesis.

# Chapter 1

## The hand

In this Chapter hand is investigated. In first section hand principal anatomical concepts are reported, stressing out force generation mechanisms. Then, main pathophysiologies involving use of hand are briefly described in the second section of the Chapter. Thus, an overview of current state devices for pathological hand assistance and rehabilitation, is presented in section three. The Chapter ends with a brief resume of the current state of devices and with the description of some unsolved issues.

### 1.1 Anatomical concepts

The hand is fundamental for the upper limb and is a great versatile instrument. Hands have a lot of different capabilities: we use them to communicate, to express ourselves and above all to manipulate objects. These functions make the hand absolutely fundamental in the *activities of daily living* (ADL). This incredible potential is strictly correlated with hand amazing neuromechanical complexity.

The whole hand is composed of 19 bones connected through joints, which ideally provide 21 degrees of freedom. Each finger has 4 degree of freedom, and the thumb is provided of 5 degree of freedom. Moreover these degrees of freedom are controlled by 27 muscles and tendons, which can cross multiple joints. Therefore a neural signal control can influence more than one target, because in addition to the target the signal has the side effected to influence even the segments connected through the same joint.

Motor control is defined as the coordination of muscular, skeletal, and neuro-

logical functions to produce a movement. Due to the complexity of hand anatomy, an exhaustive description of its motor control is particularly challenging. Moreover hand motor control is, in most actions, a precise motor control aimed to produce small and precise movements, e.g. picking up a small item with the index finger and thumb.

Moreover, in order to better describe hand motor control complexity, apparently similar muscles for the same finger may be selectively excited for different movements and in the same way different compartments of the same muscle may be activated independently [21].

Hand motoneurons are controlled by cortex with specific excitation signal, such as monosynaptical input. Moreover cortical major influence is further evidenced by the limited control action exerted by other parts of brain over hand movements, like brainstem pathways which are sparse and of questionable physiological significance [37]. There are various representations of hand motions or tasks located in the motor cortex, the most known is that of the "*Motor Homunculus*" (see Figure 1.1).

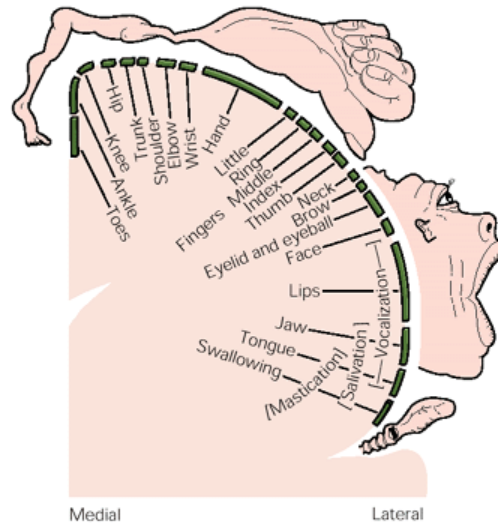


Figure 1.1 – Motor Homunculus from [34]

In addition to the cortex devoted to motor control, the somatosensory cortex plays an important role, as it is indispensable for movements coordination. Sensory feedback information heavily influence a coordinated motor control, so it makes sense that hands are completely covered by sensory innervations. Indeed, sense of touch in hands is really enhanced, e.g. finger kinesthesia relies on skin



sensation: a recent research has found that kinesthesia-based haptic perception relies strongly on forces experienced during touch [47]. In detail, haptics is the science of applying touch (tactile) sensation and control to interaction with computer applications by using special input/output devices, e.g. joysticks or data gloves [47]. In some case users can even receive feedbacks from computer applications. In combination with a visual display, haptics technology can be used to train people for tasks requiring hand-eye coordination, e.g. for games.

Due to the high haptic perception, hands proprioceptive acuity is superior than other segments of the body. In detail, proprioception (from the Latin meaning "one's own", "individual" and "perception") can be defined as the ability of an individual to determine body segment positions and movements in space and is based on sensory signals provided to the brain from muscle, joint, and skin receptors [16]. Our sense of proprioception is the most important source of feedback for promoting neural plasticity, and to support hands great sensory precision even a bigger area of somatosensory cortex is devoted to them.

Another element of complexity of hand control comes from the disposition of innervation pathways. Upper limb dermatomes, i.e. sensory areas of nerves that affers to the same cervical zone, and myotomes i.e. cervical zone that innervates different muscles for the motor control, are differently organized: dermatomes and myotomes do not necessarily individuate the same limb area, besides each limb area muscle and peripheral nerve distribution refer to different cervical zone. This is schematically represented in picture 1.2.

### 1.1.1 Force generation in hands

Hands motor control and coordination alone are not able to fully describe hand capabilities, because every movement needs a precise amount of force to be performed. Force is a critical parameter, and it is neurologically controlled by numerous regions of the cortex. Indeed strength depends even on the capabilities of motoneurons to be activated, on the recruitment of the correct amount of motor units and muscular fibers, and on all kinds of feedbacks.

In detail, motor unit recruitment is the progressive activation of a muscle by successive recruitment of contractile units (motor units) to accomplish increasing gradations of contractile strength [32]. A motor unit consists of one motor neuron and all the related muscle fibers it contracts.

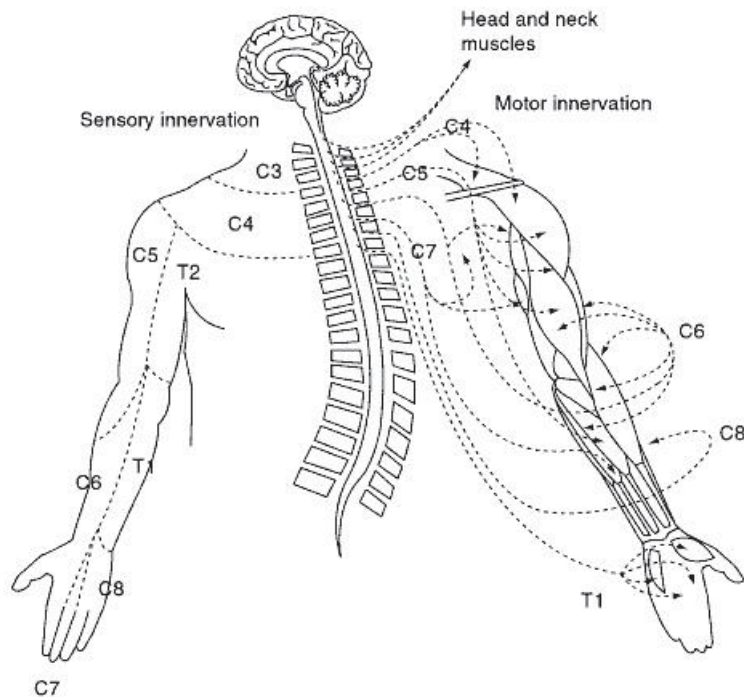


**Figure 1.2** – Sensory innervation areas (*on the left*) are defined by dermatomes, and motor innervation areas (*on the right*) are defined by myotomes.

All muscles consist of a number of motor units, and the fibers belonging to a motor unit are dispersed and intermingle amongst fibers of other units. A motor unit muscle fibers can be spread in a part, or all over the muscle, depending on the number of fibers and size of the muscle [32]. When a motor neuron is activated, all of the muscle fibers innervated by the motor neuron are stimulated and contract.

The activation of one motor neuron will result in a weak but distributed muscle contraction. The activation of more motor neurons will result in more muscle fibers being activated, and therefore a stronger muscle contraction [32]. The higher the recruitment the stronger the muscle contraction will be. Motor units are generally recruited in order of smallest to largest (fewest fibers to most fibers) as contraction increases.

Hands muscles are divided in intrinsic and extrinsic. The intrinsic muscles are small and generate forces directed to move fingertips and thumb tip, while the extrinsic muscles, located in the forearm, are long, relatively large and provide most of the power of the hand. As a result, high forces can be created in the hand

while maintaining dexterity. In particular voluntary forces at the index fingertip can exceed 60 N, and thumb tip forces can exceed 100 N [10].

Forces generated by the hand can be measured with appropriate systems: these measurements are the sum of the contributes of numerous muscles of the hand so it is difficult to attribute them to a single muscle or to a specific stimulus pattern, but they can be directly related to the task that has to be performed.

From the rehabilitative point of view, the goal is to have quantitative measurements that can undergo mathematical and statistical analysis in order to evaluate both the performance of a therapy and the effectiveness of a protocol.

## 1.2 Pathophysiology

The great importance of cortical innervation on hand control clearly emerges in case of reduction of cortical inputs. This happens primarily after strokes, spinal cord injuries or other neurological disorders. The resulting loss of motor control can have a deep impact on self-care ADL, individuals' employments and social interactions, so it can be understood that the rehabilitation of hand and upper limb functions have been identified as the primary desire of tetraplegic patients [10].

### 1.2.1 Stroke

A stroke is produced by either occlusion of blood vessels or brain haemorrhage, that can vary widely in location and extension. Usually is situated in only one of the two hemispheres, therefore the impairment consequences affect just one side of the patient body. Despite the wide spectrum of stroke events, in survivors stereotypical patterns of impairment emerge, such as initial paresis and flaccidity typically followed by hyperexcitability of specific hand muscles. For example the occurrence of spasticity is a signature phenomenon of stroke events.

In ischemic strokes different regions of the brain (cortical and subcortical) can be affected causing two possible states of damage: transient impairment or brain structural detriment. In both types the probability that centres of hand motor-somatosensory control get involved is high, due to the great amount of brain space devoted to them. So involvement of these areas in stroke event often causes the impairment of hand functions. Roughly 30 - 50 % of stroke survivors have

hemiparesis [52] involving use of hand and voluntary digits extension. Moreover, motor functions are highly influenced by the ability of imagine, plan, organize and perform a required action. Thus, brain damage of areas not directly concerning motor control can still cause hand impairment. In detail, after-stroke impairment of upper limb is often due to damage of descending central motor pathways and involvement of premotor areas devoted to the ability of motor planning.

Stroke episodes diffusion is described by the statistics, both Italian and American, reported as follows. According to statistics [40] in Italy 200.000 new cases of stroke occur approximately every year and 80 % of them are new episodes. Stroke is the second worldwide cause of death and the first cause of disability with loss of independence. To alleviate the costs of the impairment due to stroke, in many Italian hospitals new dedicated welfare areas called *Stroke Units* have recently been established. These units are specialized in giving the first aid in cases of stroke.

Focusing on American situation, the *American Heart Association* (AHA) in the *Executive Summary: Heart Disease and Stroke Statistics - 2012 Updates* [1], reports that a stroke happens on average every 40 seconds in the United States. So stroke is the leading cause of major long-term disability within the United States. Approximately 795.000 persons in United States have a new or recurrent stroke each year [1], a value that would probably grow along with the population age. Stroke disease results in substantial costs: in particular, according to [52], the combined direct and indirect costs of stroke in USA are projected to be \$62.7 billion (in 2007).

From these data can be seen that there is a real need to prevent strokes and also to identify effective therapies for the victims of stroke with incomplete tetraplegia.

### **1.2.2 Spinal cord injury and other neurological disorders**

Spinal cord injury (SCI) is one of the principal reasons of chronic disability in young people: in the United States around 12.000 are the new cases of SCI every year. Main causes of SCI are falls and car accidents, as reported in the statistics edited by *National Spinal Cord Injury Statistical Center* [31].

The impairment of upper limb functions in case of SCI concerning the cervical zone is peculiar and differentiates a lot from neurological disorder impairments,

e.g. caused by stroke, multiple sclerosis or peripheral nerve damage. For example, in contrast with stroke impairment consequences, a common result of SCI is the substantial atrophy of hand muscles that causes muscle imbalance. Moreover, in SCI patient brain usually is not damaged, so cerebral areas which lost their natural targets on hand are associated, thanks to brain plasticity, to other tasks or parts of the body, while in after-stroke patients the brain areas themselves are damaged.

The functional impairments resulting from SCI depends on the location, extent and type of damage to the spinal cord, but injury within the cervical region usually leads to impairment of all four limbs. The improving of today treatments is changing this trend: the number of incomplete SCI is increased with respect to the complete ones. Regarding the cervical portion of spinal cord, the different kind of loss of sensory-motor functions is related to the segmental level of the lesion and results in the deprivation of afferent inputs and efferent outputs, causing movement control to not work properly. Unlike all other types of impairment causes, cervical SCI patients suffer from a rather symmetrical and bilateral impairment which eliminates the possibility to compensate the movement with the other limb to accomplished the action. The compensation movement is what happens in patients with disability due mainly to neurological diseases, who try to accomplish tasks supporting impaired hand with the ipsilesional one, i.e. the uninvolved or non-paret side. This is classified as a wrong behaviour in rehabilitation even if it gets patient to fulfil therapist request, because it prevents the impaired hand to be fully trained.

At last, another disease which cause hand impairment is the multiple sclerosis. In this pathology the musculoskeletal weakness and impairment of hand depends on the demyelination of axons in the pathways between brain and spinal cord. In the deterioration process implied by the pathology, there is high variability in both time and extension of the interested areas. This leads to inconsistent and atypical impairment of hand functions. So it is quite difficult to identify an effective hand rehabilitation method for the wide spectrum of disabilities following this disease.

Finally in peripheral nerve injuries of hand-arm nerves (i.e. median and ulnar nerves), the sensory-motor control deficit heavily depends on the involved peripheral part of innervations. Peripheral nerve damages present very specific

deficits, the causes include traumatic injuries and nerve entrapment syndromes, that can be disclosed by neurophysiological recordings, but they are quite challenging to treat with a standard rehabilitative protocol.

## 1.3 State of the art

Many instruments have been developed to facilitate hand rehabilitation for both stroke and SCI survivors but their nature change depending on the specific application. In some cases the priority is set to provide assistance for tasks that the user could no longer perform, and therefore devices are intended for chronic use. Alternatively, therapeutic tools are intended to facilitate rehabilitation to promote recovery: in particular the therapeutic technology has focused on stroke survivors whose functional limitations of the upper limb are generally less imposing than those in tetraplegia.

### 1.3.1 Therapeutic devices

The best outcome for a patient, in particular an after-stroke one, would be to regain sufficient motor control so that assistive technology would no longer be needed. Thus, in recent years, there has been a substantial change of direction from the development of assistive devices to therapeutic ones to facilitate rehabilitation of impaired movements. This shift has also been supported by neurological researches showing that even mature nervous system is constantly changing and adapting, and it exhibits much greater plasticity than previously imagined [10].

Experimental evidences suggest that repeated practice of hand movements, such as performed by musicians, can lead to cortical changes and that an intensive training can induce long-term brain plasticity [36]. While this finding seems to be applicable to motor re-learning even after brain injuries or stroke, the more effective type and methods for the rehabilitative practice based on repeated training remains a matter of debate. Usually a number of researchers and therapists recommended task-specific training, also called functional training, in which patients must focus on tasks to be performed during their ADL.

Additionally, it has been shown [51] that functionally based training, similarly to strength and motor control protocols, in which the rehabilitative exercises are focused respectively on increasing hand force and regaining hand spatial motor

control, was superior to standard care post-treatment, that attention concerns generic hand movements recovery. In particular most benefits of the functional-task rehabilitation protocol emerge within the first 9 months after stroke event. Moreover for stroke survivors, reaching toward physical objects as part of a task led to enhance quality of movement, in contrast to the task of simply reaching a location in space [48]. A drawback of functional rehabilitation is the great complexity and number of tasks that limit the repetitions and the type of exercises that can be performed. Indeed as a consequence of these limits the individuation of the more effective exercises is a fundamental necessity.



**Figure 1.3** – HandTutor of MediTouch

Although functional tasks with physical objects can help to maintain the engagement of the patient on the activity and thus enhance beneficial results, many virtual rehabilitation systems have been developed. For example the *HandTutor* (see Figure 1.3) developed in 2010 from MediTouch is an open glove dedicated to rehabilitation, which records biomechanical parameters like velocity, active and passive range of motion and movement analysis of fingers and wrist, but mainly it works with hand extension and abduction.

Another device for movements analysis is the *Modular system* developed by *TecnoBody* (see Figure 1.4): the modular system detects and reproduces real movements on screen and records the data along with task performances. It implements rehabilitation exercises and in particular occupational therapy ones, but the drawback is that it only has a visual feedback.

Performing a specific task with the hand may be challenging even with the guide of a therapist, so to facilitate this phase of hand rehabilitation a number



**Figure 1.4** – Modular system for occupational therapy developed by Tecno-Body.

of mechatronic devices have been developed in the last 10 years. One approach followed was to focus on a single movement of the hand and promote the practice of it. Thus, mechatronic devices have been created to expand or contract, to open or close the hand such as the *MIT-MANUS* module (see Figure 1.5).

A different kind of devices directly deal with hands by anchoring to fingertips, external grounding or self-coupling to user arms and hands. An example of device anchored to fingers is the *HandCARE* system [12] (see Figure 1.6). In this system each finger is attached to an instrumented cable loop which allows force control and a predominantly linear displacement of finger spatial movements.



**Figure 1.5** – *MIT-MANUS*

The design of the device is based on biomechanical measurements in order to assist subjects in opening and closing hand movements. *HandCARE* records hand biometric signals relative to strength and spatial trajectory [12]. A drawback of this system is that the hand position must be fixed as the devices are externally grounded so exercises or practice with real object or functional protocols are not



possible.



**Figure 1.6** – *HandCARE3 system. Cables attached to the fingertips can pull the digits open.*

The approach of *Hand Mentor* (see Figure 1.7) produced by *Kinetic Muscles* [22] is to anchor the device on subject hand and arm with a linkage mechanism which assists the patient with the desired movement. The exoskeleton moves multiple digits simultaneously, in detail it can move in coordination with the arm and it can rotate all four metacarpal joints of the long fingers together, but it does not actuate the thumb. The *Hand Mentor* provides three types of visual feedbacks: force, position and electromyography (EMG), i.e. electrical activity of the muscle.

Moreover, *Hand Mentor* exoskeleton use have been investigated by Kutner et al. [24]. The authors assigned participants to two groups: subjects of one group received 60 hours of repetitive task practice (RPT), while the others received 30 hours of RPT plus 30 hours of robotic-assisted therapy executed by mean of the Hand Mentor (HM). Therapy took place over the course of 3 weeks and the participants of the combined therapy group divided their time equally between the RTP activities and supervised HM use. The two different therapy approaches obtain similar results of improvement in hand function, but reported an higher overall stroke recovery.

To increase the range of hand tasks allowed, some devices have provided independent control of each digit. Some of the first instruments created use pneumatic cylinders on the palmar side of the digits to move the fingertips such as *The Rutgers Master II-ND* or air bladders such as the *PneuGlove* [10].

The developed tools for hand rehabilitation exploited several directions, each



**Figure 1.7** – *Hand Mentor* exoskeleton system produced by *Kinetic Muscle*.

answering a specific set of requests. To build a really effective rehabilitative device, more aspects should be integrated, e.g. fingers and hand spatial coordination, or strength and functional exercises. For example the *CyberGrasp* (see Figure 1.8) is an actuating system created by *CyberGlove Systems*, that integrate a rehabilitation virtual reality paradigm. The *CyberGrasp* can provide extension forces to each digit independently and can be used either with real or virtual objects. On the contrary this system is really encumbering and uncomfortable, therefore its clinical use results quite difficult.

### 1.3.2 Assistive devices

Assistive devices are usually focused on facilitating a specific subset of tasks through a set of adaptive tools, e.g. modified utensils and brushes, so the hand is no longer required for grasping them. While this equipment can be very effective, it requires some external assistance to be worn and to be changed.

To provide more careful assistance robotic assistants have been developed, they include mechanical arms or entire robotic workstations, as for example that in picture 1.9. Moreover, robotic arms or mechanics could be located at grounded workstation, on mobile platforms or even on wheelchairs. One of the first was the *Handy 1* (see picture 1.9) that could be controlled through a simple switch and had a gripper end effector [10]. It was controlled through a computer and the user could get the system to operate by activating a single switch. From *Handy 1* newer robotic workstations have been updated and more services have been incorporated, e.g. to provide feeding assistance.

To increase the performance robot assistants could be mounted directly to the

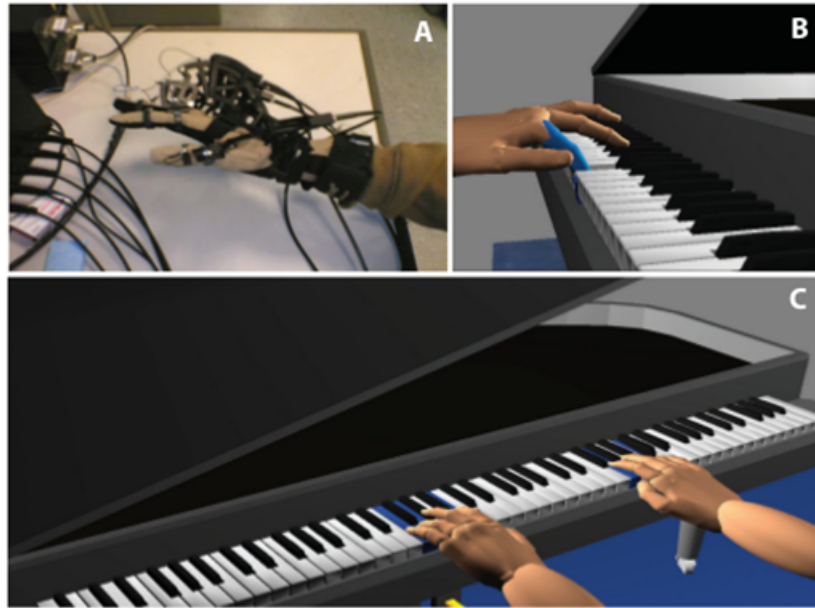


**Figure 1.8** – Example of a rehabilitation exercise with a virtual piano player. A) CyberGrasp haptic device worn over a CyberGlove instrumented glove. B) Depiction of virtual key press. C) Piano trainer simulation.

wheelchair. For example the *KARES* system (see Figure 1.10) created at the Korea Advanced Institute of Science and Technology (KAIST) has six degrees of freedom in its robotic arm and a gripper at his end [19]. Another device is the *Raptor Wheelchair Robot System* that was developed by the Rehabilitation Technologies Division of Applied Resources Corp. (RTD-ARC): its arm has four degrees of freedom with a gripper which permits grasping of objects [10].

Two products stand above others, in terms of commercial success. More than 250 *Handy 1* have been sold by *Rehab Robotics* and *Exact Dynamics* since 1990 have sold more than 150 *Manus* robots and financing the purchase of *Manus* by end users has been under discussion with the Dutch Government [17].

The *MANUS*, commercially successful wheelchair-mounted device has evolved into the *iARM*, which provides six degrees of freedom and both a gripper and an effector. The *iARM* is designed for close interactions with the user and can perform a wide variety of tasks depending on the residual capabilities and preferences of the user [10].

More hand-dedicated assistive devices have been developed such as the *Rehabilitation Glove* created at the Royal North Shore Hospital of Sydney, Australia

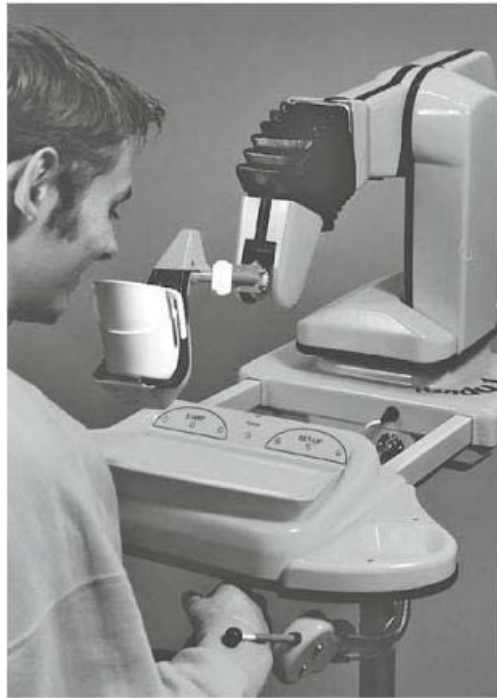


**Figure 1.9** – An assistive workstation example. In detail the *Handy 1* workstation, intended to help users with eating, drinking, and grooming. First developed by Mike Topping at Staffordshire University [10].

or the *Soft Extra Muscle Glove* developed by Bioservo Technologies in Sweden which could amplify grasping force of hand of the user who wears it [10]. Another example of exoskeleton, that allows a basic pinching motion using a natural sequence of muscle activation, is presented in [26]. By means of this orthotic exoskeleton it have been proved that even with only one muscle signal from the natural sequence, a reliable and robust pinching motion can be produced (see Figure 1.11).

A key limitation of the assistive devices control is that our hands perform a lot of tasks with a limited conscious input, while with assistive technology user intent must be transmitted to the device in a translatable manner. For example, in case of the above mentioned exoskeleton [26], the problem is solved using the residual EMG of a specific muscle target as input and an algorithm to translate the signal for the exoskeleton.

Thus, while joysticks and trackballs may be good inputs for some users, they may not be feasible for other individuals, where instead head trackers or eyelid switches may be better inputs. In this wide research of means to provide control,



**Figure 1.10** – *KARES* workstation is intended to help users in tasks such as grasping objects and turning off and on light switches.

other directions have been attempted too. A promising one is that of implantable electrode arrays which can be placed directly into the human motor or premotor cortex. The cortical signals collected by the electrodes are mapped into intended movements to drive external devices. For example, recordings from motor cortex have been successfully used in monkeys to drive a robot [45]. In another research electrodes have been implanted in individuals with tetraplegia to control a mouse on a computer screen [11]. A non-invasive alternative developed for cases of SCI is that of electroencephalogram (EEG) signals used as inputs [35].

## 1.4 Open issues

Substantial efforts for rehabilitation of hand and arm functions have been directed toward developing new robots, passive workstation and functional electrical stimulation (FES). Nevertheless the clinical advantages and the effective rehabilitation practice of these technologies suffer of significant limitations.

For the assistive robots the overall costs remains high but the ageing of population has led to a new rush in the this area of devices to meet the needs of the geriatric population.

While a number of therapeutic devices continue to be developed and evolved with new actuators and promising materials for post-stroke hand applications, scientific and comparative studies concerning their effectiveness remain sparse and in major part consist in single or multiple cases studies.

One of the key benefits of the therapeutic devices is their extended practice,

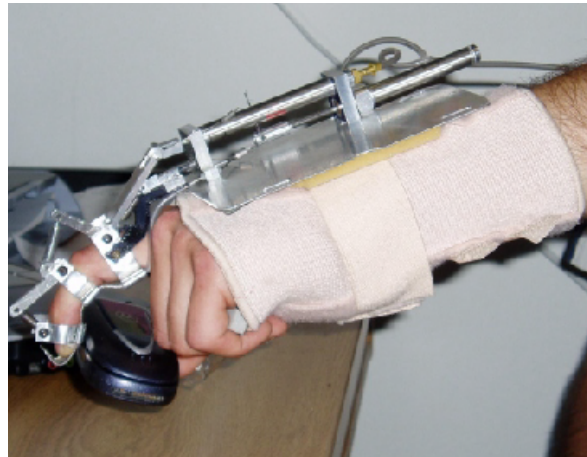


**Figure 1.11** – Orthotic exoskeleton system that allows basic pinching motion using natural sequence of muscle activation. Pinching motion between the index finger and the thumb provides the ability to perform a wide range of ADL.

either in clinic or ideally at home. In particular, to perform the rehabilitation exercises at home is an important opportunity for patients, whose often have limited possibility to access the therapy due to its costs or hospital physical distance. Nevertheless primary obstacle in terms of hardware remains the interface between the physical device and the hand, but the effective benefits of these devices in therapeutic rehabilitation of hands deserves exploration.

# Chapter 2

## Application of the system to hand functional rehabilitation

This Chapter focuses on hand functional characteristics, then briefly introduces some hints about rehabilitation protocols, performance and validation. The last two sections of the Chapter present Sollerman protocol and describe in detail a trial test performed during this Thesis.

### 2.1 Hand functionality

Hand shape is highly correlated to its functions: thanks to the independent movements of each finger, hands can perform an incredible amount of tasks with dexterity, and this is the reason why hands are such an useful and valuable tool for human life.

Each hand has five fingers which can be flexed toward the palm or extended moving away from it. Four fingers are long and similar, while the thumb has a unique role in hand functionality.

Each long finger has three bones connected by joints to form a chain (as can be seen in the scheme of Figure 2.1). These three bones are the phalanges, which are divided in proximal, intermediate and distal, named in sequence starting from the metacarpal bones.

Long fingers movement capabilities are to flex and to extend the three phalanges, toward or away from the palm. They are disposed on the same plane and have little range of lateral or rotational motion.

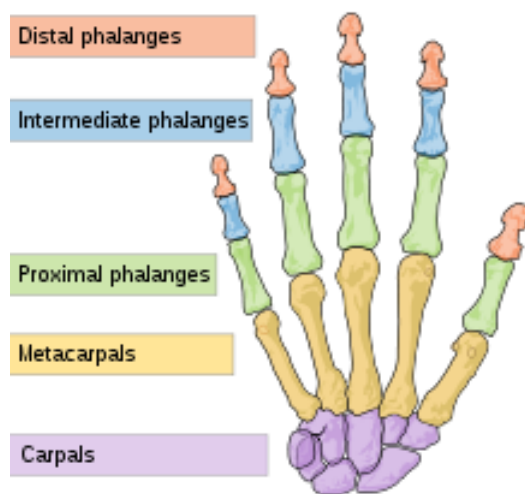


**Figure 2.1** – Scheme of hand bones and phalanges structure.

The thumb is lateral to hand main axis, and in a lower position compared to the other fingers. Differently from the long fingers, thumb has only two phalanges and its proximal phalanx is rotated of  $40^\circ$  in front and  $30^\circ$  lateral respect to the medial axis of the hand. These characteristics of the thumb are fundamental to allow different, and sometimes complementary, movements respect to other fingers from the other fingers.

Thumb motion range is really wide and permits grips otherwise impossible to perform. All the possible movements of the thumb are represented in Figure 2.2. The most useful thumb movement is the opposition one, which characterize all the most important hand functions by enabling grips.

### 2.1.1 Hand strength in Scientific Literature

Some past research has focused on whole-hand grip strength and how variables such as gender and handle width affect peak grip capability. On the other side the investigations which have specifically addressed the force capabilities of the fingers in practical situations are few, and there is little research that has examined the force capabilities of single digits. A brief overview of previous hand strength studies can be found here in the following.

Investigations concerning the strength capabilities of the hand began with explorations of grip strength. In 1956 Napier [30] identified and classified applications of various hand couplings using grips and multi-digit pinches (as described



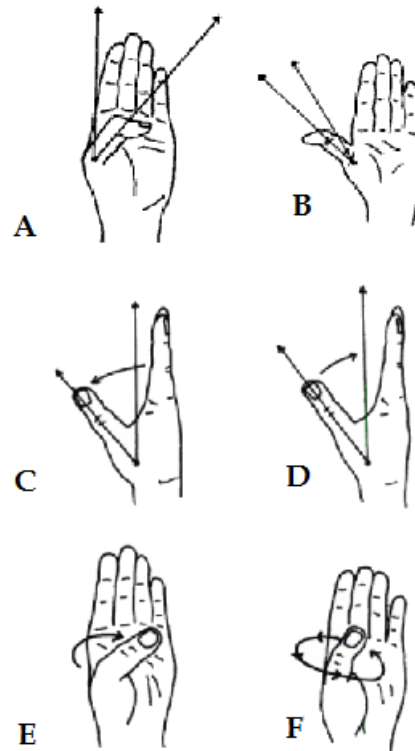


**Figure 2.2** – Possible thumb movements. A) Flexion; B) extension; C) abduction; D) adduction; E) opposition; F) rotation.

in **Chapter 2.2.4**). In 1970 Schmidt and Toews, using a Jamar dynamometer, reported average grip strength for males as 504.2 N and that of females as 311.0 N [39], and a regression model with predictor variables that included age, weight and height was derived with a reported predictive reliability of 95 % for grip strength. Swanson et al. in 1970 [44], also using a Jamar dynamometer, found comparable average male grip strength of 467.0 N and that of females as 241.3 N.

However, strength measurements can vary depending on the instructions provided to the individual and the postures maintained during the force exertions. Mathiowetz et al. in 1984 [28] investigated the reliability of grip and pinch strength evaluations by taking measurements that were separated in time by more than one day. After recording strength measurements for 27 women, it was concluded that standardizing positioning and instructions could achieve high reliability in repetitive tests. Furthermore, the average of three trials was found to be the more reliable and accurate measurement, compared to one trial or to the highest

value of the three trials.

Research pertaining to hand strength has continued to include additional measurements, such as pinch strengths. A number of these studies still include the collection of grip strength data in their results (for examples: Imrhan, 1989 [18]; Kinoshita et al. , 1996 [23]; Mathiowetz, Rennells et al. 1985 [27]; Radwin et al. 1992 [38]). Previous experimentation has included the collection of force data for various pinch exertions and extensive data on the strength of the fingers during multi-digit exertions. Some available results available are here briefly reported.

Mathiowetz, et al. in 1985 [29] determined clinical norms for adults of various ages using a large sample ( $n = 628$ ) of subjects. Their analysis focused on differences in maximum voluntary contractions produced among individuals in several age groups and of different hand dominance. Clinical norms were provided for 12 age groups for both sexes. No significant difference was found in the forces produced by right and left hand dominant individuals.

Imrhan [18] collected pinch strength data to determine quantitative relationships among different types of maximal pinch forces. He concluded that composite pinches, i.e. pinches executed with more than one finger, produced greater strengths. In addition, differences between the sexes and hand laterality were investigated. The results showed that the absolute strength differences between the sexes are slight in children, greatest in adults, and decrease slightly in the elderly. Furthermore for right hand dominant individual, pinches with the right hand are slightly greater (106 %) than pinches produced by the left hand. Finally, no significant correlations between strength and anthropometry (stature, body weight, hand length, hand breadth) were found.

Procedures used during data collection appear to affect the results of strength measurement. Caldwell, Chaffin et al. in 1974 [5], proved that the standardization of procedures is necessary for accurate comparison of research findings. Procedural recommendations included the elimination of any instantaneous feedback during the exertions and a minimum of two minutes of rest between exertions. The "Caldwell Regimen" dictates that participants have to increase force to maximum in approximately one second, after which a steady exertion has to be maintained for four seconds. This steady exertion must remain within a  $\pm 10\%$  band to be considered an acceptable trial. The force is then decreased during the last one second period. Strength is determined as the average of the first

three seconds of the steady exertion [5]. These procedural details were determined after comparison of three sets of instructions ("jerk", "increase", "hold"). The "hold" technique was the most reliable, providing the least variable results among repeated measurements.

Despite the suggestions of Caldwell et al. [5], no shared protocols have been developed neither for strength measurements nor for the procedures used during strength measurements of hand and fingers.

Berg et al. [3] examined the effects of instructions on three multi-digit pinches and showed that it is difficult for participants to maintain forces within the recommended  $\pm 10\%$  band during pinch strengths. Furthermore they proved that peak strength differed according to the duration of effort. So they recommended to reduce the steady exertion to two or three seconds.

To measure grip strength Williamson and Rice [50] re-elaborated the grip Caldwell Regimen testing three different sets of instructions:

1. sudden maximal contraction maintained;
2. sudden maximal contraction peaks;
3. built-up force maintained.

They found that participants were able to achieve the band requirements during grip strength measurements, but alterations in instruction significantly affected the produced forces.

It is important to note that the configuration and location of the fingers are not solely responsible for the magnitude of pinch force exertions: the posture of the participants and the orientation of relevant body parts (e.g. wrist and elbow) can affect the levels of force produced.

Arm positioning can significantly affect the maximum force exertions produced during grip and pinch exertions. Mathiowetz [29] examined the effect of elbow position on grip and lateral pinch strength. These strength values were significantly higher when the elbow was in a 90-degree flexed position as compared to the fully extended position. Results supported the use of the standardized position that includes the elbow at 90-degree flexion as recommended by the American Society of Hand Therapists [14].

In addition to the posture of the whole body and the position of the arm, many additional variables affect the force capabilities of individuals during pinch

exertions. The influence of gender, grasp type, pinch width and wrist position on sustained pinch strength was investigated by Dempsey and Ayoub [9]. They used the modified Caldwell Regimen recommended by Berg [3] and postures recommended by the American Society of Hand Therapists [14]. Females were 62.9 % as strong, on average, as male subjects when considering all pinch exertions. Changes in pinch width resulted in a 16.5 % reduction in strength while wrist position caused a reduction of 24 % in strength.

Radwin et al. [38] studied single digit forces during submaximal five-finger static pinches. Average forces produced by the individual fingers depended on the weight of the load being held. The index and middle fingers exerted 1 N to 5 N of force greater than that of the ring and small fingers across all pinch conditions.

Type	Mean [N]	Standard Deviation [N]	Coeff. of Variation [%]
Poke	45.95	17.8	38.7
Press	43.05	18.43	42.8
Pull	60.09	25.24	42.01
Lateral	80.93	28.15	34.79
Chuck	79.75	28.96	36.31
Palmar	54.16	18.84	34.78
Grip	370.671	117.729	31.761

**Table 2.1** – Summary of strength and variability in each finger couplings and for simple grip across 100 subjects tested by Astin [2].

In Astin study [2] one hundred volunteers between 18 and 65 years of age were selected with an equal number of female and male participants. Participants were asked to perform seven hand couplings that simulated a wide variety of hand intensive tasks typically performed in industrial settings, i.e. setting for typical hand activities of companies workers like pushing buttons, sliding levers and inserting fasteners.

The results of Astin study were that across all subjects, strength was higher for multi-digit couplings as compared with single digit couplings, whereas grip strength was considerably higher than all digit couplings (see Table 2.1). Referring to Table 2.1, it can be noted that standard deviations increase proportionally

to the mean strength magnitude, with the largest standard deviation associated to the mean grip force, due to the wide spectrum of participant individual characteristics, e.g. sex and age. Indeed, considerable differences between genders for all seven exertions were found, with males generating an average 30 % more force than females. Furthermore, Astin classified the participants by their age providing data that revealed little differences in force capabilities for three age groups: 18 - 29 years, 30 - 39 years and over 40 years [2]. Anyway age division is not particularly relevant.

There is little investigation on forces exerted by single fingers in literature, one of them is that of Radwin et al. [38]. The results of Radwin study are reported in the Table 2.2: the forces reported are averages on finger strength with their standard deviation (SD) reported below them.

Study	Index [N]	Middle [N]	Ring [N]	Little [N]
Radwin [38]	61 (SD=15)	58 (SD=21)	36 (SD=13)	28 (SD=11)
Swanson 1970	52	55	37	23
Dickson 1972	45	43	31	27
Average	53	52	35	26

**Table 2.2** – Summary of average finger strength and comparison with results of other studies [38].

A Valero et al. study in 2003 [49] outlines with precision thumb forces. He measured thumb forces for the different movements and possible positions and proved that forces of thumb never exceed 100 N even with different positions.

In after stroke cases grip force values drastically decreased to the 70 % of not paretic limb values. In Table 2.3 can be seen the comparison values [4].

### 2.1.2 Weakness

Several scientific evidences suggest that weakness presents a more serious compromise to movement function in post-stroke hemiplegia than spasticity, therefore

Subjects		Session1 [N]	Session2 [N]	Session3 [N]
Stroke	Paretic limb	123 ± 89	133 ± 81	135 ± 81
	Not paretic limb	370 ± 104	386 ± 86	389 ± 72
Control	Right limb	347 ± 111	336 ± 116	356 ± 106
	Left limb	320 ± 105	324 ± 102	338 ± 101

**Table 2.3** – Evaluation of grip force in normal subject (control subjects) and after-stroke patients (stroke subject) [4].

it is worth to be considered in any hand strength study. The capacity to produce muscle force, or strength, involves:

1. Structural factors: muscle size, muscle mass or cross-sectional area, which depends on the number, size, and relative proportions of muscle fiber types;
2. Mechanical factors, including the length-tension and force-velocity relationships of muscles;
3. Neural factors: the capacity of the nervous system to activate muscle through motor unit recruitment and rate coding.

An impairment of any of these factors affects the capacity to exert force and comprises the operational definition of weakness.

Usually in patient with disability weakness has typically a deep impact, even in moderately impaired subjects grip strength of the affected hand is only 50 % of that of the other hand.

Moreover the relative weakness in a finger is not symmetrically distributed, for example index finger extension force is only 9 % of the normal value, while flexion reaches 27 % of normal levels [8]. This exacerbates the problem of motor control, because it increases the difficulty to coordinate movements and moreover because typically absolute flexion force in fingers is greater than absolute extension one.

Weakness can be found in a large variety of central and peripheral neurological disorders, as well as ageing. All these diseases involve some level of immobilization or markedly decreased physical activity, and all of them typically involve other systemic clinical conditions.

Weakness following stroke is referred to as either hemiparesis, mild to moderate degree of weakness, or hemiplegia, severe or complete loss of motor function on one side of the body. However, evidence is now emerging that weakness also occurs at the uninvolved or non-paretic side [33].

In the literature, post-stroke weakness has been described not only as impaired force magnitude, but also as a more broadly defined phenomenon. It includes slowness to produce force, a rapid onset of fatigue, an excessive sense of effort, and difficulty to effectively produce force within the context of a task [33]. In this context, the term "post-stroke weakness" includes all aspects of weakness following a stroke event.

Although weakness in stroke survivors may depend on many factors, the primary cause is neurological, due to the inability to fully activate the existing muscle fibres. This may be caused by the reduced peak firing rates in motor units, and abnormal activation patterns may provoke excessive co-activation of concord/antagonist muscles along with substantial reduction in electromyographic (EMG) signals [33].

Correlation between weakness and physiologic mechanisms in persons who have suffered neurologic insult, remains not well defined. Functional muscular force is the product of both muscular and neural factors and compromise to either of these factors impairs the capacity to produce and regulate force.

### **2.1.3 Muscular factors**

In a study of hemiparetic persons with minor motor impairment, Sunnerhagen et al. used computed tomography (CT) and found no differences in muscle structure between the affected and ipsilesional limbs [43]. Another investigation by Jorgensen and Jacobsen using dual-energy X-ray absorptiometry demonstrates that patients who were not-ambulatory at 2 months post-stroke lost only 6 % of lean body mass in the paretic leg, that increased slowly in the following months. While a concurrent 5 % loss on the ipsilesional leg was regained completely at 12 months post-stroke [33].

Only a few studies have examined the fiber-type composition in hemiplegic muscles. Despite this, the findings are reasonably consistent and can explain a component of weakness in post-stroke hemiplegia. There is predominant atrophy of white fibers (Type II) that can be accompanied by compensatory hypertrophy

and so increased predominance of red fibers (Type I) [33].

These changes are not specifically due to stroke because they are also common findings in muscles of healthy older adults and in cases of severe inactivity. Thus, the degree of atrophy appears to be more closely related to spontaneous daily physical activity to stroke severity or to ADL score.

Remarkably little information is available regarding muscle structure in persons with post-stroke hemiplegia. While structural changes in muscle may occur in post-stroke weakness, considerable variability can be found between individual subjects. Moreover, the available data suggest effects of immobility and inactivity more than of intrinsic neuropathic change [33].

#### 2.1.4 Neural factors

Without evidence that structural differences in muscle contribute significantly to hemiparetic weakness, attention have turned to the neural aspects of strength and control of force at the motor unit level. The neural mechanisms controlling muscular force involve task-dependent motor unit activity: recruitment, rate coding of already active motor units, and the interaction of infinite gradation of muscle forces involved in motor execution.

Damage of brain tissue following stroke affects corticospinal and other supraspinal motor pathways and leads to transsynaptic degeneration at the segmental level [33]. The consequent reduction in neural traffic at the spinal segmental level results in motor neuron loss and disruption of these primary force control mechanisms.

Previous literature suggests that compromise to motor units in hemiplegia is non-uniform between and within persons, and that considerable motor unit remodelling occurs between 2 and 6 months post stroke event. Motor unit firing rates tend overall to be decreased even in the ipsilesional limbs, and reduced firing rates may affect the capacity to produce fused contraction [33].

## 2.2 Rehabilitation techniques

The best rehabilitation strategy has not yet been identified, but it is long known that the right choice of timing is extremely important in planning a proper protocol. The different phases of the therapy depend on the specific stages of the



pathologies: for example in case of stroke, the major part of brain plasticity and reorganization take place in the first four weeks after the event and motion recovery occurs mainly within three months after it, even if functional ability slowly increases along the first year [46].

Another important factor is the aim of the rehabilitation: in the past the goal was a general recovery of motion ability, while now the main purpose of rehabilitation is to regain first of all the ADL, so it is called functional rehabilitation. To remark the importance given to this specific functionally regain, in these last years traditional physiotherapy as been flanked by the occupational one, which is focused on restoring first of all some level of independence of the patient in the occupations of every day living such as eating, drinking, getting dressed and getting washed.

### 2.2.1 Clinical classification of hand functions

To enable comparison between different approaches in the treatment and rehabilitation of upper limb functions, a common classification is needed. A framework has been proposed [10] for upper limb classification and performance assessment.

A classification of upper limb function should describe the remaining motor functions of the hand, forearm and shoulder. The one proposed by Oess and Curt in [10] classified hand functions in five levels of clinical relevance. Patients' upper limb functions are continuously evaluated during the hospitalization, and every evaluation score can be related to one of the hand function levels reported below. Changes in the patient levels can be considered as clinically meaningful changes, e.g. hand functions improvement or deterioration.

Additionally, the third validated version of the spinal cord independence measure(SCIM III) is a disability scale of performance test, which can reveal changes in the upper limb function. The SCIM III total score range is between 0 to 20, and each task performed is evaluated by a scale from 0 to 4. For each level of the upper limb function classification described below [10], the referred total range of SCIM III (tasks of self-care) score have been estimated.

The five hand function levels [10] are:

1. *Level 1 - No hand function*: Patients have no voluntary control of the elbow, wrist and hand muscles. They have no grasping function or active placing and reaching of the arm. [SCIM III: 0]

2. *Level 2 - Passive tenodesis hand*: Includes patients with neither voluntary control of extrinsic and intrinsic hand muscles nor ability to actively extend the wrist. Opening and closing of the hand is only possible by passive tenodesis effect. That is by supination or pronation of forearm to induce passive movements to the wrist and fingers. Bimanual grasping is effective only in a limited workspace. [SCIM III: 0-4]
3. *Level 3 - Active tenodesis hand*: Patients have no voluntary control of extrinsic and intrinsic hand muscles but can actively extend the wrist. Thus, an active tenodesis effect can be performed by the wrist to generate passive finger movements. Single handed grasping function is limited to a reduced workspace. [SCIM III: 4-13]
4. *Level 4 - Active extrinsic tenodesis hand*: Includes patients with voluntary control of the wrist and some extrinsic hand muscles. Thus, grasping with or without tenodesis effect and opening and closing of the hand can be carried out. Dexterity and workspace remain reduced. [SCIM III: 4-16]
5. *Level 5 - Active extrinsic intrinsic hand*: Patients have voluntary control of extrinsic and intrinsic muscles within an entire workspace. They have the ability to grasp in different forms, nevertheless muscle strength and dexterity can be limited. [SCIM III: 12-20]

Tasks evaluated in the SCIM III for self-care scale are:

- Feeding;
- Bathing upper body part;
- Bathing lower body part;
- Dressing upper body part;
- Dressing lower body part;
- Grooming.

In particular the maximum score of SCIM III that a patient sit on a wheelchair can reach is 18 points out of 20. This is because the "bathing" and "dressing body lower part" can not be performed without wheelchair [10].

Moreover the basic level needed to start some rehabilitation protocols is that patient can move the limb at least to oppose gravity, so higher than the score 0 of SCIM III scale.

### 2.2.2 Ability and performance measurements

Although intuitively the benefits of a stroke rehabilitation protocol may seem obvious, determining the impact of this treatment has proved to be difficult. This difficulty is due in part to problems of test study, design and methodology like lack of randomization, inappropriate control group selection, failure to blind assessors and difficulty in controlling for all possible confounders. Other difficulties are inherent to stroke rehabilitation such as controlling for spontaneous neurological recovery, daily fluctuation in individual function and, of main importance, difficulties in measuring functional and objective outcomes [15].

Many different clinical protocols have been applied to assess upper limb functionality, e.g. electro-physiological and biomechanical data collection. These measurements assess very specific aspects, mainly targeted to disclose effects of different types of hand interventions [10].

Clinical measurements of capacity and performance consist in set of specific movements and ADL tasks, that the patient has to perform in standardized environments and from which defined parameters are measured and scored according to pre-defined scale.

Capacity tests such as GRASSP (Graded and Redefined Assessment of Strength, Sensibility and Prehension [10]), VLT-SV (Short Version of the Van Lieshout Test for Arm/Hand Function [10]) and MSC (Motor Capabilities Scale [10]) are based on raw movements or ADL tasks that patient carries out specifically for the evaluation in an artificial environment, like laboratory or clinic.

Conversely, performance tests such as the THAQ (Tetraplegia Hand Activity Questionnaire [10]), assess ADL tasks that patients execute in their usual life course in a normal environment.

Thus, in capacity tests specific parameters are measured precisely, whereas performance tests evaluate tasks accomplishments. The advantage of capacity tests is that they are more reliable but they do not accurately reflect reality necessarily well. On the other side, performance tests provide less precise measurements but reflect reality more closely.

### 2.2.3 Evaluation and validation

Reliability and validity are important clinimetric properties of upper limb function evaluation tests, and have been studied by Oess and Curt [10] to ensure precise and accurate assessment tools.

Reliability is defined as the reproducibility of results obtained when the protocol is repeatedly used to perform tests. A common used index of reliability to measure reproducibility is the Intraclass Correlation Coefficient (ICC), which can vary in a range between 0, i.e. no agreement in repeated measures, to 1 that indicates perfect agreement.

The validity is defined as the precision to which an instrument actually measures what it is intended to measure. Three types of validity can be found: content validity, which is how much the instrument reflects the domain of interest; construct validity, which relates scores obtained to measurements of other tools based on the same theoretical hypothesis; and criterion validity, that represents how much the results are related to other tools previously shown to be accurate.

Among the instruments considered in Oess and Curt study [10], only five have been assessed for reliability and validity.

These five tools are:

- the GRASSP: Graded and Redefined Assessment of Strength, Sensibility and Prehension [10];
- the VLT-SV: Short Version of the Van Lieshout Test for Arm/Hand Function [10];
- the MSC: Motor Capabilities Scale [10];
- the CUE: Capabilities of Upper Extremity Instrument [10];
- the Sollerman Test [42].

The tools were all developed for clinical or research purpose to assess upper limb functions. For four out of five tools Oess et al. [10] have assessed reliability and validity both for proximal and distal arm analysis protocols both for proximal and distal arm. The only one focused on the distal arm and hand is the Sollerman Test.

Moreover the absolute clinical relevance of these techniques in order to evaluate the outcomes and validate the protocols still needs to be completely established.

#### 2.2.4 Rehabilitation protocols

Capacity and performance measurements of upper limb functions are based on various parameters, such as timing, counting, ordinal rating or weighting [10]. Ordinal scales generally rate the grasp pattern or capacity to execute a task, so they are subjective. Also the time to complete a task is sometimes used as parameters, for example in Sollerman Test, or weighing can be used to measure force strength with a dynamometer, for example WMFT test (Wolf Motor function Test [10]).

Tests based mainly on timing are objective but do not rate quality of movement. As a result they can neither differentiate normal from compensatory movements nor distinguish between a patient who can not perform a grasp pattern and a patient who can execute it but not to complete a given task.

Actually hand force is measured only from few instruments. The results of a recent review [10] which analyzes many existing methods for upper limb rehabilitation [10], are that only 5 % of them are based on weighing.

Thus, most of the upper limb function capacity and performance test rely on ordinal rating and therefore are subjective and somewhat imprecise.

### 2.3 Sollerman functional protocols

In the 1980 Christer Sollerman designed and presented in his Thesis [41] a hand function test based on seven (out of eight considered in a previous work [41]) of the most common and frequently used hand-grips. In the article of 1994 titled *Sollerman hand function test* [42] is reported a standardised test. The test is described in procedure and method, and it was used to evaluate hand function of fifty-nine tetraplegic patients before reconstructive surgery of their hand [42].

The aim of the method is primarily to give a picture of the grip function, as well as the ability and the quality of the hand, not of elbow or shoulder, in activities of daily living. The hand function test is based on the concept that the prehensile movements of the human hand can be described as variations of seven

basic grips: pulp pinch, lateral pinch, tripod pinch, five-finger pinch, diagonal, transverse and spherical volar grip, even if human hand naturally has many other functions in addition to these main grips.

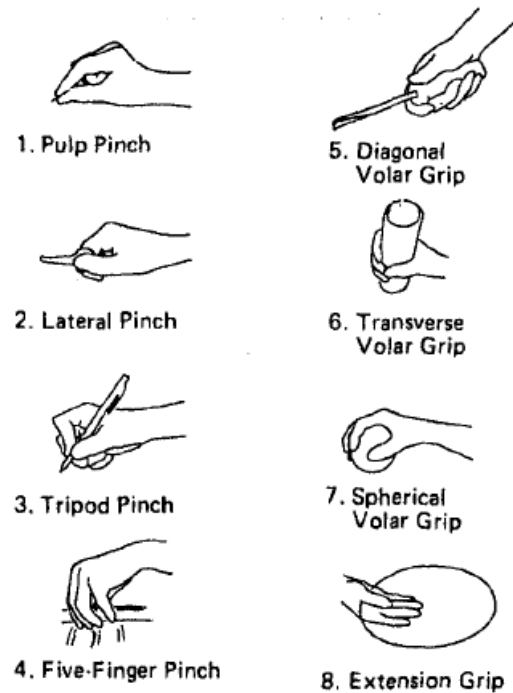


**Figure 2.3** – Eight main hand-grips individuated by Sollerman [42].

In reference to the Figure 2.3 the different grips were described as follow [42]:

1. *Pulp pinch*: the object is held between the thumb and the index.
2. *Lateral pinch*: the object is held between the thumb and the radial side of the index finger.
3. *Tripod pinch*: the object is surrounded by the thumb, index and middle finger.
4. *Five-finger pinch*: the object is held between the thumb and the four fingers together. It has no contact with the palm.
5. *Diagonal volar grip*: the object is held with the thumb against the four fingers. It has contact with the palm and its axis is diagonal to that of the hand.

6. *Transverse volar grip*: same as the *diagonal* one, but the axis of the object is transverse to that of the hand.
7. *Spherical volar grip*: the object is surrounded by the thumb and the four fingers and has contact with the palm.
8. *Extension grip*: the object is held between the thumb and the four fingers, which are extended in the interphalangeal joints. It has no contact with the palm.

The percentage use of the main grips in activities of daily living was calculated in a previous study [41]. The last grip presented (*Extension grip*) is the one discarded from the initial eight grips that Sollerman considered in [41], due to its low percentage of ADL usage (as can be seen by the data reported in Table 2.4 [41]).

Pinches (involving fingers)	[%]	Grips (involving whole hand)	[%]
Pulp pinch	20	Diagonal volar grip	15
Lateral pinch	20	Transverse volar grip	14
Tripod pinch	10	Spherical volar grip	4
Five-finger pinch	15	Extension grip	2

**Table 2.4** – The percentage use of the eight most common hand-grips in ADL according to [41]

The evaluation of the test was organized in two parts. One was called subjective estimation of hand function, and it consisted in a self evaluation of the patient who was instructed to put a mark somewhere on a line 10 cm long. The edges of the line were defined as "no hand function" and "full hand function" respectively, so that the distance of the mark from the endpoints corresponded to their estimated hand function. The second part of the valuation is claimed to be reproducible and reliable, and consists in a score evaluation by the examiner (C. Sollerman in [42]) based on a scale from 4 to 0 points according to the guidelines for scoring shown in the Table below 2.5.

The claimed of reproducibility and reliability is supported by good correlations indexes obtained by comparison between Sollerman and other two therapists that

independently assessed of the same patients.

Description	Score
The task is completed without any difficulty within 20 seconds and with the prescribed hand-grip of normal quality.	4
The task is completed, but with slight difficulty, or the task is not completed within 20 seconds, but within 40 seconds, or the task is completed with the prescribed hand-grip with slight divergence from normal.	3
The task is completed, but with great difficulty, or the task is not completed within 40 seconds, but within 60 seconds, or the task is not performed with the prescribed hand-grip.	2
The task is only partially performed within 60 seconds.	1
The task cannot be performed at all.	0

**Table 2.5** – Guidelines for scoring of subtests according to [41]

Although the test gives a good idea of the functional level of a pathological hand, it is not supported by truly objective records of the requested movement. Anyway the main importance of Sollerman test relies in its general nature. The test is not specifically designed for tetraplegic patients or for a specific pathology, so hand function data can be compared between groups of patients with different pathologies and with those with normal functions.

The Sollerman test was created to fulfil the need of hand surgery to have an index of overall hand function to decide the treatments and to assess surgical results. Anyway a test for the evaluation of the overall functions of the hand that requires a short period of time to be performed and with reproducible results obtained with objective measurements of tasks based on ADL, is still not used in therapy.

The system of electrical transduction of multiple biometric signals discussed in this Thesis has been created to help reaching this standardised test. In particular its main contribution lies in the capability of the system to record quantitative force signals generated by hands during force exertion.



## 2.4 Prehension patterns

The analysis of prehension patterns during the performance of ADL tasks plays an important role in the upper limb function evaluation test, particularly in capacity test. Indeed, most capacity test are based on raw movements and/or ADL tasks, which have been selected to perform specific types of grasps [10].

Numerous taxonomies of prehension have been established the first simple division came by Napier [30], who divided movements of the hand into two main groups :

- *Prehensile movements*: movements in which an object is seized and held partially or wholly within the compass of the hand.
- *Non-prehensile movements*: in which no grasping or seizing is involved. This group includes hand manipulations performed by pushing or lifting of objects. The movement can involve either the whole or single digits.

The only group of movements taken in analysis in the follow is that of *prehensile movements* one, which is important for functional rehabilitation.

### 2.4.1 Types of grips

In 1956 J.R. Napier [30] classified hand grips in two big groups, and thanks to its simplicity the partition is still used with efficacy. Napier purpose was to present a method of classifying prehensile movements, and his approach to the problem consists in investigate functions of the overall hand.

At first sight it would seem that the prehensile activities of the hand are really extensive and varied. However, on closer examination, this diversity is an expression of a multiplicity of movements rather than a vast range of purposive actions involving objects of all shapes and sizes that are handled during everyday activity.

So the theory of Napier is the following: although the size and the shape of an object may influence the type of prehension employed, it is actually the nature of the intended activity that finally influences the type of the grip.

Napier study of the normal hand suggests that there are only two distinct patterns of movement in man and that these, either separately or in combina-

tion, provide the anatomical basis for all prehensile activities whether skilled or unskilled.

The two discrete patterns of movement that had emerged through Napier study were analysed from both the anatomical and functional points of view and were called *precision grip* and *power grip* [30].

- *Power grip*: performed when power is needed. The object is grabbed full hand and makes contact with the palm and the fingers partially flexed, while the thumb exerts opposite pressure.
- *Precision grip*: identifies a grip of manipulation, where the object is held using only fingers and thumb.

Thus, combinations of these two prehensile patterns (see example of them in Figure 2.4) give all the possible prehensile movements that a human hand can perform.

This division is based on the main functional activities that hand can perform, and even if anatomically is not possible to find different biometric parameters for the two types of grips, the role of the different parts of the hand changes. For example when an object is really small the grip shifts to index and thumb which are the fingers with higher level of precision ability.

Next studies introduce more partitions in the *precision grip* group, for example based on the reciprocal forces exerted by the fingers [13]. An important result of hand grips research is that thumb and index have a principal role in all kinds of grips and the other fingers role is mainly to stabilize grips.

### 2.4.2 Static grip evaluation method

Landsmeer [25] suggested a further distinction for all hand activities: a static terminal phase and a dynamic initial one, which includes the opening of the hand, the positioning of the fingers, and the grasping of the object.

In the article of Kamakura et al. [20], static prehensile patterns of normal hand were classified into 14 patterns and 4 categories, according to the finger positions and the contact areas. To produce this classification the prehension patterns of 7 subjects holding each 98 objects were taken into account. In the study, prehension is defined as *the state of the hand in which an object is held without*

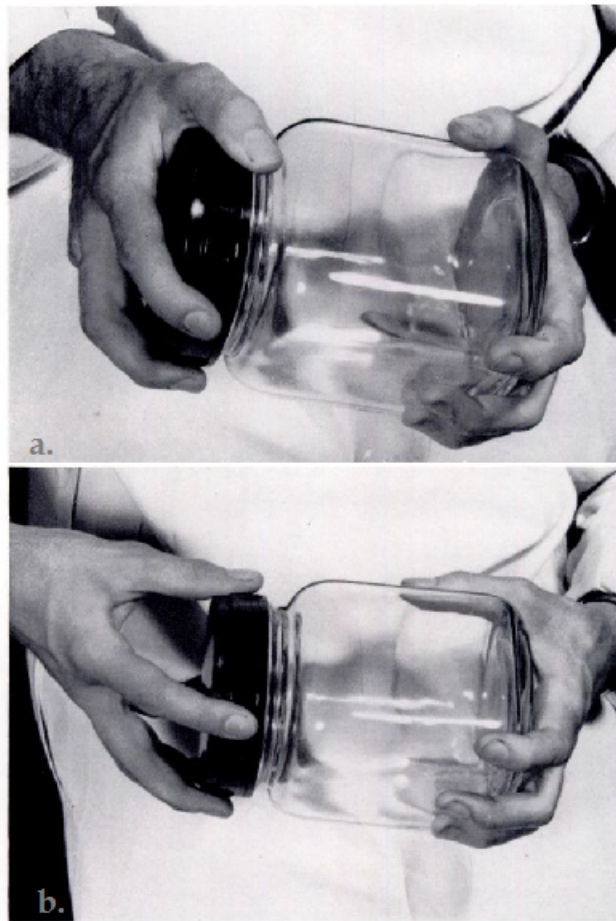


**Figure 2.4** – Two types of prehensile pattern of a right handed subject, in a everyday living task [30]. a) Power grip posture. b) Precision grip posture.

*changing contact with it*, thus static or relatively static phases of prehension were investigated.

The method used in Kamakura et al. [20] was to photograph the hand from different directions during the static phase of the grip (see Figures 2.5 and 2.6). Then, the object was smeared with ink and other pictures were taken of the open hand, after grasping, to record the contact areas revealed by the ink residue (see Figure 2.5 and 2.6).

The data analysis consisted in comparing photos of the finger positions and of contact areas on each object for each subject and among subjects. Any two prehension patterns were considered identical when both posture and contact areas were alike, so each pattern was identified by a name.

As a result five patterns of power grip, four of intermediate grip, four of precision grip, and one without thumb use were identified. Indeed the four categories

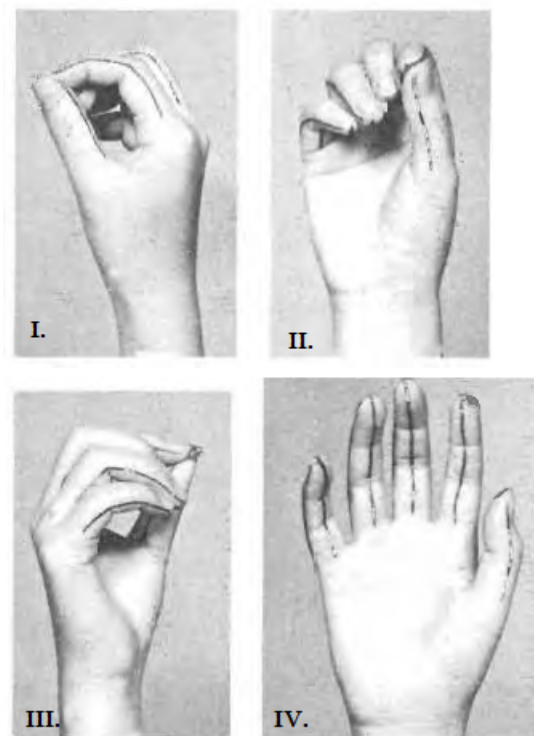


**Figure 2.5** – An example of a sequence for Tip prehension taken in a Kamakura test [20].

individuated by Kamakura et al. are

1. *Power Grip Category*: this major group was named after Napier's classification [30] and includes five patterns. Generally, in this group a wide area of the hand and a part of the palm make contact with the object.
2. *Precision Grip Category*: this group was also named after Napier's classification [30] and is subclassified into four patterns. Generally, in this group an object is held between the volar regions of the fingers and the pulp of the thumb. The flexion of the fingers is generally mild.
3. *Intermediate Grip Category*: this major group is intermediate between *Power Grip* and *Precision Grip*. The palm is no longer included as a contact area. The contact areas include the radial aspect of the index or the middle finger.
4. *Grips not involving the thumb*: this category does not contemplate the use of the thumb and consists prevalent in prehension pattern of small, light

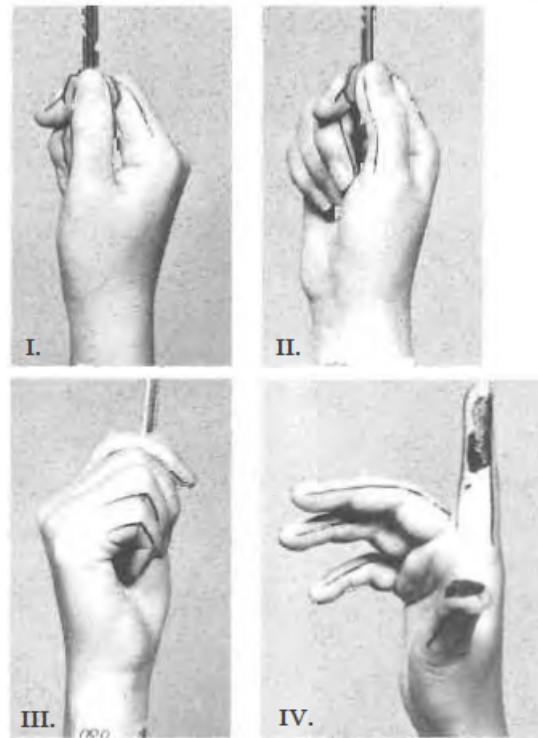


**Figure 2.6** – An example of a sequence for Lateral Grip taken in a Kamakura test [20].

object held between adjacent fingers.

Eighty-six percent of the grips shown by the subjects could be fitted into one of these prehension patterns, and the remaining fourteen percent into similar or combined patterns. In addition, individual differences were noted: sometimes a subject grasped an object using different patterns within the same category of other subjects or in a totally different way, but 31 out of 98 objects were grasped in an identical pattern.

The idea presented in Kamakura article [20], of studying prehension patterns in this simple way, seemed as effective as Sollerman individuation of principal ADL grips. So in collaboration with the rehabilitation equipe of San Bortolo hospital of Vicenza a similar Kamakura test has been performed. The purpose of the test was to individuate finger position and contact areas by mean of a previously identified set of static grips and the set used was that described and standardised by Sollerman [42].

### 2.4.3 Tests for contact area definition

In literature, the names of the grips are used rather inconsistently, so the names of the Sollerman grips presented in the following may be find with different names.

Object Description	Object picture	Reference Grip	Category
Little and Cylindrical Bicycle Pump		Transverse Grip type 1 (Vertical or horizontal)	Power Grip
Kitchen Knife		Diagonal Grip	Power Grip
Shirt Sleeve		Five finger Grip	Power Grip
Big Jar Cap		Three Point Grip	Power Grip
Little Jar Cap		Tripod (or Tridigit) Pinch	Precision Grip
Normal size glass		Transverse Grip type 2	Precision Grip
Dice		Index and Thumb Pinch (or Pulp pinch)	Precision Grip
Plastic Petri Dishes		Lateral Pinch	Intermediate Grip

**Figure 2.7** – Objects used to execute grips chosen from *Sollerman Table 84* (see appendix B).

In order to obtain the finger postures and the contact areas for each selected grip of the list, eight objects have been identified for grip executions. The list of chosen grips is coherent with the *Table of Sollerman 84 (Functional Balance)* (which can be found in appendix B) that was provided by the Occupational

Therapists of San Bortolo hospital equipe.

The objects used have been photographed and are reported in the Table 2.7.

In Table 2.7 the third column reports the grip meant to be obtained with the object, and they are divided in three categories based on Kamakura article [20].

The last category of Kamakura pattern classification (*Grips not involving the thumb*) is not present in the list of chosen grips and it is the only one of no interest in functional rehabilitation.

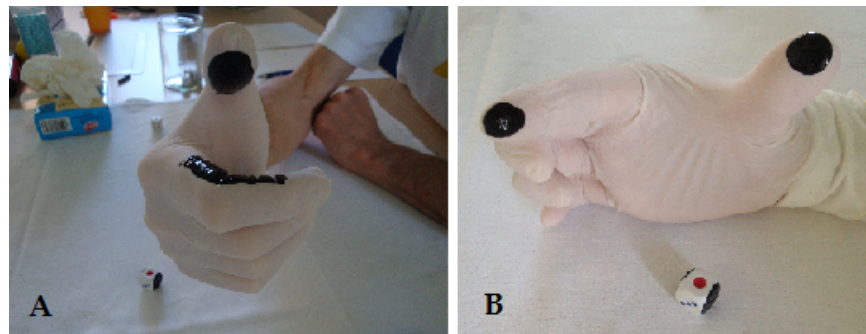


**Figure 2.8** – Picture taken in collaboration with San Bortolo hospital equipe.

A) The grip performed was the Index and Thumb pinch (or Pulp pinch) similar to Tip Grip of Kamakura test 2.5. B) The grip performed was the Lateral one similar to Kamakura test 2.6.

Lattice gloves have been used to perform grip tests and the objects have been smeared with black ink before starting tests. The glove was worn on the hand of the three therapists who collaborate at the test, and the object was grasped with a static grip for a while. Then the gloves with the highlighted contact areas of the grips were catalogued. Example of the obtained results can be seen in the Figure 2.8.

Some of the grips were performed also in Kamakura test [20], and comparing the results the patterns appear to be identical for the lateral grip (see Figure 2.6 and the 2.8 (A)) and similar for the index and thumb pinch (see Figure 2.5 and 2.8 (B)). In this second case the contact areas are not perfectly matched, this is because in Kamakura test the prehension was performed with the very fingertips, instead in the test executed in collaboration with San Bortolo hospital equipe, the goal of the grip was to grasp firmly the object in order to have a functional result, so the areas involved are principally represented by the last phalanx of the fingers.

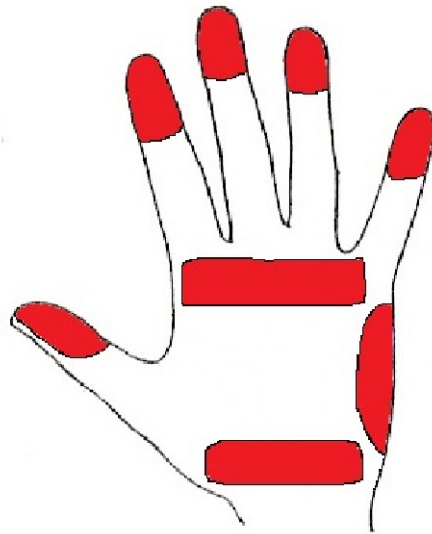


**Figure 2.9** – Hand diagram of the contact areas results.

In a second phase some of the same grips were performed by two patients with pathologies involving the use of the hand:






- Patient 1 had a non-severe problem and good mobility;
- Patient 2 had poor hand mobility.

As seen in Table 2.10, the test points out different static patterns between normal hand and pathological hand.

The main purpose of the test was to identify the contact areas of normal hand for the list of grips described (see the appendix B). So, patterns obtained on lattice gloves were compared to identify the fundamental hand contact areas in grips. Results are schematically reported in Figure 2.9.

Beside this, the test proved that pathological hand has different patterns and even if the grip was fully explained to patient, the lower mobility compromises the result. The aim of functional rehabilitation is to fulfil this gap.



Grip Name	Normal Hand	Good Mobility	Poor Mobility
Tripod (or Tridigital)			
Trasversal 1			
Trasversal 2			

**Figure 2.10** – Pictures taken in collaboration with San Bortolo hospital equipe.

# Chapter 3

## Software description

This Chapter describes the software part of the system. The first section focuses on the graphic interface while the second explains implementation features and how data were recorded. In the last part of the Chapter some future developments are described.

### 3.1 System graphic interface

Software basic idea was to create an effective rehabilitation tool with an intuitive graphic interface for occupational therapists. For this reason, *Wetware Concepts* collaborates with San Bortolo hospital team to design this proper graphic interface. These feedbacks were a fundamental contribution to the implementation of an intuitive tool for therapists really useful for hand treatments.

The whole system software was implemented in *LabVIEW 2011* (National Instruments) programming language, both for data acquisition and for interface implementation.

The interface has a main view through which therapists can control the rehabilitation exercise options, and an analysis view which permits clinicians to compare different exercise results. The proposed functional rehabilitation protocol and the two interfaces are described here in the following sections.

#### 3.1.1 Implemented functional rehabilitation protocol

The system graphic interface allows hand functional rehabilitation treatments of patients with different diseases, e.g. stroke or spinal cord injury. To obtain

this, a protocol based on Sollerman test has been developed. In 2.3 and 2.4 the Sollerman test has been described along with the *Table of Sollerman 84* (see appendix B), that was provided by San Bortolo hospital equipe.

The proposed protocol consists in a preliminary patient data collection and grip selection. The required patient data are of personal (e.g. name and surname, which are compulsory) and clinical (e.g. anamnesis, which can be freely added) kind. The grip task to be performed is up to therapists and can be chosen among the grips listed in *Table of Sollerman 84 Functional Balance* plus a "free-hand" exercise, i.e. performing hand movements without the purpose to achieve a specific grip execution.

The execution of an exercise could be targeted to either record a database of correct grip performed by normal hands, or collect data of patient grip for clinical interest. The correct grip data are used to compare patient executions. The comparison purpose is to monitor ability, force and trend of patient hands during the whole rehabilitative period.

The comparisons between patient different performances, or patient and correct grip executions, are fundamental for therapist treatment choices. So in the implemented protocol the analysis is based on hand color map schemes, which report execution information and enable comparisons.

### 3.1.2 Main interface

The main interface is user friendly and interactive, as shown in Figure 3.1. Its main features, like visual style and feedbacks, have been implemented at the *BioDevices laboratory of the Department of Information Engineering (University of Padova)* in collaboration with *Wetware Concepts* (University of Padova spin off) and San Bortolo hospital equipe of severe spinal/brain injured (Vicenza). The software has been implemented using LabVIEW 2011.

Thanks to the visual-oriented programming language, the interactive interface is based on intuitive elements like clickable buttons, multiple choice menu, writeable boxes and real-time graphics. During the execution of a software-supported rehabilitation treatment the biometric hand signals are instantly shown in the interface graphics.

The interface is divided into four main parts:

- *Option panel* (see Figure 3.2)

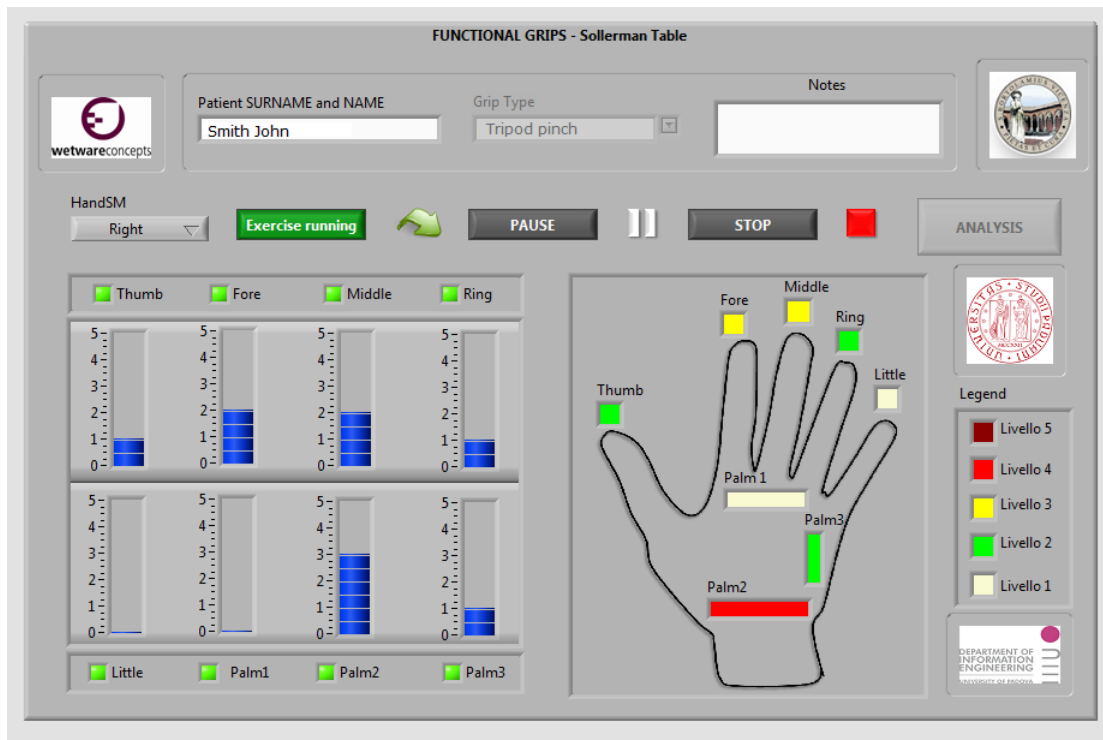


Figure 3.1 – System main graphic interface

In the first box of this panel the patient's name and surname has to be written (see number 1), and it is the only mandatory option of the whole interface: in fact the exercise can not be started until clinician do not log in the patient. The second element is a multiple choice menu for grip type selection (see number 2) and the third one is a note box where therapist can annotate comments or daily treatment specifics (see number 3).

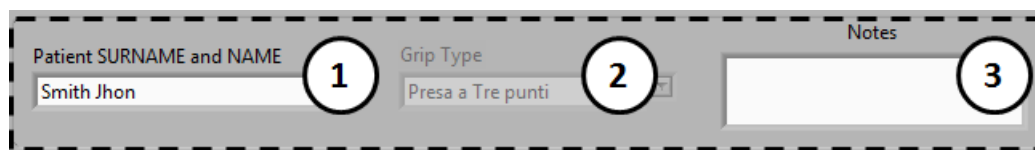


Figure 3.2 – Option panel. 1) Patient's name and surname box; 2) grip type box; 3) free note box.

- *Control panel* (see Figure 3.3)

On this panel the operational buttons can be found. The first field is a multiple choice menu to select the left or the right hand for the exercise execution (see number 1). Then at number 2 there is the "Start" button

(in this image the exercise is running so the button appears to be pressed), buttons at numbers 3 and 4 allow respectively to pause and to stop the exercise.

Pressing the "Analysis" button will enable the analysis interface. In the image the button is disabled because during the exercise running mode, the interface can not be accessed.



**Figure 3.3** – Command panel. 1) Left or right hand option; 2) "Start" button; 3) "Pause" button; 4) "Stop" button; 5) "Analysis" button.

- *Histograms panel* (see Figure 3.4)

In this part of the main interface, there are the histograms which show hand activity in real-time (see number 2). In detail, during exercise execution the force exerted by the hand is detected by the sensors and each signal is visualized using an histogram. Each sensor is linked to an histogram, so histograms number corresponds to sensor number.

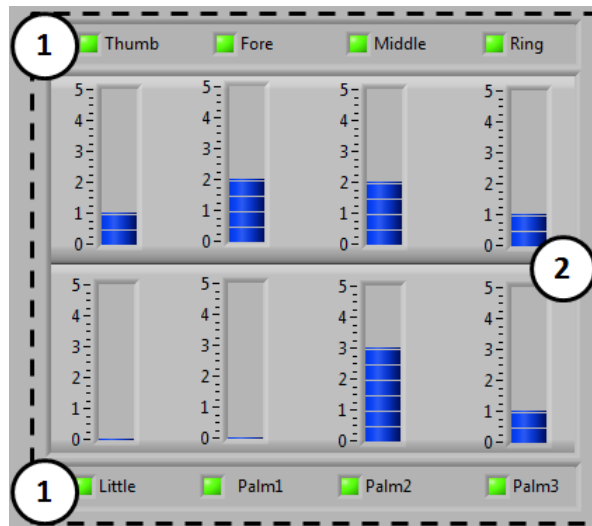


**Figure 3.4** – Histogram panel. 1) Hand contact-area names and in green is shown their selection LEDs; 2) sensor histograms.

Above and below the histograms their correspondent hand contact-area names are shown (see number 1). Moreover, each green LED associated to

the zone name (number 1) allows the selection or de-selection of the related histogram visualization.

- *Hand schematic representation* (see Figure 3.5)

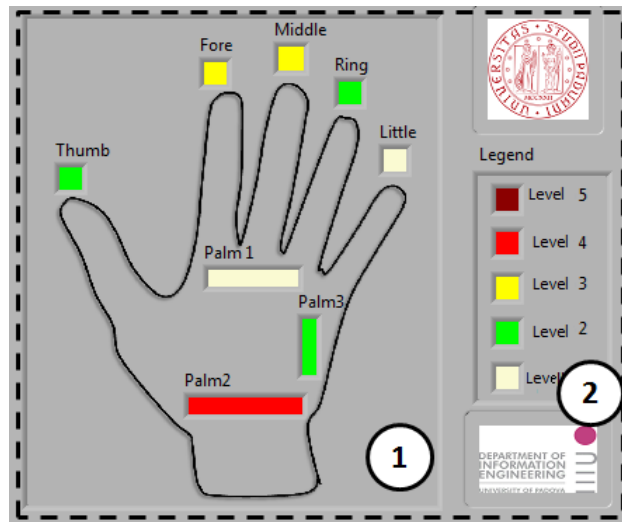


**Figure 3.5** – Hand schematic representation. 1) Hand color map scheme; 2) color map legend.

On the right part of the main interface a schematic hand color map allows the immediate and intuitive correlation between contact areas and their names. Moreover each contact area is provided of a coloured strip to approximately visualize the position of the sensor on glove.

Furthermore, every LED changes colour level in real-time during the exercise according to the force value registered. The colour legend is depicted at number 2.

This interface is meant to be mainly used by therapists, but actually it has been used also as a visual feedback for patient. The force level can be estimated by the real-time changing of colors in the hand color map (see Legend in Figure 3.5). This implementation allows intuitive real-time interpretation of force exerted both for therapist and patient during the exercise.

### 3.1.3 Report of a performed exercise

The grips in the list menu are those of *Table of Sollerman 84 Functional Balance*, moreover the grip box is initially blank and if the exercise is started in this way,

it is recorded as a free-hand exercise (see box number 2 of Figure 3.2).

While exercise is running, real time changing in exerted force can be seen from the histograms panel and from hand color map scheme (see figure 3.4 and 3.5). Overall task duration is up to clinician who can stop the exercise by pressing the "Stop" button when the task is considered executed or failed.

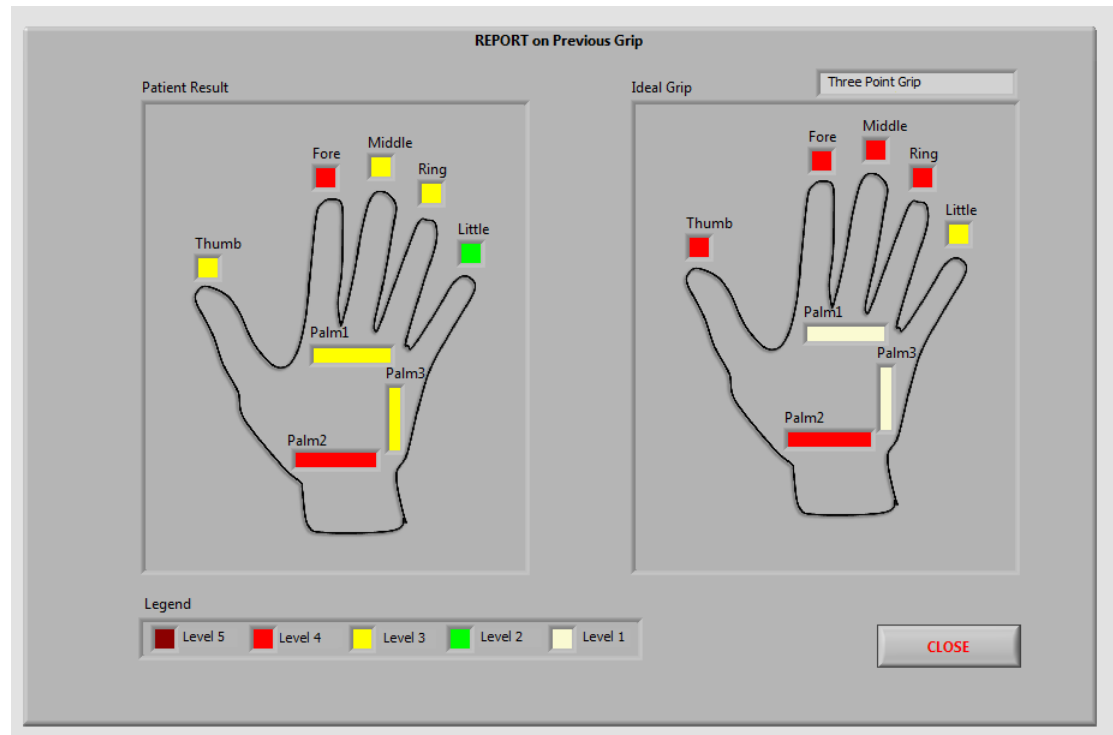


**Figure 3.6** – Resume after exercise execution page

When the "Stop" button is pressed a "Resume Page" appears: these hand color map schemes visualize both the results of the exercise just stopped, and the standard comparison scheme of a normal hand for that grip. Resume page can be seen in Figure 3.6.

### 3.1.4 Analysis interface

In this interface the results of exercises executed in different treatment sessions can be compared. In Figure 3.7 is depicted the page that allows the comparison between different executions of the same patient and with the database of standard grips.

The analysis page can be reached by pressing the "Analysis" button on the main interface (see "Analysis" button in Figure 3.3), which is enabled only when

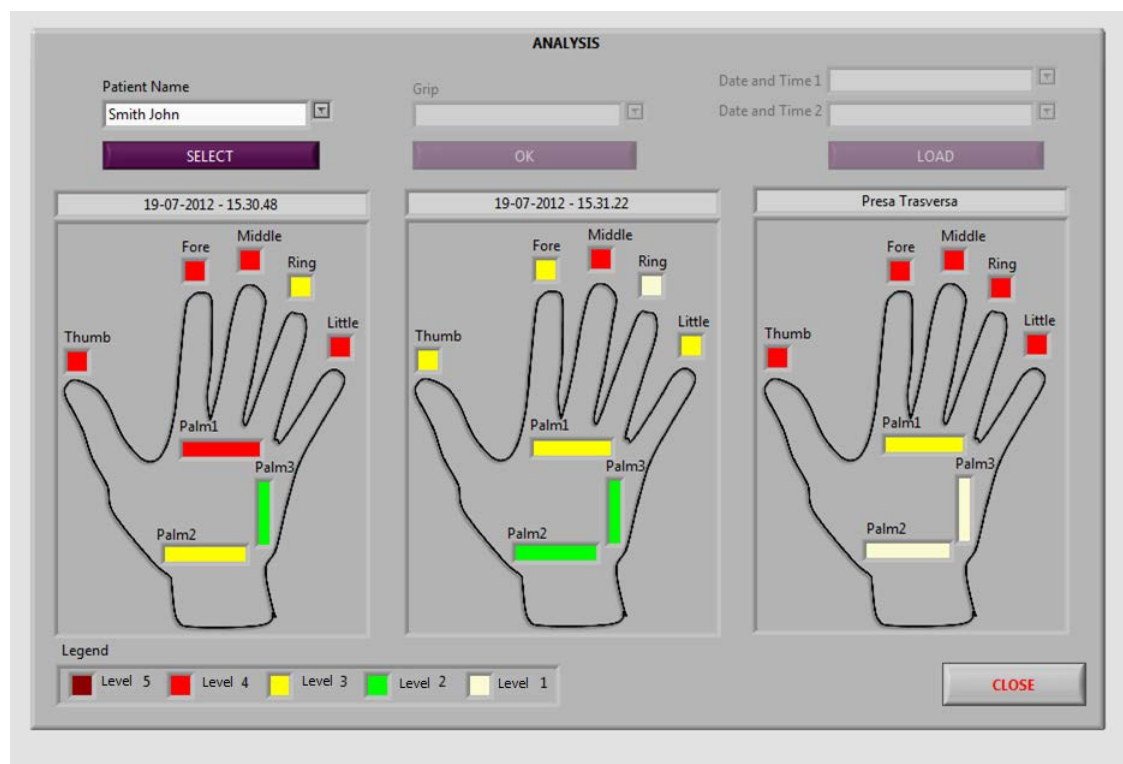


Figure 3.7 – Analysis interface

the exercise is not running.

This page is divided into two principal areas:

- *Selection panel* (see Figure 3.8)

This area of the analysis interface allows to choose which exercise has to be visualized in the graphs.

The first element required by the panel is the patient's name, which can be picked up in the box menu list (see number 1). Menu list collects all names of the patients who had previously used the rehabilitation system to perform treatments by indexing the database of results.

Once the name field is completed in the first box, the "Select" button has to be pressed to proceed to the second box. In this way the second part of the panel reaches the enable state, while the first one is disabled.

The second element on the panel allows the selection of the grip type (number 2). Like the first one the second box has a menu list which collects all the different grips performed by the selected patient. To fill this second box,



user has to choose one of the grips in the list and press the "OK" button below it.

The "OK" button enables the last step of the selection panel and disable the second one. The third step of the panel (see number 3) allows the choice of the test to be displayed. As it can be seen at number 3 there are two multiple choice menus to fill in, and each box has the same menu list where all the tests performed for each grip by the selected patient can be found.

**Figure 3.8** – Analysis selection panel. 1) Field for the selection of the patient; 2) box for grip choice; 3) exercise selection areas.

Finally, once the last two elements (see number 3) have been completed and the "Load" button has been pressed, test results will appear in the visualization panel of the analysis interface (see Figure 3.9). Moreover, the selection panel returns to the initial step of the selection sequence to allow another comparison session.

- *Visualization panel* (see Figure 3.9)

This panel uses the schematical color map representation of hand to visualize results of the tests. In this panel there are three hand schemes (see number 1 and 2).

In the first two schemes (number 1) the results of the test identified in the selection panel are loaded, when the "Load" button is pressed (see Figure 3.8). Above each hand scheme there is the result identification, given by the date and hour when the test was performed.

The third hand scheme (see number 2) reports the results of the selected grip, performed by a normal hand. Above the third scheme the name of the chosen grip is reported. To understand scheme information a legend is reported below (number 3).

When information required have been visualized, user can either close the analysis page by pressing the "Close" button, or continue the analysis session choosing different options from the selection panel (see Figure 3.8).

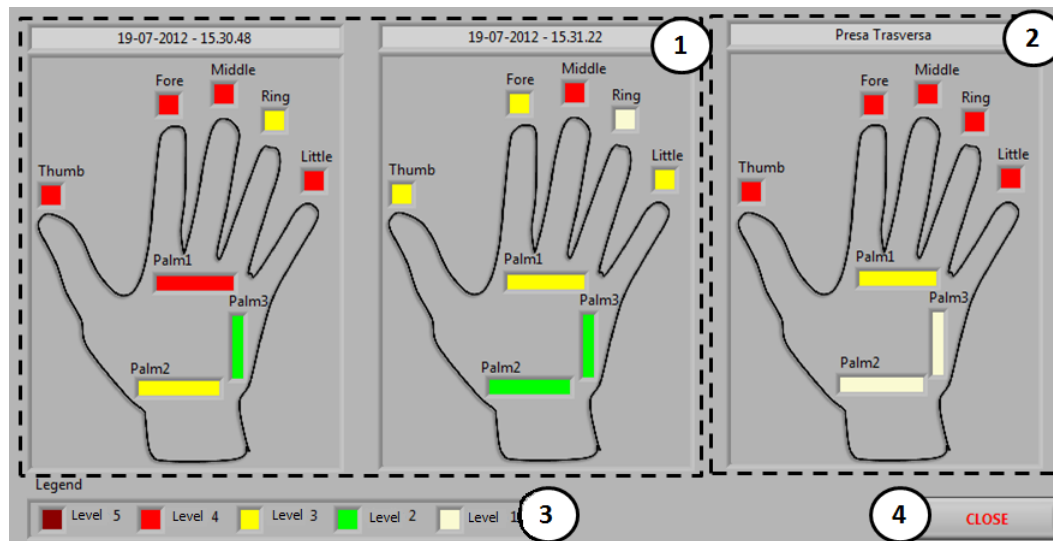


**Figure 3.9** – Analysis visualization panel. 1) Schematical hand color map representation that visualizes exercises results; 2) color map that reports typical non-pathological hand results; 3) color legend; 4) "Close" button to exit the analysis session.

This kind of visualization allows an immediate comparison between two patient's performances, even performed in completely different periods, and a non-pathological one of the same grip.

Actual analysis interface allows multiple comparisons of different executions, and gives the therapist indications about patient's performance improvement or deterioration during the rehabilitation period.

## 3.2 Data record format

Each time an exercise has been concluded a record file is generated. The record file template, reported in Figure 3.10, is organized in different sections. A section can be identified by standard names, usually a section begins with "*StartNameSection*" and ends with "*EndNameSection*".

Date and time are stored not only as file name, but also in the first line of the record file. Then the section "*RealTimeData*" starts and it includes all options or data entered by the user in the main interface, as well as the data sampled during the exercise execution.

The "*RealTimeData*" subsections are:

- "Comments", where some hints about the file organization are given;
- "PatientData", in which all the data of the option panel are stored (see Figure 3.2);
- "Options", which includes only the right or left hand selection operated in the control panel (see Figure 3.3);
- "Data" subsection which stores all the samples obtained from the sensors.

### FILE RECORD TEMPLATE :

```

Date and time
DAY-MONTH-YEAR - HOUR.MINUTES.SECONDS

StartRealTimeData
StartComments

"Real Time" data
[time[sec] sensor1-8[V]]

EndComments
StartPatientData
Surname and Name: NAME SURNAME;
Notes: FREE NOTES;
Grip Type: GRIP TYPE;
EndPatientData
StartOptions
Hand: RIGHT (OR LEFT);

EndOptions
StartData
Time[sec] - Sensor1[V] - Sensor2[V] - Sensor3[V] - Sensor4 [V] - Sensor5[V] - Sensor6[V] - Sensor7[V] - Sensor8[V];
[...]

Maximum instants:
IstantMaxSensor1[sec]- IstantMaxSensor2[sec]- IstantMaxSensor3[sec]- IstantMaxSensor4[sec]- IstantMaxSensor5[sec]-
IstantMaxSensor6[sec]- IstantMaxSensor7[sec]- IstantMaxSensor8[sec];

Maximum instant values:
MaxValueSensor1[sec]- MaxValueSensor2[sec]- MaxValueSensor3[sec]- MaxValueSensor4[sec]- MaxValueSensor5[sec]-
MaxValueSensor6[sec]- MaxValueSensor7[sec]- MaxValueSensor8[sec];

EndData
EndRealTimeData

```

Figure 3.10 – Record file template.

Each line of samples in "Data" subsection has been divided in: sampling instant (in seconds) and values (in Volts). Sampled values are stored sequentially for each sensor. Samples number can vary according to the running period length, which is set by the therapist.

In the last two lines of data in "Data" subsection are identified and memorized the "Maximum instants": these lines store the maximum value registered by each sensor during the whole exercise and the corresponding time.

Information of the maximum values are used in the analysis interface and in the resume page, due to the hypothesis that the maximum value recorded by the sensors corresponds to the instant successful execution of the grip. As indicated by San Bortolo hospital equipe, the comparison between maximum results of patient grip and those of the same grip performed by a normal hand, is an useful clinical information for functional rehabilitation protocols assessment.

### 3.2.1 Maximum identification

Maximum value is identified with a progressive method:

- The maximum array is initialized to a zero array;
- then, during the exercise running time, each new incoming sample is compared to the correspondent sensor value stored in the maximum array;
- if the incoming sample is greater than the value stored, the stored value is substituted by the incoming one;
- otherwise, if stored value is still the highest one, it is not substituted;
- the loop stops when the exercise execution is stopped.

An example is reported here following in Figure 3.11, and depicts a screen-shot of a part of the implemented software.

## 3.3 Future developments

The implemented interface is clinically usable by San Bortolo hospital equipe. To improve the existing interface, another one could be implemented by split the main interface into two parts, one for therapist and one to give dedicated

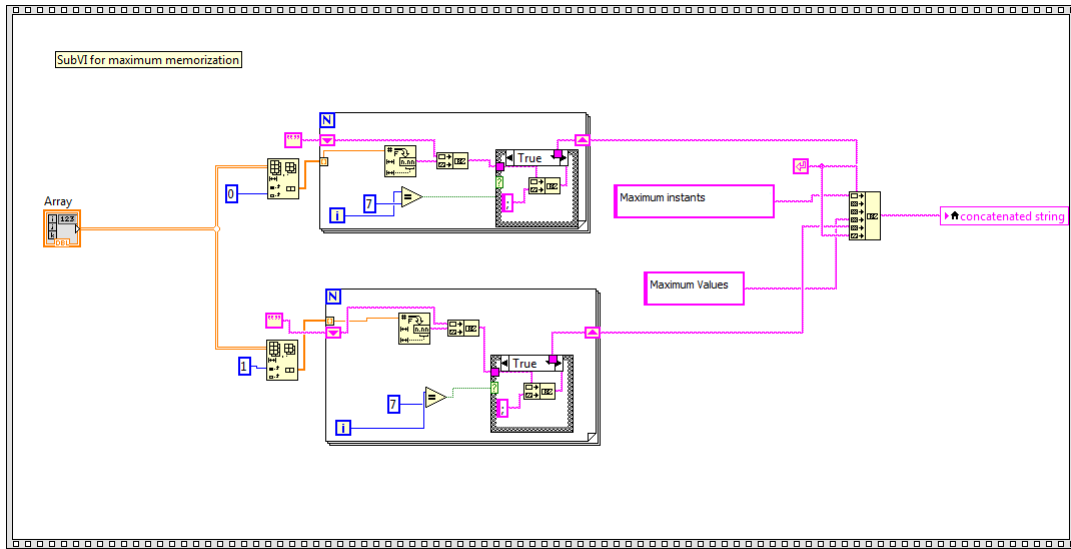


**Figure 3.11** – Example of *LabVIEW* software implementation of the function that converts and organizes the maximum values and corresponding time in data to be stored.

motivational feedback to patient. This new interface should be implemented using visual feedbacks and sounds to help and to direct patient grip execution. To give a better support to therapists, the main interface should include more information and should implement more types of functional exercises and analysis.

Moreover the biometric signal analysis can be deepened and other important parameters can be studied to increase the amount of available information obtainable from an exercise. This option would be useful when planning clinical treatments, so it should be added to the information provided by the analysis interface.

Another possible improvement is related to the storage of data: actual organization of data storage is functional to the prototype and is suitable for small amounts of data. To deal with a greater amount of data and with more information about patients clinical history, a proper and more robust database will be implemented.



# Chapter 4

## The prototype

This Chapter describes the manufacturing process of *Wetware concepts* prototype. In particular, in the first section components are introduced, then in next sections there is a detailed description of each one. At last, the ending section outlines possible future improvements of the prototype.

### 4.1 Prototype components

The system prototype is based on three principal components: the software interface, the hardware circuits and the sensorized glove.

Software interface, explained in **Chapter 3**, accomplishes many different tasks: the main one is to implement the functional rehabilitation protocol, which gives the therapist several choices about the treatment; then it records and analyse data to provide a visual feedback both to patient and therapist.

The hardware part of the prototype is outlined here in the following sections and it includes mainly two elements: a printed circuit board (PCB) and a commercial data acquisition device (DAQ). Moreover, a computer is needed to run the software interface, to acquire data and to interact with patient and therapist.

A shaped and sensorized glove is the mean used on patient's hand to identify biometric signals. The sensors included in the glove structure are transducers which produce electrical signals correlated to the applied force.

As it can be seen in Figure 4.1 the prototype aims to create a rehabilitation loop, including the patient as an active part of it. The patient wears the glove connected to the hardware, which amplifies and samples incoming biometric sig-

nals. Then the conditioned signals passing through USB undergo the phase of data elaboration in order to obtain and visualize feedbacks presented to patient.

System principal components are schematically represented in Figure 4.1.

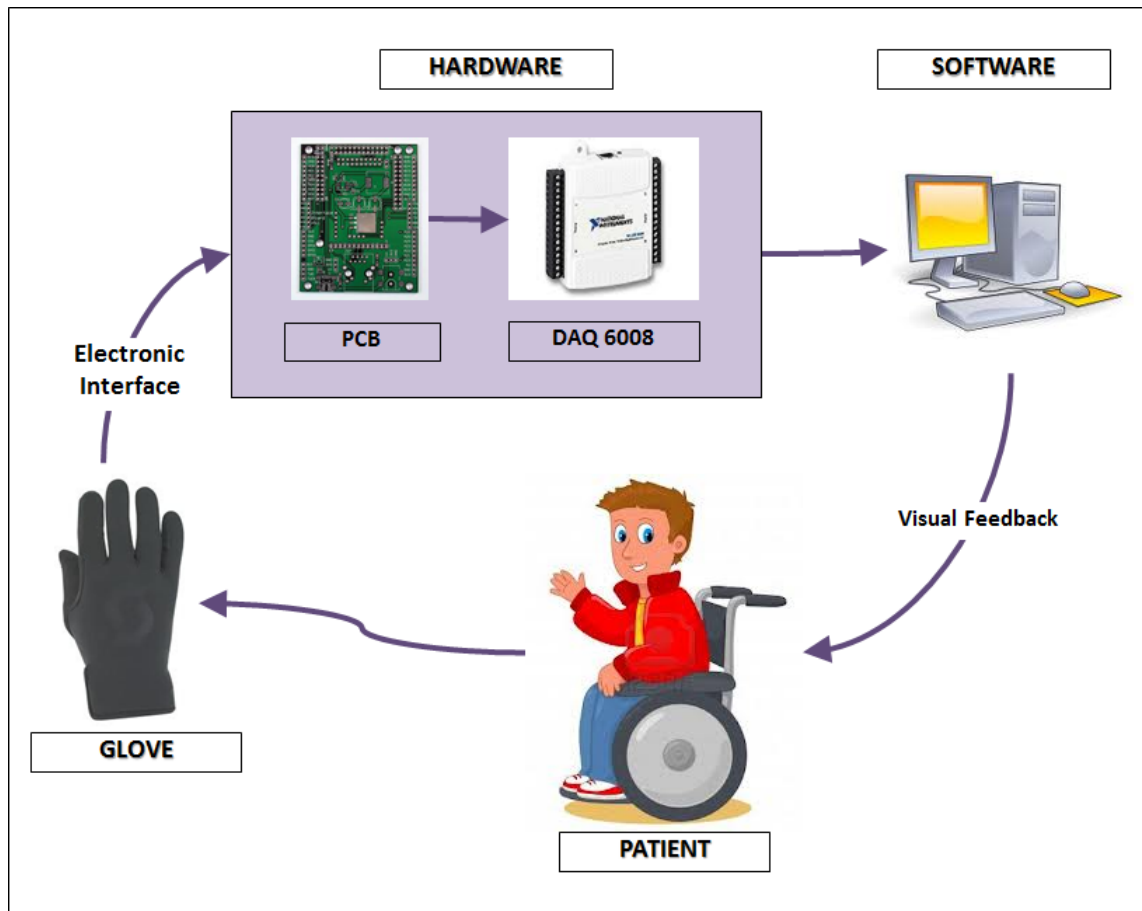


Figure 4.1 – Biofeedback loop including patient.

## 4.2 Glove

Electromechanical exoskeletons for rehabilitation used to acquire hand biometric signals, are usually encumbering, big and heavy. Moreover they often allow a limited range of motion (see section 1.3 in **Chapter 1**), so they do not permit the execution of the proper movements to fully perform functional rehabilitation.

The glove included in the system is shaped to be wearable for different types of pathological hands and the technology used to sensorize it is flexible, comfortable and allows the movements needed to carry out a functional rehabilitation



protocol. In detail, pathological hands can present a wide spectrum of unconventional shapes, like upper extremity hypertonicity, i.e. tensed muscles caused by increased tone, or flaccidity, i.e. muscles lack of tone. To increase glove possibilities to be worn some practical features have been considered:

- the palm side of the glove can be opened to be put on;
- glove finger parts correspondent to proximal phalanges (see Figure 2.1) are open too, so fingers have only two phalanges worn;
- finally, in correspondence of the wrist, a fabric strap is placed to fasten and secure glove to patient limb.

#### 4.2.1 Sensors behaviour and features

Hand biometric signals are measured by force sensors included in glove structure and placed in correspondence of the contact areas identified through preliminary trials described in 2.2.4.

Force sensors are devices which measure in specific areas the contact force values between sensor and object. To develop force sensors, many physical principles have been exploited and it has been decided to include in glove structure sensors which base their functioning on the force sensing resistance principle.

Force sensing resistors are constituted by a material whose resistance changes when a force is applied. They are also known as force sensitive resistors and are sometimes referred to with their initials: FSRs [7]. The material is a piezoresistive conductive polymer, which changes resistance in a predictable manner following application of force to its surface.

The piezoresistive effect describes changes in the electrical resistivity of a semiconductor when mechanical stress is applied: this electrical resistor may change its resistance when it experiences a strain or a deformation. This effect provides an easy and direct transduction mechanism between the mechanical and the electrical domains [6].

The resistance value of a resistor with length  $l$  and cross-sectional area  $A$  is given by

$$R = \rho \cdot \frac{l}{A} \tag{4.1}$$

The resistance value is determined by both the bulk resistivity ( $\rho$ ) and the geometrical dimensions. Consequently, there are two important factors that can change the resistance value according to the applied strain: the dimensions, including the length and cross section, and the resistivity, which depends on the chosen material. In detail, resistivity of certain materials may change as a function of strain, and the resistance change in magnitude that strain provokes is much greater than what is achievable through dimensions change.

By strict definition, piezoresistors refer to resistors whose resistivity changes with applied strain, e.g. sensors based on doped silicon. Also metal resistors change their resistance in response to strain, but mainly because of the shape deformation mechanism; such resistors are typically called strain gauges.

In the microscopic description of a piezoresistive behaviour under normal strain, the resistivity depends on the mobility of charge carriers, while in the macroscopic description of a semiconductor material the change ( $\Delta$ ) in resistance  $R$  is linearly related to the applied strain, according to equation 4.2:

$$\frac{\Delta R}{R} = G \cdot \frac{\Delta L}{L} \quad (4.2)$$

where  $L$  is the geometrical dimension and  $\Delta L$  quantifies its variation. The proportional constant  $G$  in the above equation is called *gauge factor* of a piezoresistor and the terms can be rearranged to get to an explicit expression for  $G$  as reported in the equation 4.3,

$$G = \frac{\Delta R/R}{\Delta L/L} = \frac{\Delta R}{\epsilon \cdot R} \quad (4.3)$$

where  $\epsilon$  is equal to  $\frac{\Delta L}{L}$ . The resistance is typically measured along its longitudinal axis. However, externally applied strain may contain three primary vector components: one along the longitudinal axis of a resistor and two at  $90^\circ$  respect to the longitudinal axis. A piezoresistive element may behave differently in conformity with each strain component. The change of measured resistance under the longitudinal stress component is called longitudinal piezoresistivity and similarly the one under transverse strain component is called transverse piezoresistivity [6].

The longitudinal and transverse strains are often present at the same time, and one of them may play a clearly dominating role. The total resistance variation is the sum of the changes in the longitudinal and transverse stress components [6].

The piezoresistive material can be a conductive polymer or, more precisely, intrinsically conducting polymer. Conductive polymers are generally organic polymers that conduct electricity. Such compounds may have high conductivity or can be semiconductors, and their biggest advantage is their processability, mainly by dispersion. They can offer high electrical conductivity properties which can be tuned using the methods of organic synthesis and by advanced dispersion techniques.

Thus, piezoresistive polymer is normally supplied by a polymeric sheet on which the sensing film has been applied by screen printing technique. The sensing film consists of both electrically conducting and non-conducting particles suspended in matrix. The particle sizes are of the order of fraction of microns, and are designed to reduce the temperature influence, improve mechanical properties and increase surface durability [7]. Applying a force to the surface of the sensing film causes particles to touch the conducting electrodes and change the resistance of the film.

Force sensitive resistor, as all resistance based sensors, requires a relatively simple interface and can operate satisfactorily in moderately hostile environments. Compared to other force sensors, the advantages of FSRs are their size (thickness typically less than 0.5 mm), low cost and good shock resistance.

A drawback of FSRs sensor type is that they can be damaged if force is applied steadily for a long time, i.e. hours, but this is clearly not the case of the functional rehabilitation protocols executed with the glove. Another possible disadvantage is the limited precision: measurement results may differ up to 10 %, but this mainly depends on the whole system features. Indeed, typical precision range in force sensitivity depends on mechanics, and its resolution depends on measurement electronics.

The electrical transducers used to build the prototype are customized FSR commercial devices produced by *Interlink Electronics* (see FSR data sheets in appendix D). These FSRs are robust polymeric film devices that exhibit decrease in resistance at the increasing of force applied onto the surface of the sensor (see Figure 4.2). The range of force sensitivity (according to data sheets in appendix D) goes from the actuation force, as low as 0.1 N, up to 10 N. Force sensitivity is optimized for human touch control in electronic devices such as medical systems and automotive, and for industrial or robotic applications.

Other characteristics of this sensor are fundamental to build a reliable electronic device:

- highly repeatable force behaviours;
- a large number of actuations, because the sensor is granted for 10 Million times without failure;
- long term drift smaller of 5 % (per  $\log_{10}$  time) in a 35-day-test with 1 kg load.

These and further specific data are reported in appendix D.

To include force sensing resistors in the glove structure, the commercial standard long strip sensor was cut down to a very short length and each sensor produced in this way has been placed at the glove contact area and has been electrically contacted driving circuits.

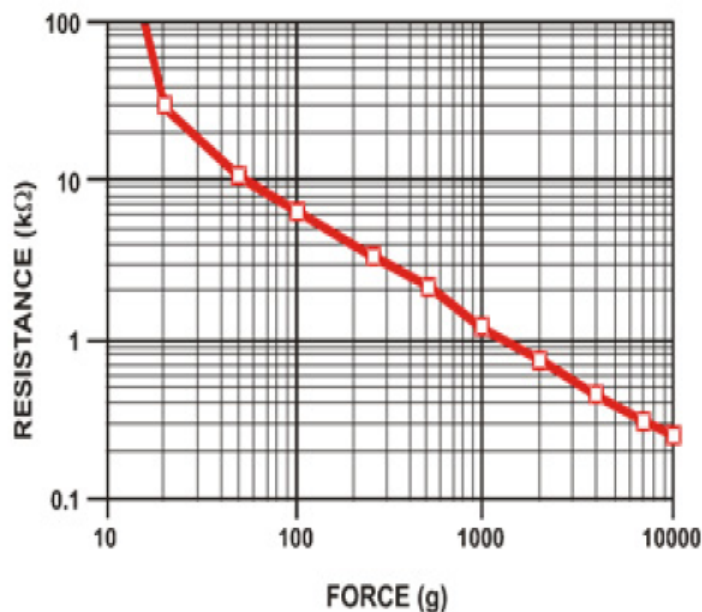


**Figure 4.2** – Sensor typical force curve, reported in FSR 408 Data Sheet (see appendix D)

According to the sensor data sheets (see appendix D) the *stand-off resistance*, i.e. the resistance of the sensor without any force applied, is greater than  $10\text{ M}\Omega$  while, with force application, the resistance can decrease to some hundreds

of Ohms (as represented in graph 4.2). The lowest resistance values presented in graph 4.2 and specified in the data sheets (see appendix D), appears at 100 N force. Moreover, referring to Figure 4.2, the operative range of resistance is exponentially proportional to applied force.

The commercial sensor thickness range, classified as ultra thin is between 0.2 and 1.25 mm (see appendix D). So sensor inclusion in glove structure do not modify its shape nor its comfort. By doing this a fabric layer is inserted between sensor and the real object used for functional rehabilitation. This layer is made of neoprene, that is glove fabric, and its thickness is of approximately 3 mm. Due to neoprene characteristics of elasticity and plasticity, sensors included in the glove undergo changes in sensor transduction characteristics presented in graph 4.2 and reported in data sheets in appendix D. To characterize sensor resistance when placed inside the glove, a resistance curve was plotted using data obtained from several tests performed with the glove (refer to graph 4.3).

The force curve in graph 4.3, obtained for glove sensors reports the resistance values (in Ohms) vs time (in seconds). Quantitative measurements of forces exerted by a finger wearing the glove were recorded using a peculiar sequence. In detail, the finger wearing the glove belonged to a normal female subject, who exerted on the sensor a slowly increasing force up to its maximum.

Referring to graph 4.3, the main phases are:

- In the *initial phase*, that is from 0 to approximately 8 seconds, the *stand-off resistance* of about 215 k $\Omega$  is found. The resulting trend is almost constant and the value recorded is definitely higher than the working range of interest.
- Then the *wearing phase* starts when the glove is worn, and usually in 2-3 seconds (see the Figure 4.3 from 8th second) the sensor resistance trend stabilizes at the wearing contact value. In about 8-10 seconds the resistance decreased from the *stand-off* value, passing through a negative pick, to the wearing value, which is about 20 k $\Omega$ . In the interval between 10 to 42 seconds, finger worn stood still and so the resistance wearing value remained constant. The punctual fluctuations depends on involuntary finger or body (e.g. respiration and heart beat) movements.
- In time range from 42 to 60 seconds the *force application phase* took place.

Therefore, data trend graph reported a progressive decrease in sensor resistance values until it arrives to the minimum of  $540 \Omega$ . Thus, the sensor resistance range of interest for the functional applications is between approximately  $20 \text{ k}\Omega$ , when glove is correctly worn, and hundreds of  $\Omega$ , when force is applied on the sensor. Some factors like subject's age or gender (see **Chapter 2**) can possibly affect the resistance range of interest, so they deserve further insights to be defined.

- In the *release phase*, the interval between 60 and 61 seconds in Figure 4.3, corresponds to the actual complete release of force applied to the sensor and the next period of 19 seconds consists in the resistance value stabilization during which the finger stood still.
- At last, the *final phase* data records (interval between 80 and 84 seconds) correspond to the finger undress, and the sensor resistance value returns to the initial *stand-off* value.

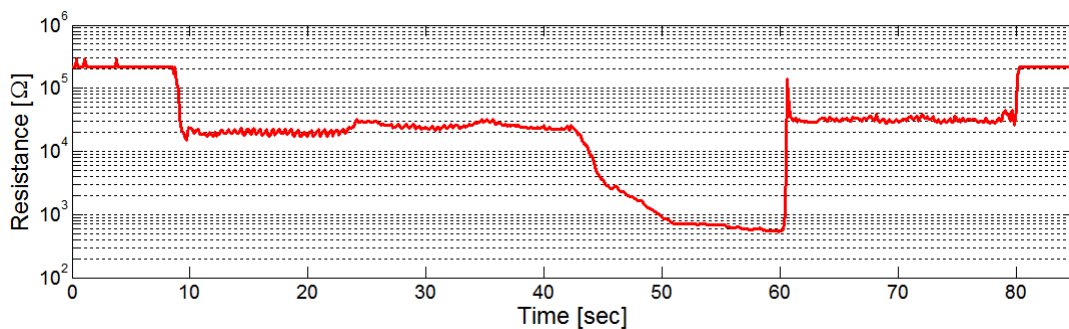
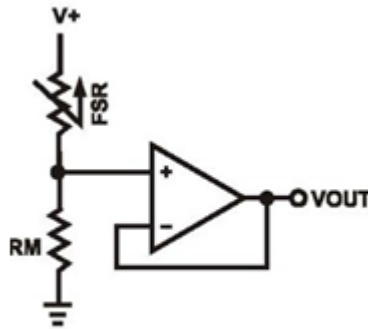


Figure 4.3 – Mounted sensor force curve.

### 4.3 Driving electronic interface

The main purpose of the system electronic interface is to design the driving circuits of the sensor in order to maximize the force curve range where voltage modulation is proportional to force. In this way the proportional modulation range matches the mounted sensor range of variation.

Sensor typical schematic (refer to appendix D) is reported in Figure 4.4 where *FSR* resistance stands for the variable sensor resistance and  $R_M$  indicates the fixed resistance on which the linear interval is calibrated.



**Figure 4.4** – Typical schematic of a single sensor (see appendix D)

The voltage signal is measured at the  $V_{OUT}$  connector and its equation, reported below (equation 4.4), is a voltage divider formula where  $V_+$  is the voltage signal at the positive input of the buffer.

$$V_{OUT} = \frac{R_M \cdot V_+}{R_M + R_{FSR}} \quad (4.4)$$

Moreover, between the two resistances and the voltage connector there is a dual operational amplifier schematic which is used as voltage buffer in a follower configuration.

The aim of the application of the voltage buffer amplifier is to retain the sensor output voltage and supply sufficient electrical current to the acquisition stage. In detail it is used to transfer a voltage from the first circuit represented by the sensor, which have a low output impedance level, to a second circuit, the system data acquisition device (DAQ, see 4.3.2), with an high input impedance level (144 k $\Omega$ ).

The interposed buffer amplifier prevents the DAQ from overloading the sensor circuit and avoiding interferences with its sampling operation. In the ideal voltage buffer, the input resistance is infinite and the output resistance zero. More properties of the ideal buffer are: perfect linearity, regardless of signal amplitudes, and instant output response, regardless of the speed of the input signal. The features of the operational amplifiers that have been used (LM258, Texas Instruments) can be found in App F.

Therefore, the dual operational amplifier is used in a buffer configuration to transfer the  $V_+$  input voltage unchanged to the output connector  $V_{OUT}$ , and buffer

voltage gain is equal to 1.

The complete electronic circuitry is composed by a cluster of basic driving circuits (see appendix 4.4) for each of the 8 sensors mounted on the glove. It was implemented on a printed circuit board (PCB), which is used to mechanically support and electrically connect electronic components using conductive pathways etched from copper sheets laminated onto a non-conductive substrate. The complete schematic and the printed circuit board scheme can be found in appendix A.

### 4.3.1 Sensing circuit fixed resistance

To maximize the operative resistive range as a function of exerted force, the fixed resistance value ( $R_M$ ) of the sensor driving circuits has been investigated. The electrical behaviour of the sensor has been modelled by several fixed resistors with different values, ranging from the stand off to the maximum force ones. In this way, the variable resistance of the sensor has been substituted by 13 fixed resistances, here called  $R_{FSR}$  (see Table 4.2), in order to better identify and increase the confidence on  $R_M$  calibration curves (graph 4.5).

As can be seen in graph 4.5 the curves of the signals have been measured for the different  $R_M$  values reported in Table 4.1.

Resistance	Nominal Value [k $\Omega$ ]	Real Value [k $\Omega$ ]
R1	1.5	1.49
R2	15.0	14.74
R3	150.0	149.00
R4	2.1	2.15

**Table 4.1** –  $R_M$  fixed resistance values used in the calibration curves 4.5.

Fixed resistance values reported in column *Real Value* of the Table 4.1 and 4.2 have been measured with the HP3458A multimeter at *BioDevices Laboratory*, and by comparing them to values reported in column *Nominal Value* some light deviations can be observed. Real values measurements allow to obtain the more accurate calibration curves reported in graph 4.5.



Nominal Value [k $\Omega$ ]	Real Value [k $\Omega$ ]
0.10	0.098
0.56	0.552
1.80	1.770
3.90	3.860
5.60	5.520
22.00	21.900
56.00	55.400
82.00	81.300
120.00	117.800
330.00	327.000
680.00	679.000
1000.00	989.000
4000.00	3970.000

**Table 4.2** –  $R_{FSR}$  resistance values used to represent sensor variable resistance in the calibration curves 4.5.

The  $R_{FSR}$  resistance curves vs  $V_{OUT}$  for each  $R_M$  value, are shown in graph 4.5. In detail, these typical curves have been obtained with the supply voltage of 5 V to feed the buffer.

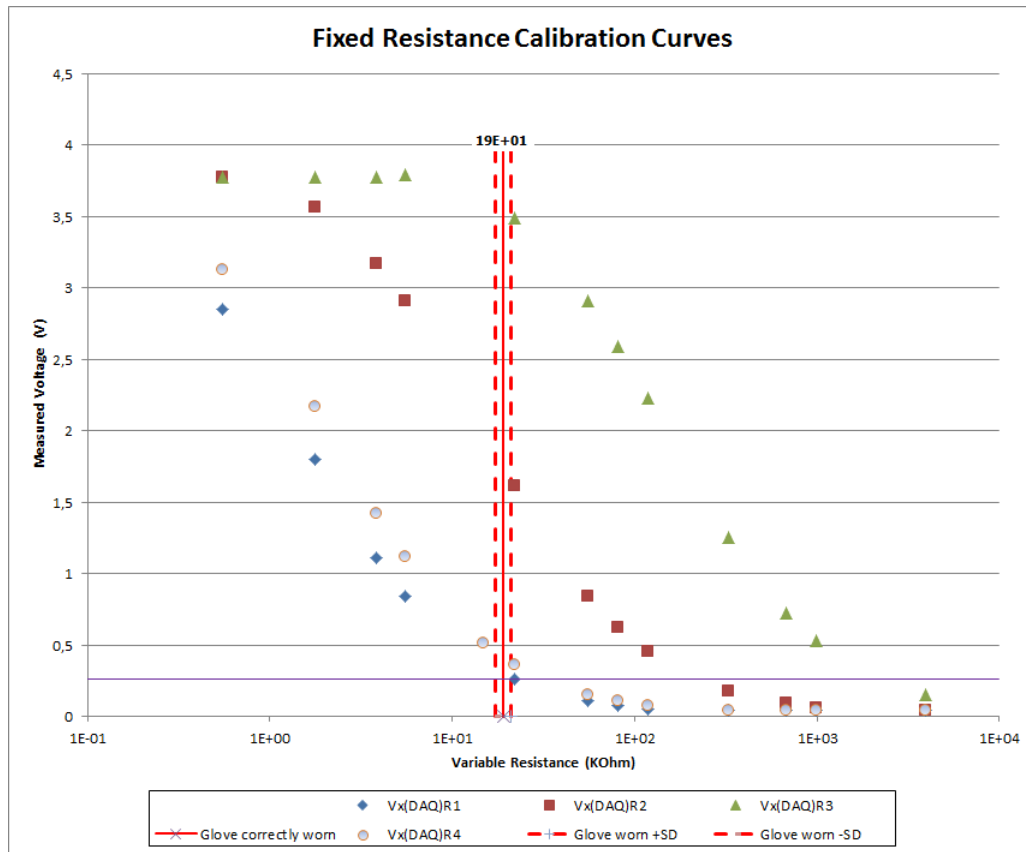


**Figure 4.5** – Typical curves measured for different values of resistances. Red lines indicates the mean resistance for a correctly worn glove (see **Chapter 5**).

On graph 4.5 is reported also the value of the resistance found in correspondence of a correctly worn glove ( $R_{cw}$ ) and the range identified by the standard deviation (SD, see **Chapter 5**).

From Figure 4.5, the range suitable for functional protocol application is between some kilo Ohms and hundreds of Ohms, therefore the  $R_M$  resistance curve which better reflects the range of interest was  $R_4$  2.1 k $\Omega$

By using this value for  $R_M$  it can be ensured a correct response of the sensor during functional tasks executions, avoiding the upper and lower tails due to operational amplifiers saturation.

### 4.3.2 DAQ

The PCB is connected to a data acquisition device (DAQ), that is the electronic interface which is used to condition the incoming voltage signals produced by the transducers. Signal conditioning generally means manipulating an analogue signal to meet the requirements of the next processing stage. In this case the DAQ is used mainly as an analog-to-digital converter to sample signals and transmit them to computer interface through an USB channel .

The DAQ used in the system is an USB-6008 commercial device produced by National Instruments, which can be connected to the main computer through an USB for various type of measurement applications. The connectivity is up to a plug-and-play USB, so this device can be easily used for quick measurements, and nevertheless it is versatile enough even for more complex measurement applications.

This device supports 8 analog inputs of 12 bits up to 10 kS/s, that have been used to connect the analog signals coming from the PCB. Than the two analog outputs at 12 bits have been occupied as power supplies, to feed the circuits.

At last, DAQ output sampled signals are transmitted through the USB channel to the connected computer and processed by the interface presented in **Chapter 3**.

For further technical informations about the DAQ commercial device, data sheets and block diagram of DAQ functional components are reported in the appendix E.

## 4.4 Future improvements

*Wetware Concepts* prototype can already be used for research, studies, and first functional rehabilitation trials, but it needs some improvements for effective clinical use.

For enhancing the system capability some possible hints to pursue may be:

- to deepen studies about sensor and circuit characterization;
- to increase the number of sensors included in the glove;
- to shape new glove configurations adjustable to even more pathological hands;

- to investigate more PCB configurations;
- to use different technological data acquisition devices (that may use a wireless connection channel).

These and other improvements could lead to a robust measurement system, which could be used by occupational therapists in clinics to enhance hand rehabilitation.

# Chapter 5

## Application of the prototype

In this Chapter data obtained with the prototype are reported and discussed. The first section shows data of a correct glove wearing process, the second one reports functional grip data produced by the prototype, and outlines the grip execution procedure followed by discussion. In these sections only normal hand trends were investigated and possible clinical hand grips are imitated.

### 5.1 Glove wearing features

In order to correctly wear the glove, fingers have to be accurately inserted and positioned against sensors, then the glove palm side has to be fasten through the wrist fabric strap. Data used to create graph 5.1 were produced using the prototype described above and the graphic interface with the grip type selection field left blank (see Figure 3.2).

In detail, to allow a better visualization of data only three meaningful series were chosen: thumb, fore and middle fingers. Usually ring and little fingers have similar trends even if, due to their smaller dimension, their trends may show lower amplitude values. The dimensions of little finger make it difficult to properly wear the glove on it, moreover it is often less important in hand grips, so in these wearing tests it is not reported (see graphs 5.1 and 5.2). Also ring finger is not reported in graphs 5.1 and 5.2 because it does not add further information to the following discussion.

Graph 5.1 depicts the typical phases of the glove wearing procedure. During the *initial phase* the software interface was already in a running mode, but the

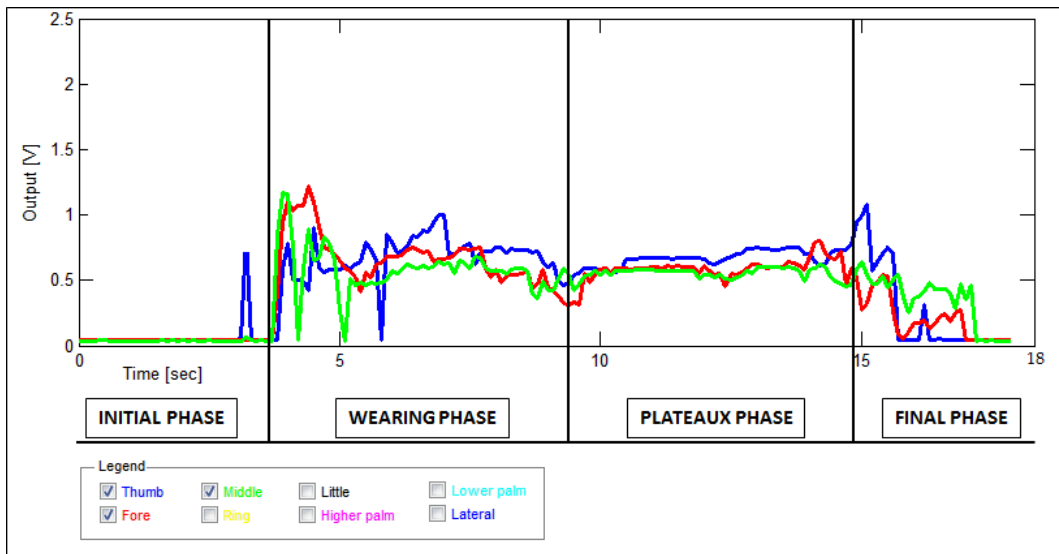


**Figure 5.1** – Glove wearing phases for fingers.

glove was not worn, so the voltage signals reported are at a zero level.

Then the *wearing phase* starts, the fore and the middle fingers were worn and adjusted so voltage values suddenly reach the first peaks. After that also the thumb was worn and adjusted as can be confirmed in the graph by the appearing of the thumb peak some instants later. As can be seen in Figure 5.1 at the end of the *wearing phase* trends decrease toward the *plateaux phase*, and this decreasing behaviour is not as rapid as the increasing one. This is because sensor answer needed some time to reach a stable contact voltage value.

During the *plateaux phase* the glove was just worn without any additional force application, therefore trends are approximately constant, some minor variation can depend on involuntary movements of hands or of the whole body, e.g. those caused by respiration. At last in the *final phase* hand was undressed, so voltage signal may pass through local increase, caused by undress operations, but finally they go back to zero.

Graph 5.2 is reported to stress differences in palm sensor during the wearing process, allowing an immediate and informative comparison. Trends reported are both those of the three fingers and that of the lower palm. Time length in Figure 5.2 do not include the *initial phase* (which is zero like observed before) and starts with the *wearing phase*. In comparison with the *wearing phase* of graph 5.1, in Figure 5.2 the phase lasts more due to the inclusion of the lower palm trend.

In the wearing process, after dressing the finger part of the glove, the fabric

strap is fasten to place palm sensors in contact with the hand. Therefore, the palm wearing peak (indicated by the left arrow in graph 5.2) appears later than finger ones and it is higher because the fabric strap needs to be fasten hard to secure the glove. Then *plateaux* and *final phase* trends are similar to the ones observed before, the only main difference noted is the last peak (indicated by the right arrow in graph 5.2), which corresponds to the unfasten of the fabric strap during the undress operation.

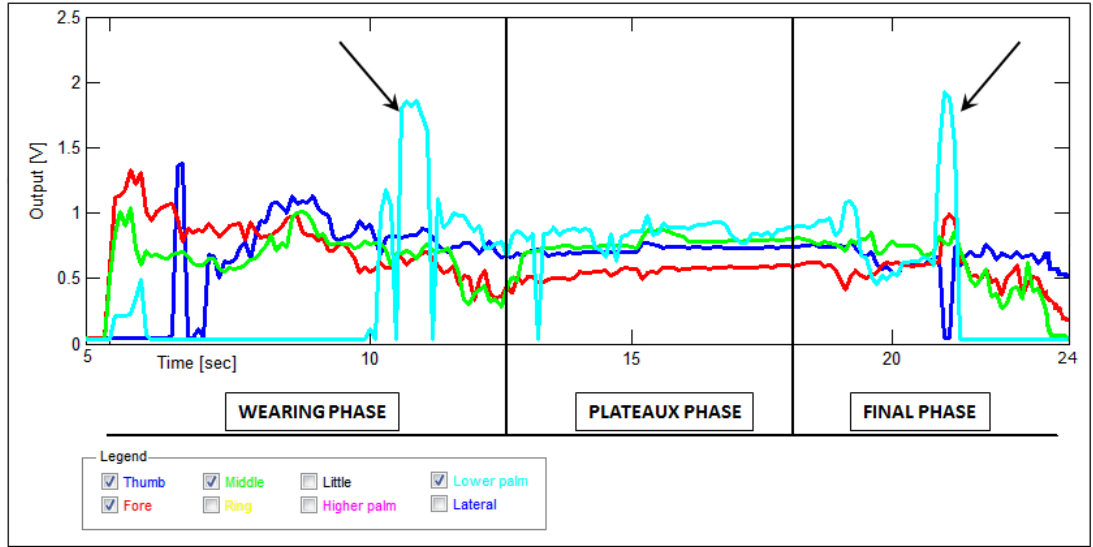


**Figure 5.2** – Glove wearing phases for fingers and palm.

The constant voltage signal value, reached by each sensor during the *plateaux phase*, can differ slightly in value among fingers or palm contact areas, but it is given by an almost constant sensor resistance ( $R_{FSR}$ ). The  $R_{FSR}$  has been evaluated throughout series of measurements, acquired during the *plateaux phase*, for a correctly worn glove configuration. The average on the 40 measurements obtained for the correctly worn resistance is:

$$R_{cw} = 19020\Omega \pm 10\% \quad (5.1)$$

where 10 % is the standard deviation calculated on the 40 values. The  $R_{cw}$  and its standard deviation (SD) values are reported in the resistance calibration graph 4.5. The voltage value that corresponds to the  $R_{cw}$ , deduced from graph 4.5 interpolation, is approximately of 0.41 V, congruent with the series of data presented above.

## 5.2 Grips executions

Some functional exercises of the rehabilitation protocol, described in Chapters above, were performed to test the prototype. These trials have demonstrated the effective role that the system has in distinguishing grip executed in accordance to Sollerman standards.

The whole system was operatively used to perform the following trials and data recorded have been elaborated and reported in graphs using custom MATLAB (Mathworks, 2009) Graphical User Interfaces. In usual exercise carried out with the prototype, the data shown in the results and analysis interfaces (see **Chapter 3**), are just functional to the rehabilitation use as therapist information or patient feedbacks. Instead, the graphs presented in this section reports sensor voltage output vs exercise time graphs. This signal visualization allows even more technical considerations, useful for further investigations on hand force.

In the following three illustrative graphs are reported. These have been obtained by executing three different grips coded in *Sollerman Table 84* (see appendix B): a lateral pinch, a transverse grip type 1 and a tripod (or tridigit) grip. For each grip all sensors traces are visualized, and in order to allow an informative comparison of trends, traces for each grip are divided in two different sub-graphs. In the graphs **A**, trends of sensors mainly involved in the hand grip are selected, while in the **B** ones all the other glove sensors are visualized.

The lateral grip was performed using the same plastic petri dish reported in Table 2.7, used to evaluate the contact areas in the preliminary trials (see section 2.4). In this test the goal was to show how thumb and fore finger are involved in the lateral pinch. In detail, thumb and index should be the only fingers actively involved in the lateral pinch execution, according to San Bortolo hospital therapists.

In the **A** graph of Figure 5.3 the trends of the thumb (blue line) and the index (red line) are reported. Lateral pinch exercise was executed in sequence of four time by a normal hand. A single execution process starts with the contact between fingers and object, becomes a firmly static pinch for approximately 2 seconds and last with the release of the object.

The lateral pinch correct execution according to Sollerman static grip standards consists in grabbing the petri dish with thumb fingertip and index lateral proximal/medial phalanges, while a wrong pinch can involve the use of the index



lateral distal phalanx. To compare the correct and the non-correct lateral pinches the overall execution (reported in 5.3 graphs) was divided in two phases: the one between 0 and 15 seconds reports two non-correct pinches, while between 15 and 30 seconds there are two correct pinches.

Therefore, observing the four lateral pinch executions, differences can be noticed between the first two (in the interval 0-15 seconds) and later ones (in the interval 15-30 seconds). In detail, during the pinch process thumb voltage value (proportional to force exerted) is lower in the first two executions than the fore finger value, while in the last ones it is higher.

Thus, in addition to force peaks shown in the interfaces of **Chapter 3**, force values and trends can reveal how similar to a correct Sollerman standard the performed execution is. Moreover, in this trend analysis could be evaluated more parameters like rising/falling time between constant and maximum forces exerted, correlations between different signals, or other clinical meaningful variables that can be obtained with further investigations.

Hence, to show how a wrong grip can be easily detected, in graphs **A** and **B** of 5.4 are reported the sensor data recorded during a transverse grip type 1 execution. As for lateral pinch exercise, the transverse grip was executed in a sequence of four times by a normal hand. Unlikely lateral pinch the execution of this grip was not divided in two phases, but was performed imitating a possible wrong grip. In detail, the wrong behaviour imitated is the compensation movement, that is common in patients affected by hand impairment, is the compensation movement. The compensation movement is an involuntary strategy to achieve grip purpose that could involve the ipsilesional hand or impaired hand segments not considered in Sollerman standard.

The standard trends expected for this grip consist in finger sensors main activation, while palm sensors activation should not be relevant. For this reason, in graphs 5.4, trends are divided in fingers (**A**) and palms (**B**), for trend identification refer to Legends reported in graphs.

In the **A** graph of Figure 5.4, output signals show that fore (red line), middle (green line) and ring (yellow line) fingers exert the most part of the force, while thumb (blue line) and little finger (black line) have a lower output value. So finger trends are congruent with the correct static grip sequence execution. While in the graph **B**, where sensor palms are reported, lower palm (light blue line) and

---

lateral palm (dotted blue line) values have minor and not relevant fluctuations, but higher palm (pink line) perfectly follows finger trends. This means that higher palm is actively involved in the execution and hand impairment is compensated using that segment to reach the static grip.

Thus, the transverse grip execution reported in graphs 5.4 is classified as not correctly performed due to the compensation movements. So, in addition to wrong finger positions even compensation movements can be recognized and classified with the analysis of trends.

### 5.2.1 Example of a dynamic grip execution

In Figure 5.5 trends for a tripod (or tridigit) dynamic grip are reported. The grip was performed by a normal hand of a male subject who unscrewed and re-screwed the cap of the little jar presented in Table 2.7. In the tripod grip (according to Sollerman standard) the only sensor of interest are those of the thumb, fore and middle fingers, while all the other sensors output voltage should not be relevant.

The tripod grip execution was performed according to Sollerman standards, as can be seen in Figure 5.5, where relevant trends are reported in graph **A** (thumb in blue, fore finger in red and middle finger in green), while not relevant trends are in the graph **B**.

According to what expected, in graph 5.5 **B** it can not be identified any actuation trends, because all sensors of ring, little finger and palms present minor fluctuations around the correctly worn voltage value discussed above (see 5.1). On the other side thumb, index and middle fingers trends reported in graph 5.5 **A** are dynamic trends.

The process in graphs 5.5 is divided in two phases:

- *Unscrew phase*

Between 10 and 20 seconds the cap of the jar has been unscrewed with three principal movements. The three movements present an overall decreasing amount of force and range of time for each finger. Moreover, the first movement is peculiarly high in magnitude and covers a long interval of time, this is because initially the cap of the jar was closed firmly. Then, cap has been released and re-grabbed in correspondence to each of the three unscrewing movements. In the respective intervals between the three

peaks, cap releasing has been confirmed by trends in the graph **A**, where sensor outputs rapidly decrease approximately to the correctly worn voltage output.

- *Screwing phase*

Between 20 and 30 seconds the second phase has taken place and the cap of the jar has been closed again through four main movements. On the contrary of the previous phase, movements present an overall increasing trend of force exerted. The first lowest peak corresponds to the lean down movement of the cap on the jar and the following three to the consequent screwing of it. Similarly to the previous phase the pattern presents intervals of correctly worn voltage output.

It is worth noticing that output trends follow accurately the two phases of cap unscrewing and screwing in the observation period, revealing a good performance of the device in dynamic exercises. So from this dynamic grip example emerged an even greater possibility of analysis related to the whole dynamic of the grip and not only to maximum values of forces.

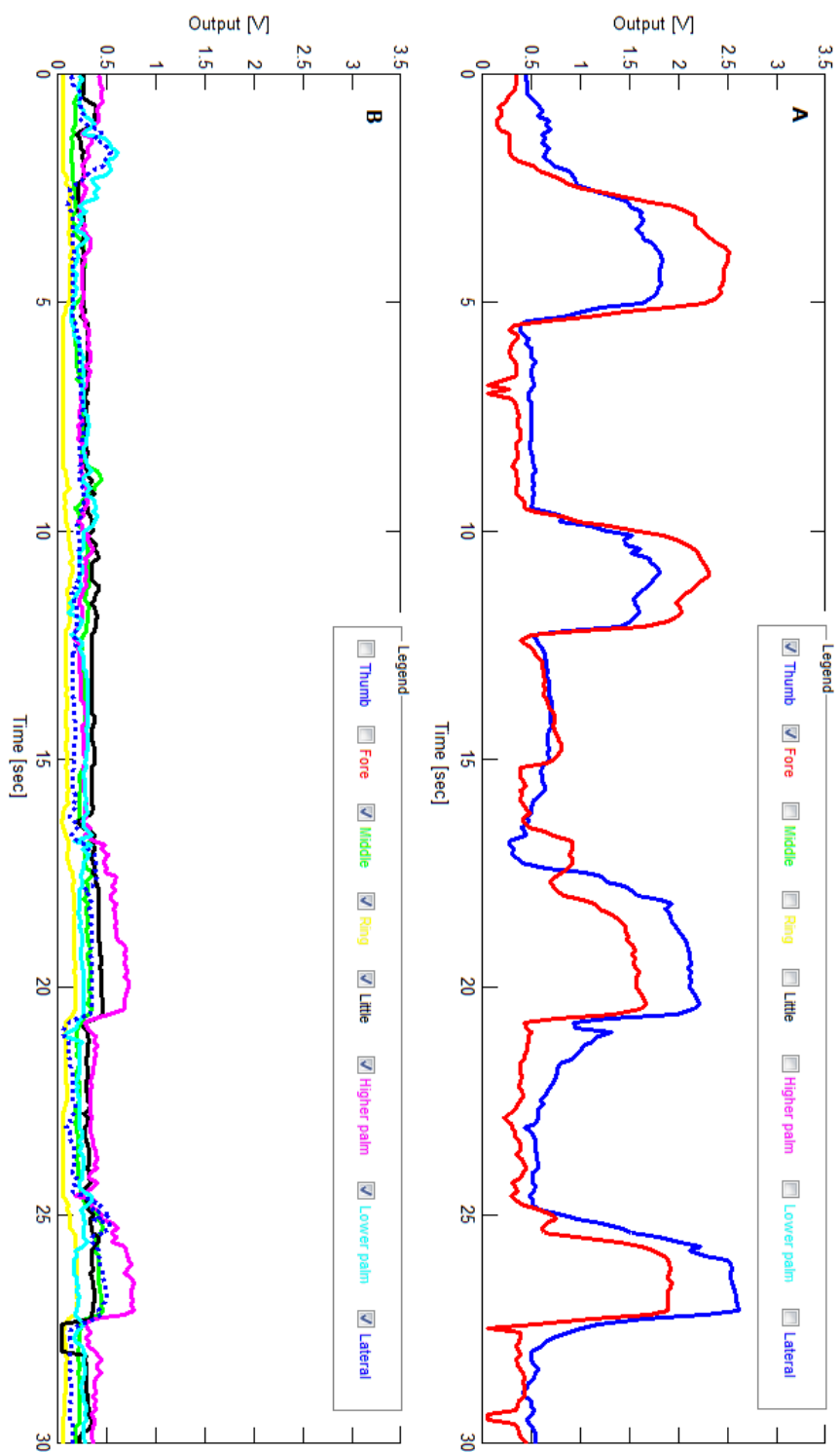
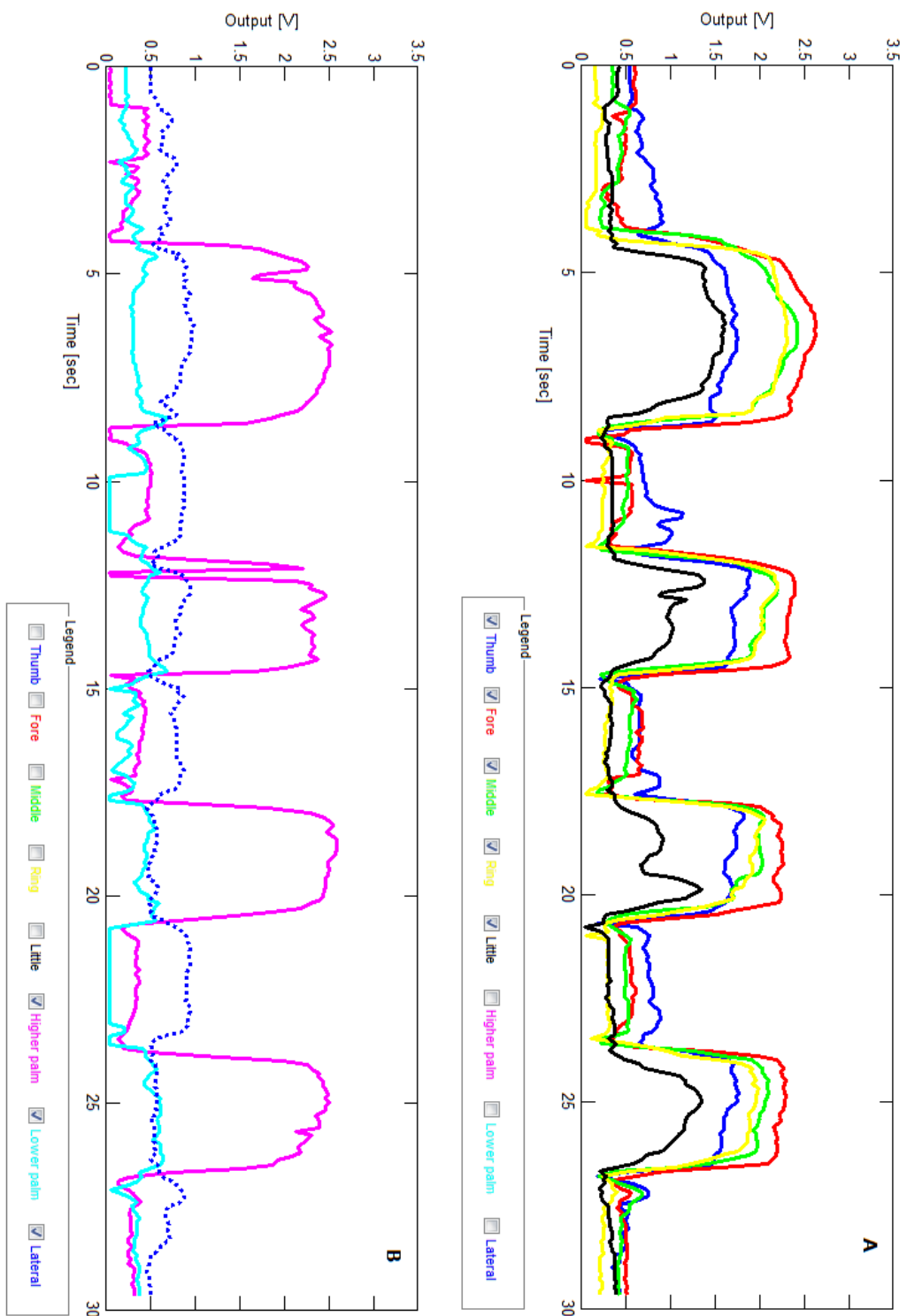
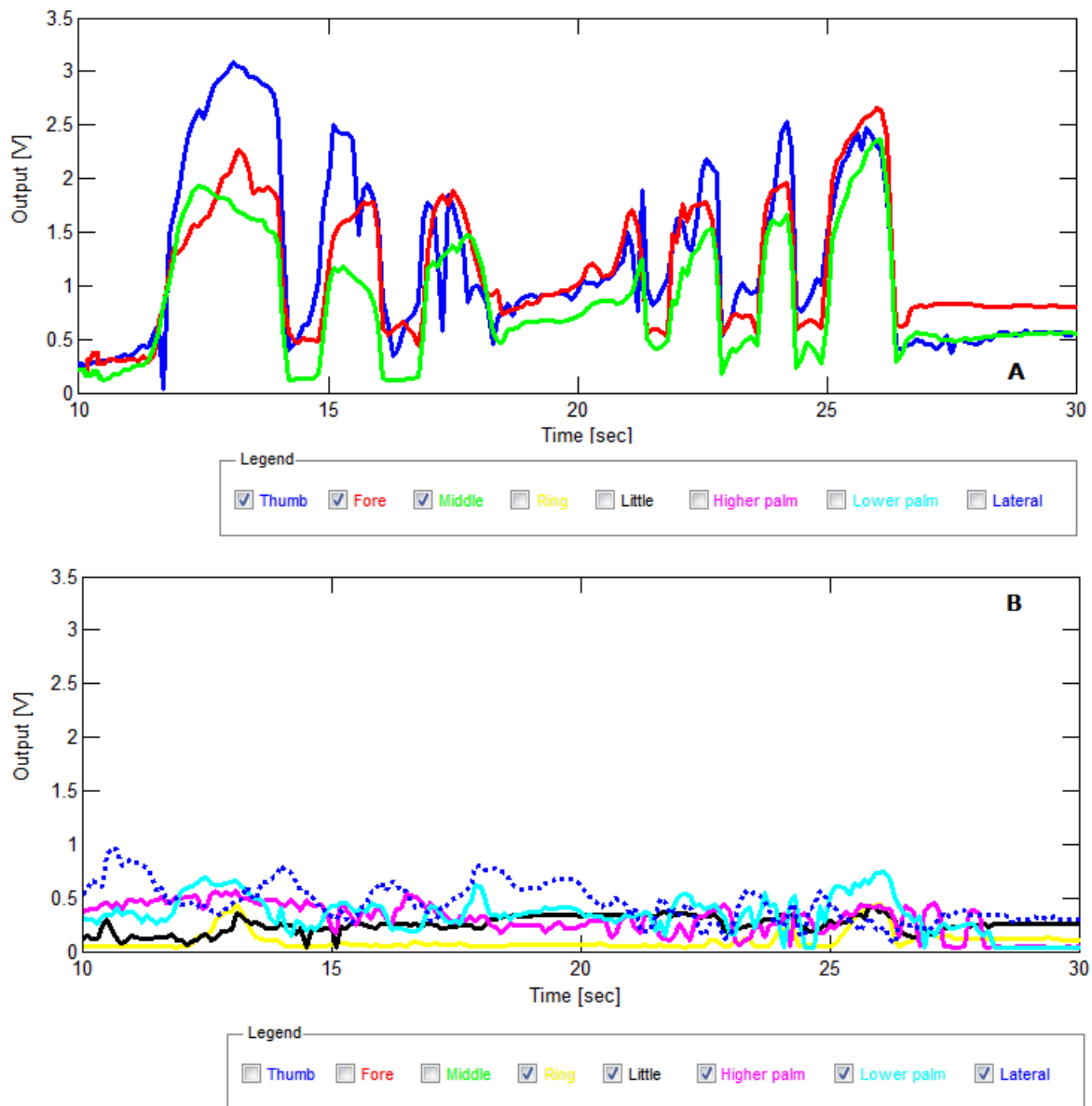


Figure 5.3 – Lateral pinch (see Figure 2.7) executed using the prototype.



**Figure 5.4** – Transverse grip type 1 (see Figure 2.7) executed using the prototype.



**Figure 5.5** – Tripod (or tridigit) grip (see Figure 2.7) executed using the prototype.

# Conclusions

In this Thesis the study and implementation of a transduction system for hand functional rehabilitation is described. The prototype is mainly constituted by a sensorized glove, a sensor driving circuitry and a visual feedback software interface. The prototype allows both to collect quantitative data and to analyze them, enabling an objective assessment of rehabilitative protocols effectiveness.

The system was developed by the *BioDevices Laboratory of the Department of Information Engineering of Padova University* in collaboration with *Wetware Concepts* (University of Padova spin off) and the equipe of severe spinal/brain injured of *San Bortolo hospital of Vicenza*.

A protocol for hand functional rehabilitation was studied and developed thanks to San Bortolo therapists' experience. An overview of hand strength and rehabilitation methods in Scientific Literature has been necessary to its definition, because of hand anatomical and functional complexity.

To identify principal hand contact areas the Sollerman standard for static grips was chosen. Sollerman grips were tested through trials based on Kamakura method, and carried out with normal and pathological hands.

At *BioDevices Laboratory* the technology to build the prototype was studied and tested with the support of *Wetware Concepts*. In detail, software interface has been implemented both to be a feedback for patient and to allow therapists comparative analysis. From the technological point of view, piezoresistive polymeric sensors have been investigated and customized to be integrated in glove structure and the related driving electronic circuits have been designed, implemented and calibrated. Finally the glove has been designed to fit various pathological hands.

Prototype application reported in the last Chapter of this Thesis shows tests carried out only on normal subject hands, that in some cases imitates wrong or pathological grips. Non-correct grips and imitated can be easily identified by data analysis. Moreover, prototype was tested for a dynamic grip which is

not considered in the actual implementation of the protocol. Even in this case prototype gives good results and confirmed its capabilities of tracking forces.

In conclusion the developed prototype proved to be a good candidate for clinical researches and trials.

### **Possible future developments**

In the functional rehabilitation field the prototype could help further investigations in finger strength, or could be flanked to other instrumentation such as electromyographs to give correlation between brain inputs and limb actuator. Moreover, the whole system could be used by therapists to improve rehabilitation methods, analysis and protocols, or by patient as a training feedback tool in remote assistance regimes.

On the other side, the prototype could be developed for sportive or musical applications, or even for brain-computer interfaces.

In final analysis the investigations on hand quantitative measurements could help a general enhancing in rehabilitation treatments, and a consequent enhance in stroke survivors quality of life.



# Appendix A

## System electronic interface schematics and boards

Here the complete electronic schematic of the printed circuit board (PCB) is reported. This has been designed to interact both with force sensors and with data acquisition system (DAQ).

APP. A SYSTEM ELECTRONIC INTERFACE SCHEMATICS AND BOARDS

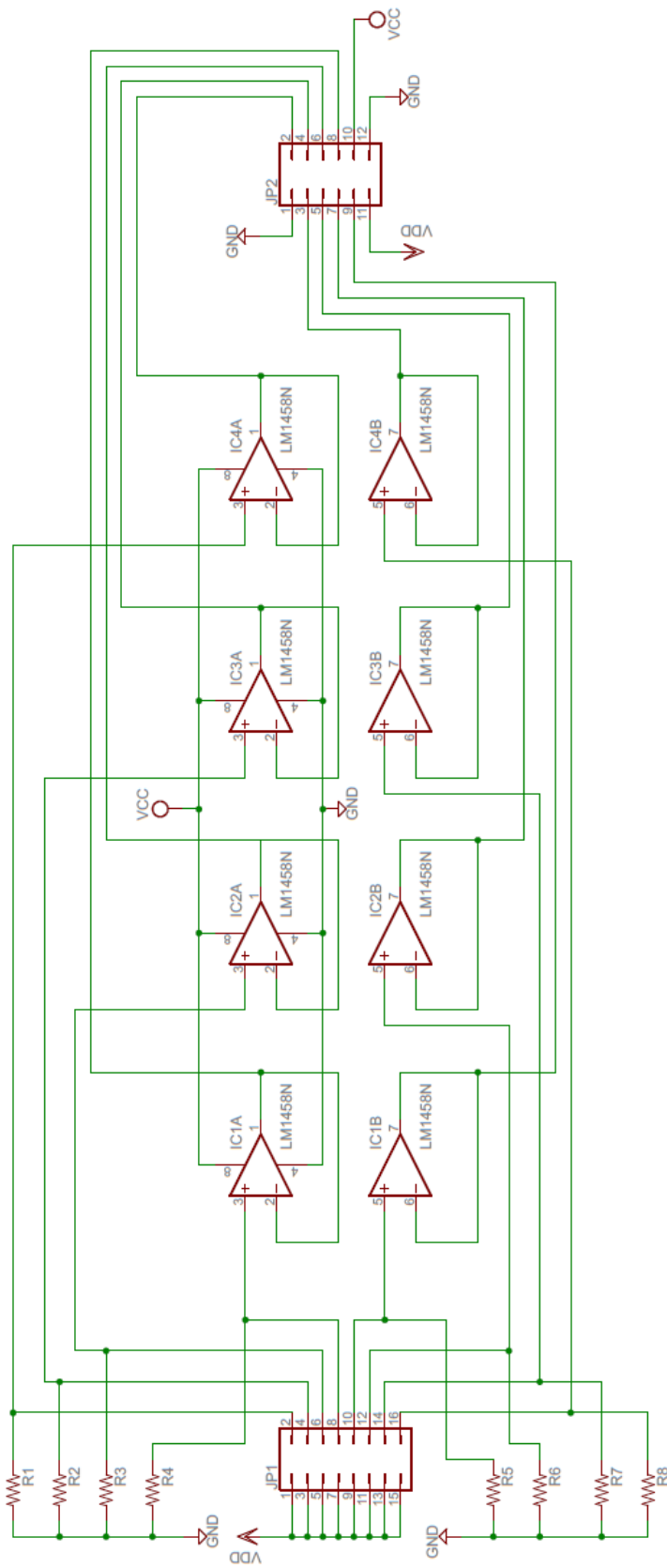


Figure A.1 – Electronic schematic.

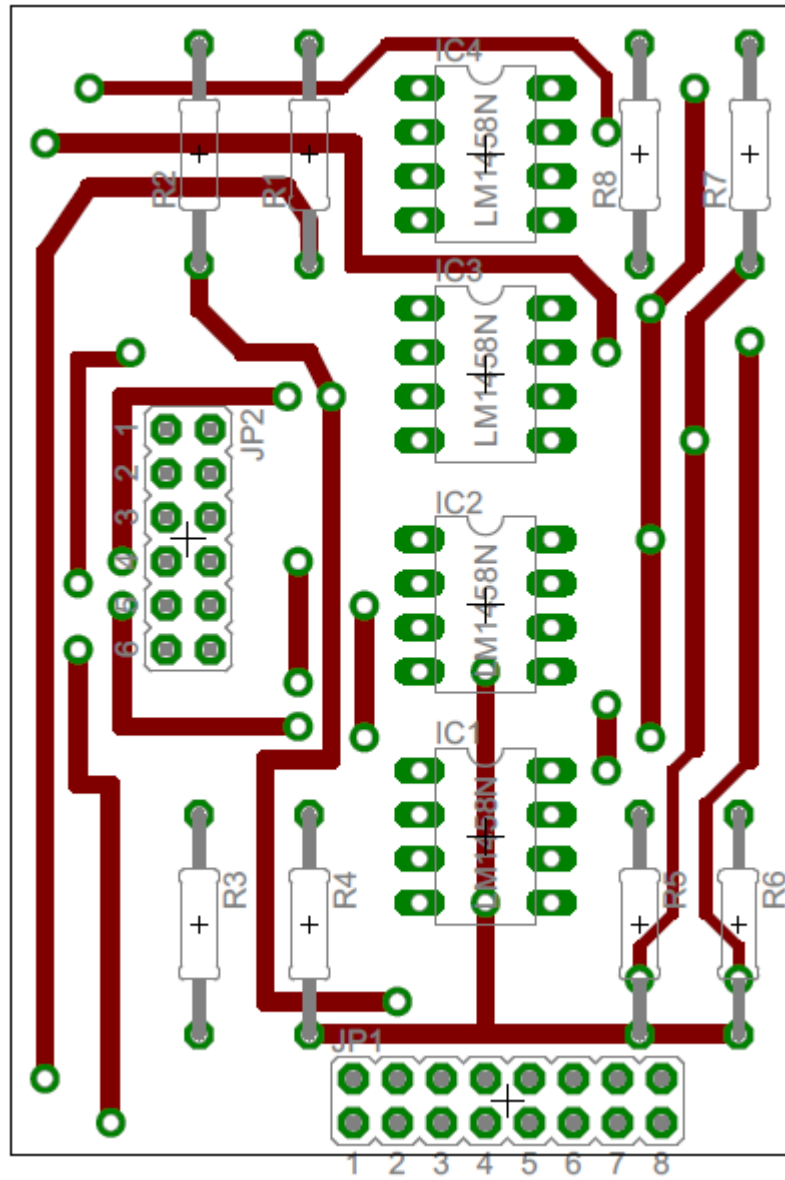


Figure A.2 – Board schematic top side.

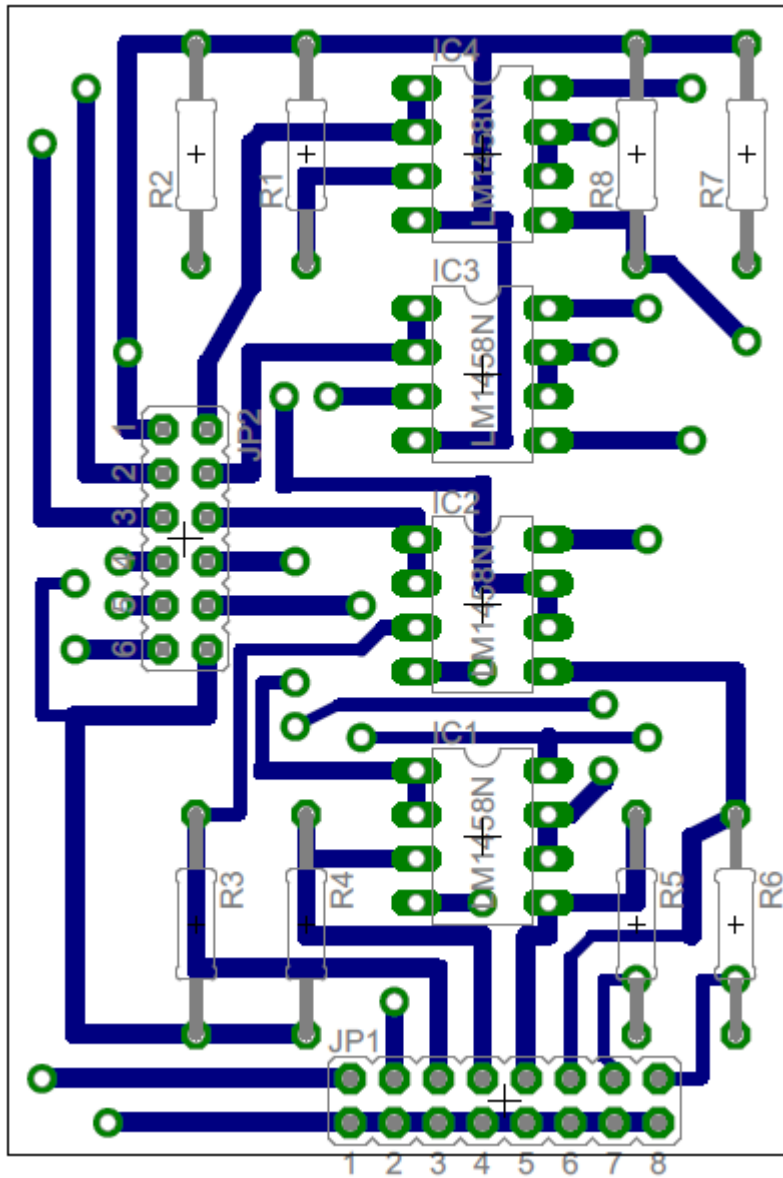


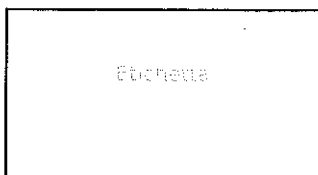
Figure A.3 – Board schematic bottom side.

## Appendix B

### Sollerman Table 84 (functional balance)

Here the Sollerman Table 84 (Functional Balance) provided by San Bortolo hospital equipe is reported. It codes all the functional grips analysed and considered for software implementation.

# TABELLA DI SOLLERMAN 84 (BILANCIO FUNZIONALE)



DATA ▶												
ESAMINATORE ▶												
LATO ▶	Dx	Sn	Dx	Sn	Dx	Sn	Dx	Sn	Dx	Sn	Dx	Sn
PRESA TRASVERSA ORIZZONTALE												
PRESA TRASVERSA VERTICALE 1												
PRESA TRASVERSA VERTICALE 2												
PRESA DIAGONALE												
PRESA A 5 DITA												
PRESA A TRE PUNTI												
PRESA A TRE DITA TRIDIGITALE (TRIPODE)												
PINZA LATERALE												
PINZA TRA POLLICE E INDICE												
<b>TOTALE</b>												

**Totale punteggi:**

- <13 severa menomazione
- 14-21 moderata menomazione
- >22 lieve menomazione

**LEGENDA**

0	Il compito non è stato svolto
1	Il compito è solo parzialmente eseguito
2	Il compito è completo, ma difficile o la presa non è come prescritto
3	Il compito è completa ma lento o la presa è un po' modificata
4	Il compito è completo e la presa è normale

# Appendix C

## Example of recorded data

The record file following is reported to present an example of data recorded. As can be seen it is organized in different sections and reports the complete execution of a transverse grip type 1. Illustrative pages reported are the first and the last of the exercise execution.

Date and time  
19-07-2012 - 15.31.37  
StartRealTimeData  
StartComments  
"Real Time" data  
[time[sec] sensor1-8[V]]  
EndComments  
StartPatientData  
Surname and Name: Antonio Dolfi;  
Notes: Good hand mobility;  
Grip Type: Transversal Grip;  
EndPatientData  
StartOptions  
Hand: Right;  
EndOptions  
StartData

0,000000 - 0,795398 - 0,041856 - 0,578022 - 0,041875 - 0,090346 - 0,230062 - 0,406274 - 0,254275;  
0,010000 - 0,795398 - 0,041856 - 0,588228 - 0,041875 - 0,090346 - 0,230062 - 0,406274 - 0,264464;  
0,020000 - 0,805585 - 0,041856 - 0,588228 - 0,041875 - 0,090346 - 0,219844 - 0,406274 - 0,264464;  
0,030000 - 0,805585 - 0,041856 - 0,588228 - 0,041875 - 0,090346 - 0,230062 - 0,406274 - 0,264464;  
0,040000 - 0,805585 - 0,041856 - 0,588228 - 0,041875 - 0,090346 - 0,219844 - 0,406274 - 0,264464;  
0,050000 - 0,795398 - 0,041856 - 0,588228 - 0,041875 - 0,090346 - 0,230062 - 0,406274 - 0,264464;  
0,060000 - 0,795398 - 0,041856 - 0,588228 - 0,041875 - 0,090346 - 0,230062 - 0,406274 - 0,264464;  
0,070000 - 0,795398 - 0,041856 - 0,588228 - 0,306746 - 0,090346 - 0,230062 - 0,406274 - 0,264464;  
0,080000 - 0,785210 - 0,041856 - 0,588228 - 0,316934 - 0,090346 - 0,230062 - 0,406274 - 0,264464;  
0,090000 - 0,775023 - 0,041856 - 0,588228 - 0,316934 - 0,090346 - 0,230062 - 0,406274 - 0,264464;  
0,100000 - 0,775023 - 0,041856 - 0,588228 - 0,316934 - 0,090346 - 0,230062 - 0,416460 - 0,264464;  
0,110000 - 0,785210 - 0,041856 - 0,588228 - 0,316934 - 0,090346 - 0,230062 - 0,406274 - 0,264464;  
0,120000 - 0,785210 - 0,041856 - 0,588228 - 0,316934 - 0,090346 - 0,230062 - 0,406274 - 0,264464;  
0,130000 - 0,785210 - 0,041856 - 0,588228 - 0,327121 - 0,090346 - 0,230062 - 0,406274 - 0,264464;  
0,140000 - 0,785210 - 0,041856 - 0,588228 - 0,327121 - 0,090346 - 0,230062 - 0,416460 - 0,264464;  
0,150000 - 0,785210 - 0,041856 - 0,588228 - 0,327121 - 0,090346 - 0,230062 - 0,416460 - 0,264464;  
0,160000 - 0,785210 - 0,041856 - 0,588228 - 0,327121 - 0,090346 - 0,230062 - 0,406274 - 0,264464;  
0,170000 - 0,785210 - 0,041856 - 0,588228 - 0,327121 - 0,090346 - 0,230062 - 0,406274 - 0,264464;  
0,180000 - 0,785210 - 0,041856 - 0,588228 - 0,327121 - 0,090346 - 0,230062 - 0,406274 - 0,264464;  
0,190000 - 0,785210 - 0,041856 - 0,588228 - 0,327121 - 0,090346 - 0,230062 - 0,416460 - 0,264464;  
0,200000 - 0,785210 - 0,041856 - 0,588228 - 0,327121 - 0,090346 - 0,230062 - 0,416460 - 0,264464;  
0,210000 - 0,785210 - 0,041856 - 0,588228 - 0,327121 - 0,090346 - 0,230062 - 0,416460 - 0,264464;  
0,220000 - 0,775023 - 0,041856 - 0,588228 - 0,327121 - 0,090346 - 0,230062 - 0,416460 - 0,264464;  
0,230000 - 0,785210 - 0,041856 - 0,588228 - 0,327121 - 0,090346 - 0,230062 - 0,416460 - 0,264464;  
0,240000 - 0,785210 - 0,041856 - 0,578022 - 0,327121 - 0,090346 - 0,230062 - 0,406274 - 0,264464;  
0,250000 - 0,785210 - 0,041856 - 0,588228 - 0,316934 - 0,090346 - 0,230062 - 0,396087 - 0,264464;  
0,260000 - 0,785210 - 0,041856 - 0,588228 - 0,306746 - 0,090346 - 0,230062 - 0,365526 - 0,264464;  
0,270000 - 0,795398 - 0,041856 - 0,588228 - 0,327121 - 0,090346 - 0,219844 - 0,324778 - 0,264464;  
0,280000 - 0,795398 - 0,041856 - 0,588228 - 0,337308 - 0,090346 - 0,219844 - 0,324778 - 0,264464;  
0,290000 - 0,795398 - 0,041856 - 0,588228 - 0,337308 - 0,090346 - 0,230062 - 0,345152 - 0,264464;  
0,300000 - 0,805585 - 0,041856 - 0,588228 - 0,337308 - 0,090346 - 0,219844 - 0,345152 - 0,264464;  
0,310000 - 0,805585 - 0,041856 - 0,588228 - 0,347496 - 0,090346 - 0,230062 - 0,355339 - 0,264464;  
0,320000 - 0,815772 - 0,041856 - 0,588228 - 0,347496 - 0,090346 - 0,230062 - 0,355339 - 0,264464;  
0,330000 - 0,815772 - 0,041856 - 0,578022 - 0,337308 - 0,090346 - 0,219844 - 0,365526 - 0,264464;  
0,340000 - 0,815772 - 0,041856 - 0,588228 - 0,337308 - 0,090346 - 0,219844 - 0,365526 - 0,264464;  
0,350000 - 0,805585 - 0,041856 - 0,588228 - 0,337308 - 0,090346 - 0,219844 - 0,365526 - 0,254275;  
0,360000 - 0,815772 - 0,041856 - 0,588228 - 0,337308 - 0,090346 - 0,219844 - 0,375713 - 0,264464;  
0,370000 - 0,815772 - 0,041856 - 0,588228 - 0,337308 - 0,090346 - 0,230062 - 0,375713 - 0,264464;  
0,380000 - 0,815772 - 0,041856 - 0,588228 - 0,041875 - 0,090346 - 0,219844 - 0,375713 - 0,264464;  
0,390000 - 0,815772 - 0,041856 - 0,588228 - 0,041875 - 0,090346 - 0,219844 - 0,375713 - 0,264464;  
0,400000 - 0,825960 - 0,041856 - 0,588228 - 0,041875 - 0,090346 - 0,219844 - 0,375713 - 0,264464;  
0,410000 - 0,836147 - 0,041856 - 0,588228 - 0,041875 - 0,090346 - 0,219844 - 0,385900 - 0,264464;  
0,420000 - 0,856522 - 0,041856 - 0,588228 - 0,041875 - 0,090346 - 0,219844 - 0,385900 - 0,254275;  
0,430000 - 0,856522 - 0,041856 - 0,588228 - 0,041875 - 0,090346 - 0,219844 - 0,396087 - 0,264464;  
0,440000 - 0,856522 - 0,041856 - 0,598433 - 0,041875 - 0,090346 - 0,219844 - 0,396087 - 0,254275;  
0,450000 - 0,856522 - 0,041856 - 0,588228 - 0,041875 - 0,090346 - 0,219844 - 0,396087 - 0,264464;  
0,460000 - 0,846335 - 0,041856 - 0,598433 - 0,041875 - 0,090346 - 0,219844 - 0,385900 - 0,254275;  
0,470000 - 0,856522 - 0,041856 - 0,588228 - 0,041875 - 0,100533 - 0,219844 - 0,385900 - 0,264464;  
0,480000 - 0,856522 - 0,041856 - 0,588228 - 0,041875 - 0,090346 - 0,219844 - 0,385900 - 0,254275;  
0,490000 - 0,856522 - 0,041856 - 0,588228 - 0,041875 - 0,090346 - 0,219844 - 0,385900 - 0,264464;  
0,500000 - 0,856522 - 0,041856 - 0,588228 - 0,041875 - 0,090346 - 0,219844 - 0,385900 - 0,264464;



5,480000 - 0,673149 - 0,500286 - 0,608638 - 0,041875 - 0,039412 - 0,270936 - 0,039542 - 0,101440;  
5,490000 - 0,683336 - 0,541035 - 0,578022 - 0,041875 - 0,039412 - 0,270936 - 0,039542 - 0,101440;  
5,500000 - 0,673149 - 0,541035 - 0,588228 - 0,041875 - 0,039412 - 0,270936 - 0,039542 - 0,101440;  
5,510000 - 0,693524 - 0,541035 - 0,588228 - 0,041875 - 0,039412 - 0,281154 - 0,039542 - 0,101440;  
5,520000 - 0,693524 - 0,520660 - 0,578022 - 0,041875 - 0,039412 - 0,281154 - 0,039542 - 0,101440;  
5,530000 - 0,662961 - 0,551222 - 0,588228 - 0,041875 - 0,039412 - 0,281154 - 0,039542 - 0,101440;  
5,540000 - 0,693524 - 0,530848 - 0,588228 - 0,041875 - 0,039412 - 0,281154 - 0,039542 - 0,101440;  
5,550000 - 0,713898 - 0,500286 - 0,588228 - 0,041875 - 0,039412 - 0,270936 - 0,039542 - 0,091251;  
5,560000 - 0,744461 - 0,561410 - 0,598433 - 0,041875 - 0,039412 - 0,270936 - 0,039542 - 0,101440;  
5,570000 - 0,713898 - 0,530848 - 0,598433 - 0,031688 - 0,039412 - 0,270936 - 0,039542 - 0,101440;  
5,580000 - 0,724086 - 0,571597 - 0,598433 - 0,041875 - 0,039412 - 0,270936 - 0,039542 - 0,091251;  
5,590000 - 0,724086 - 0,571597 - 0,598433 - 0,041875 - 0,039412 - 0,270936 - 0,039542 - 0,091251;  
5,600000 - 0,713898 - 0,500286 - 0,598433 - 0,041875 - 0,039412 - 0,270936 - 0,039542 - 0,101440;  
5,610000 - 0,744461 - 0,541035 - 0,598433 - 0,031688 - 0,039412 - 0,270936 - 0,039542 - 0,111629;  
5,620000 - 0,734273 - 0,469724 - 0,588228 - 0,041875 - 0,039412 - 0,270936 - 0,039542 - 0,111629;  
5,630000 - 0,744461 - 0,428974 - 0,588228 - 0,041875 - 0,039412 - 0,270936 - 0,039542 - 0,101440;  
5,640000 - 0,713898 - 0,469724 - 0,588228 - 0,041875 - 0,039412 - 0,270936 - 0,039542 - 0,111629;  
5,650000 - 0,703711 - 0,510473 - 0,588228 - 0,041875 - 0,039412 - 0,270936 - 0,039542 - 0,111629;  
5,660000 - 0,683336 - 0,520660 - 0,578022 - 0,041875 - 0,039412 - 0,270936 - 0,039542 - 0,101440;  
5,670000 - 0,693524 - 0,530848 - 0,578022 - 0,041875 - 0,039412 - 0,270936 - 0,039542 - 0,111629;  
5,680000 - 0,703711 - 0,530848 - 0,588228 - 0,031688 - 0,039412 - 0,270936 - 0,039542 - 0,111629;  
5,690000 - 0,693524 - 0,541035 - 0,588228 - 0,041875 - 0,039412 - 0,270936 - 0,039542 - 0,111629;  
5,700000 - 0,673149 - 0,551222 - 0,588228 - 0,041875 - 0,039412 - 0,270936 - 0,039542 - 0,101440;  
5,710000 - 0,683336 - 0,561410 - 0,588228 - 0,041875 - 0,039412 - 0,281154 - 0,039542 - 0,101440;

Maximum instants:

3,870000-3,330000-3,430000-2,950000-3,810000-4,220000-3,740000-1,630000;

Maximum values:

3,260746-3,006369-2,976283-1,171281-1,954695-2,568340-2,260172-2,794899;

EndData

EndRealTimeData



# Appendix D

## Sensors data sheets

Complete data sheets of the Interlink sensors are reported here following to provide further information.

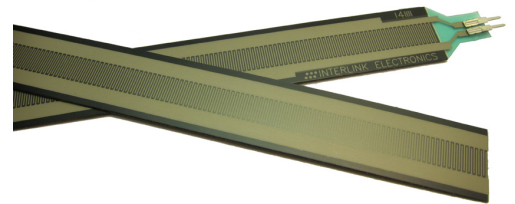
### Features and Benefits

- Actuation force as low as 0.1N and sensitivity range to 10N.
- Easily customizable to a wide range of sizes
- Highly Repeatable Force Reading; As low as 2% of initial reading with repeatable actuation system
- Cost effective
- Ultra thin; 0.40mm
- Robust; up to 10M actuations
- Simple and easy to integrate

### Description

Interlink Electronics FSR™ 400 series is part of the single zone Force Sensing Resistor™ family. Force Sensing Resistors, or FSRs, are robust polymer thick film (PTF) devices that exhibit a decrease in resistance with increase in force applied to the surface of the sensor. This force sensitivity is optimized for use in human touch control of electronic devices such as automotive electronics, medical systems, and in industrial and robotics applications.

The standard 408 sensor is a strip sensor 622.3mm in length and can be cut down to a very short length.



### Industry Segments

- Game controllers
- Musical instruments
- Medical device controls
- Remote controls
- Navigation Electronics
- Industrial HMI
- Automotive Panels
- Consumer Electronics

Figure 1 - Typical Force Curve

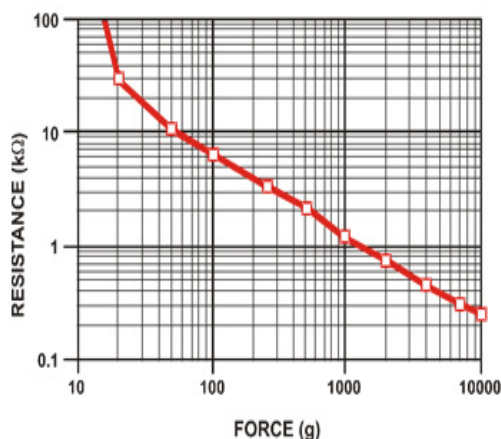
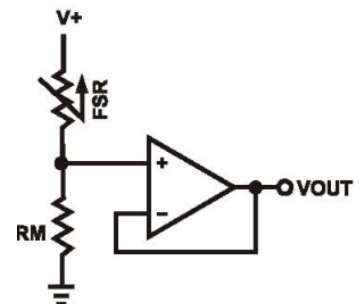


Figure 2 - Typical Schematic



Interlink Electronics - Sensor Technologies

## Applications

### Detect & qualify press

Sense whether a touch is accidental or intended by reading force

### Use force for UI feedback

Detect more or less user force to make a more intuitive interface

### Enhance tool safety

Differentiate a grip from a touch as a safety lock

### Find centroid of force

Use multiple sensors to determine centroid of force

### Detect presence, position, or motion

Of a person or patient in a bed, chair, or medical device

### Detect liquid blockage

Detect tube or pump occlusion or blockage by measuring back pressure

### Detect proper tube positioning

### Many other force measurement applications

## Device Characteristics

Feature	Condition	Value*	Notes
Actuation Force		0.1 Newtons	
Force Sensitivity Range		0.1 - 10.0 <sup>2</sup> Newtons	
Force Repeatability <sup>3</sup>	(Single part)	± 2%	
Force Resolution <sup>3</sup>		continuous	
Force Repeatability <sup>3</sup>	(Part to Part)	±6%	
Non-Actuated Resistance		10M W	
Size		622.3mm	
Thickness Range		0.2 - 1.25 mm	
Stand-Off Resistance		>10M ohms	Unloaded, unbent
Switch Travel	(Typical)	0.05 mm	Depends on design
Hysteresis <sup>3</sup>		+10%	$(R_{F+} - R_{F-})/R_{F+}$
Device Rise Time		<3 microseconds	measured w/steel ball
Long Term Drift		<5% per log <sub>10</sub> (time)	35 days test, 1kg load
Temp Operating Range	(Recommended)	-30 - +70 °C	
Number of Actuations	(Life time)	10 Million tested	Without failure

\* Specifications are derived from measurements taken at 1000 grams, and are given as one standard deviation / mean, unless otherwise noted.

1. Max Actuation force can be modified in custom sensors.
2. Force Range can be increased in custom sensors. Interlink Electronics have designed and manufactured sensors with operating force larger than 50Kg.
3. Force sensitivity dependent on mechanics, and resolution depends on measurement electronics.

## Contact Us

### United States Corporate Offices

Interlink Electronics, Inc.  
546 Flynn Road  
Camarillo, CA 93012, USA  
Phone: +1-805-484-8855  
Fax: +1-805-484-9457  
Web: www.  
interlinkelectronics.com  
Sales and support:  
fsr@interlinkelectronics.com

### Japan

Japan Sales Office  
Phone: +81-45-263-6500  
Fax: +81-45-263-6501  
Web: www.interlinkelec.co.jp

### Korea

Korea Sales Office  
Phone: +82 10 8776 1972

## Application Information

FSRs are two-wire devices with a resistance that depends on applied force.

For specific application needs please contact Interlink Electronics support team. An integration guide is also available.

For a simple force-to-voltage conversion, the FSR device is tied to a measuring resistor in a voltage divider configuration (see Figure 3). The output is described by the equation:

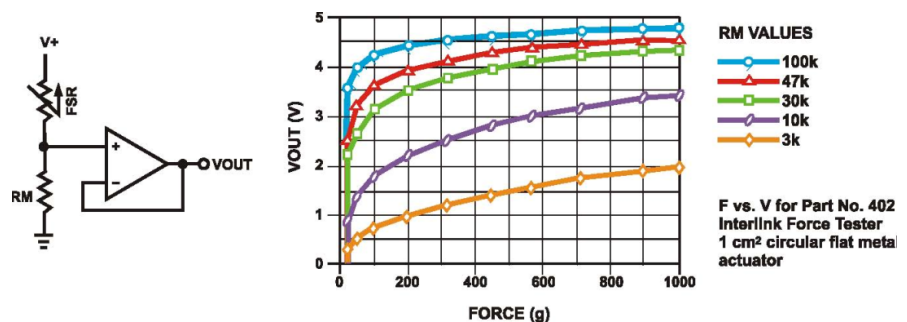
$$V_{OUT} = \frac{R_M V_+}{(R_M + R_{FSR})}$$

In the shown configuration, the output voltage increases with increasing force. If  $R_{FSR}$  and  $R_M$  are swapped, the output swing will decrease with increasing force.

The measuring resistor,  $R_M$ , is chosen to maximize the desired force sensitivity range and to limit current. Depending on the impedance requirements of the measuring circuit, the voltage divider could be followed by an op-amp.

A family of force vs.  $V_{OUT}$  curves is shown on the graph below for a standard FSR in a voltage divider configuration with various  $R_M$  resistors. A ( $V_+$ ) of +5V was used for these examples.

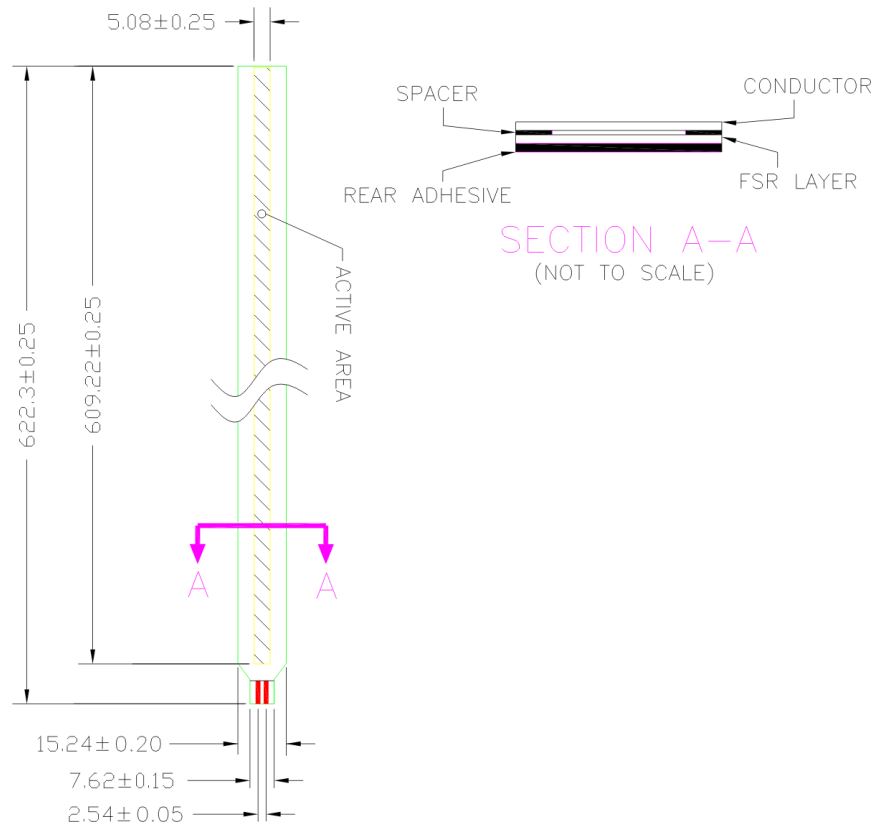
Figure 3



**Part No. 408**

- Active Area: 609.22 x 5.08mm
- Nominal thickness: 0.28 mm

**Mechanical Data**







# Appendix E

## Data acquisition device data sheets

Complete data sheets of the National Instrument data acquisition system (DAQ) are reported here following to provide further information.

Last Revised: 2012-05-07 11:16:06.0

## Low-Cost, Bus-Powered Multifunction DAQ for USB

### 12- or 14-Bit, Up to 48 kS/s, 8 Analog Inputs



- 8 analog inputs at 12 or 14 bits, up to 48 kS/s
- 2 analog outputs at 12 bits, software-timed
- 12 TTL/CMOS digital I/O lines
- One 32-bit, 5 MHz counter
- Digital triggering
- Bus-powered
- 1-year warranty

### Overview

With recent bandwidth improvements and new innovations from National Instruments, USB has evolved into a core bus of choice for measurement applications. The NI USB-6008 and USB-6009 are low-cost data acquisition (DAQ) devices with easy screw connectivity and a small form factor. With plug-and-play USB connectivity, these devices are simple enough for quick measurements but versatile enough for more complex measurement applications.

[Back to Top](#)

### Requirements and Compatibility

#### OS Information

- Windows 2000/XP
- Mac OS X
- Windows 7
- Windows CE
- Windows Mobile
- Windows Vista 64-bit
- Windows Vista 32-bit

#### Driver Information

- NI-DAQmx
- NI-DAQmx Base

#### Software Compatibility

- ANSI C/C++
- LabVIEW
- LabVIEW SignalExpress
- LabWindows/CVI
- Measurement Studio

[Back to Top](#)

### Comparison Tables

Product	Analog Inputs	Input Resolution	Max Sampling Rate (kS/s)	Analog Outputs	Output Resolution	Output Rate (Hz)	Digital I/O Lines	32-Bit Counter	Triggering
USB-6008	8 single-ended/4 differential	12	10	2	12	150	12	1	Digital
USB-6009	8 single-ended/4 differential	14	48	2	12	150	12	1	Digital

## Extended Warranty

NI offers options for extending the standard product warranty to meet the life-cycle requirements of your project. In addition, because NI understands that your requirements may change, the extended warranty is flexible in length and easily renewed. For more information, visit [ni.com/warranty](http://ni.com/warranty).

## OEM

NI offers design-in consulting and product integration assistance if you need NI products for OEM applications. For information about special pricing and services for OEM customers, visit [ni.com/oem](http://ni.com/oem).

## Alliance

Our Professional Services Team is comprised of NI applications engineers, NI Consulting Services, and a worldwide National Instruments Alliance Partner program of more than 600 independent consultants and integrators. Services range from start-up assistance to turnkey system integration. Visit [ni.com/alliance](http://ni.com/alliance).

[Back to Top](#)

## Detailed Specifications

The following specifications are typical at 25 °C, unless otherwise noted.

Analog Input	
Converter type	Successive approximation
Analog inputs	8 single-ended, 4 differential, software selectable
Input resolution	
NI USB-6008	12 bits differential, 11 bits single-ended
NI USB-6009	14 bits differential, 13 bits single-ended
Max sampling rate (aggregate) <sup>1</sup>	
NI USB-6008	10 kS/s
NI USB-6009	48 kS/s
AI FIFO	512 bytes
Timing resolution	41.67 ns (24 MHz timebase)
Timing accuracy	100 ppm of actual sample rate
Input range	
Single-ended	±10 V
Differential	±20 V <sup>2</sup> , ±10 V, ±5 V, ±4 V, ±2.5 V, ±2 V, ±1.25 V, ±1 V
Working voltage	±10 V
Input impedance	144 kΩ
Overvoltage protection	±35
Trigger source	Software or external digital trigger
System noise <sup>3</sup>	
Single-ended	
±10 V range	5 mVrms
Differential	
±20 V range	5 mVrms
±1 V range	0.5 mVrms

Absolute accuracy at full scale, single-ended		
Range	Typical at 25 °C (mV)	Maximum over Temperature (mV)
±10	14.7	138

Absolute accuracy at full scale, differential <sup>4</sup>		
Range	Typical at 25 °C (mV)	Maximum over Temperature (mV)

Absolute accuracy at full scale, differential <sup>4</sup>		
Range	Typical at 25 °C (mV)	Maximum over Temperature (mV)
±20	14.7	138
±10	7.73	84.8
±5	4.28	58.4
±4	3.59	53.1
±2.5	2.56	45.1
±2	2.21	42.5
±1.25	1.70	38.9
±1	1.53	37.5

## Analog Output

Analog outputs	2
Output resolution	12 bits
Maximum update rate	150 Hz, software-timed
Output range	0 to +5 V
Output impedance	50 Ω
Output current drive	5 mA
Power-on state	0 V
Slew rate	1 V/μs
Short circuit current	50 mA
Absolute accuracy (no load)	7 mV typical, 36.4 mV maximum at full scale

## Digital I/O

Digital I/O	
P0.<0..7>	8 lines
P1.<0..3>	4 lines
Direction control	Each channel individually programmable as input or output
Output driver type	
NI USB-6008	Open collector (open-drain)
NI USB-6009	Each channel individually programmable as active drive (push-pull) or open collector (open-drain)
Compatibility	TTL, LVTTTL, CMOS
Absolute maximum voltage range	-0.5 to 5.8 V with respect to GND
Pull-up resistor	4.7 kΩ to 5 V
Power-on state	Input

Digital logic levels			
Level	Min	Max	Units
Input low voltage	-0.3	0.8	V
Input high voltage	2.0	5.8	V
Input leakage current	—	50	μA
Output low voltage (I = 8.5 mA)	—	0.8	V
Output high voltage			
Active drive (push-pull), I = -8.5 mA	2.0	3.5	V
Open collector (open-drain), I = -0.6 mA, nominal	2.0	5.0	V
Open collector (open-drain), I = -8.5 mA, with external pull-up resistor	2.0	—	V

## External Voltage

+5 V output (200 mA maximum)	+5 V typical, +4.85 V minimum
+2.5 V output (1 mA maximum)	+2.5 V typical
+2.5 V accuracy	0.25% max
Reference temperature drift	50 ppm/°C max

## Counter

Number of counters	1
Resolution	32 bits
Counter measurements	Edge counting (falling-edge)
Counter direction	Count up
Pull-up resistor	4.7 kΩ to 5 V
Maximum input frequency	5 MHz
Minimum high pulse width	100 ns
Minimum low pulse width	100 ns
Input high voltage	2.0 V
Input low voltage	0.8 V

## Power Requirements

### USB

4.10 to 5.25 VDC	80 mA typical, 500 mA max
USB suspend	300 μA typical, 500 μA max

## Physical Characteristics

### Dimensions

Without connectors	6.35 cm × 8.51 cm × 2.31 cm (2.50 in. × 3.35 in. × 0.91 in.)
With connectors	8.18 cm × 8.51 cm × 2.31 cm (3.22 in. × 3.35 in. × 0.91 in.)
I/O connectors	USB series B receptacle, (2) 16 position terminal block plug headers
Weight	
With connectors	84 g (3 oz)
Without connectors	54 g (1.9 oz)
Screw-terminal wiring	16 to 28 AWG
Torque for screw terminals	0.22–0.25 N · m (2.0–2.2 lb · in.)

## Safety

If you need to clean the module, wipe it with a dry towel.

### Safety Voltages

Connect only voltages that are within these limits.

Channel-to-GND	±30 V max, Measurement Category I
----------------	-----------------------------------

Measurement Category I is for measurements performed on circuits not directly connected to the electrical distribution system referred to as MAINS voltage. MAINS is a hazardous live electrical supply system that powers equipment. This category is for measurements of voltages from specially protected secondary circuits. Such voltage measurements include signal levels, special equipment, limited-energy parts of equipment, circuits powered by regulated low-voltage sources, and electronics.



**Caution** Do not use this module for connection to signals or for measurements within Measurement Categories II, III, or IV.

### Safety Standards

This product is designed to meet the requirements of the following standards of safety for electrical equipment for measurement, control, and laboratory use:

- IEC 61010-1, EN 61010-1
- UL 61010-1, CSA 61010-1

**Note** For UL and other safety certifications, refer to the product label or visit [ni.com/certification](https://www.ni.com/certification), search by model number or product line, and click the appropriate link in

the Certification column.

### Hazardous Locations

The NI USB-6008/6009 device is not certified for use in hazardous locations.

### Environmental

The NI USB-6008/6009 device is intended for indoor use only.

Operating temperature

(IEC 60068-2-1 and IEC 60068-2-2) 0 to 55 °C

Operating humidity

(IEC 60068-2-56) 5 to 95% RH, noncondensing

Maximum altitude

2,000 m (at 25 °C ambient temperature)

Storage temperature

(IEC 60068-2-1 and IEC 60068-2-2) -40 to 85 °C

Storage humidity

(IEC 60068-2-56) 5 to 90% RH, noncondensing

Pollution Degree (IEC 60664)

2

### Electromagnetic Compatibility

This product is designed to meet the requirements of the following standards of EMC for electrical equipment for measurement, control, and laboratory use:

- EN 61326 EMC requirements; Minimum Immunity
- EN 55011 Emissions; Group 1, Class A
- CE, C-Tick, ICES, and FCC Part 15 Emissions; Class A



**Note** For EMC compliance, operate this device with double-shielded cables.

### CE Compliance

This product meets the essential requirements of applicable European Directives, as amended for CE marking, as follows:

- 2006/95/EC; Low-Voltage Directive (safety)
- 2004/108/EC; Electromagnetic Compatibility Directive (EMC)



**Note** Refer to the Declaration of Conformity (DoC) for this product for any additional regulatory compliance information. To obtain the DoC for this product, visit [ni.com/certification](http://ni.com/certification), search by module number or product line, and click the appropriate link in the Certification column.

### Environmental Management

National Instruments is committed to designing and manufacturing products in an environmentally responsible manner. NI recognizes that eliminating certain hazardous substances from our products is beneficial not only to the environment but also to NI customers.

For additional environmental information, refer to the *NI and the Environment* Web page at [ni.com/environment](http://ni.com/environment). This page contains the environmental regulations and directives with which NI complies, as well as other environmental information not included in this document.

### Waste Electrical and Electronic Equipment (WEEE)



**EU Customers** At the end of their life cycle, all products *must* be sent to a WEEE recycling center. For more information about WEEE recycling centers and National Instruments WEEE initiatives, visit [ni.com/environment/weee.htm](http://ni.com/environment/weee.htm).

### 电子信息产品污染控制管理办法（中国 RoHS）



**中国客户** National Instruments 符合中国电子信息产品中限制使用某些有害物质指令 (RoHS)。  
关于 National Instruments 中国 RoHS 合规性信息, 请登录 [ni.com/environment/rohs\\_china](http://ni.com/environment/rohs_china)。  
(For information about China RoHS compliance, go to [ni.com/environment/rohs\\_china](http://ni.com/environment/rohs_china).)

<sup>1</sup> System dependent.

<sup>2</sup> ±20 V means that |AI+ - (AI-)| ≥ 20 V. However, AI+ and AI- must both be within ±10 V of GND.

<sup>3</sup> System noise measured at maximum sample rate.

<sup>4</sup> Input voltages may not exceed the working voltage range.

[Back to Top](#)

---

In addition the following block diagram (in figure E.1) shows key functional components of the NI USB-6008 DAQ.

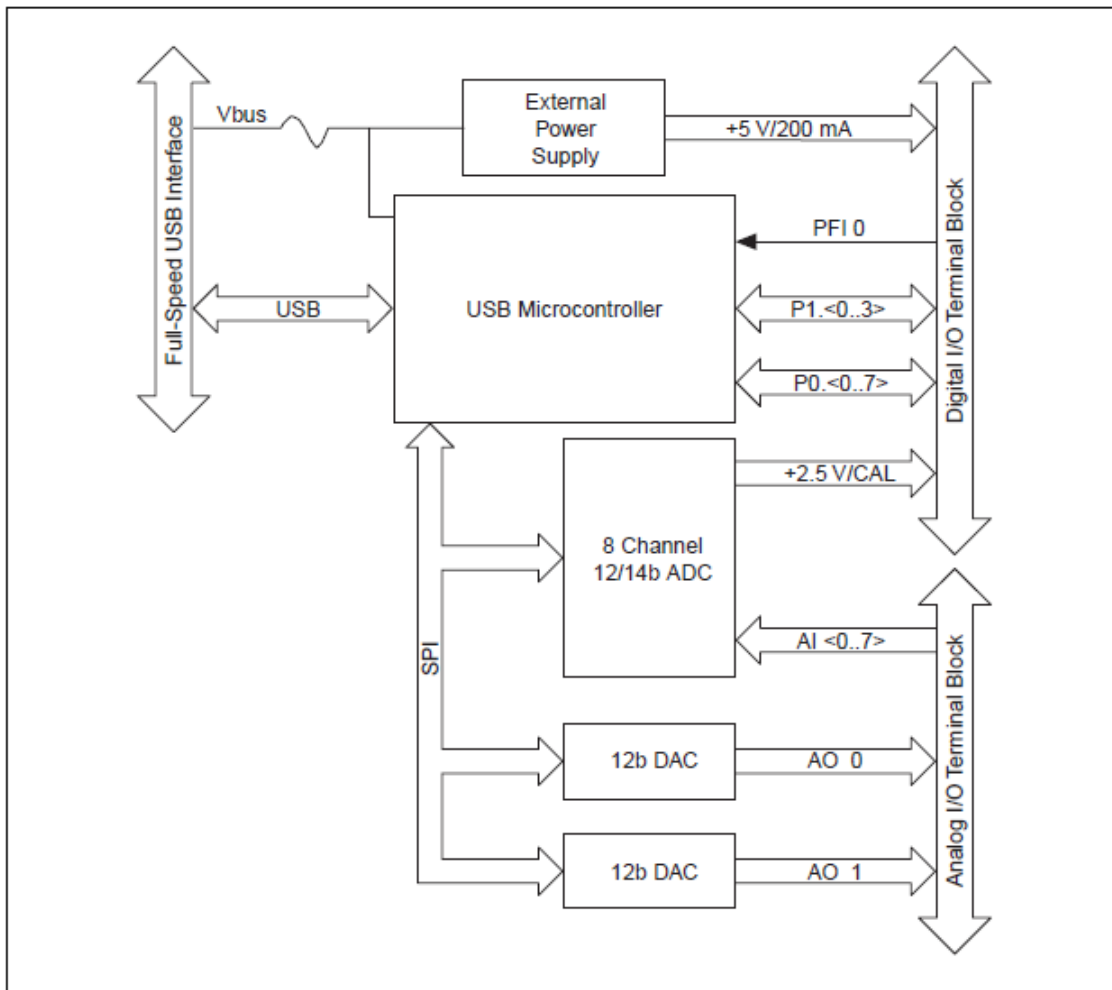


Figure E.1 – NI USB-6008 Block Diagram.



# Appendix F

## Dual operational amplifier data sheets

Complete data sheets of the dual operational amplifier LM258 (Texas Instruments) are reported here following to provide further information.

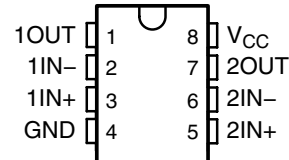
# LM158, LM158A, LM258, LM258A LM358, LM358A, LM2904, LM2904V DUAL OPERATIONAL AMPLIFIERS

SLOS068R – JUNE 1976 – REVISED JULY 2010

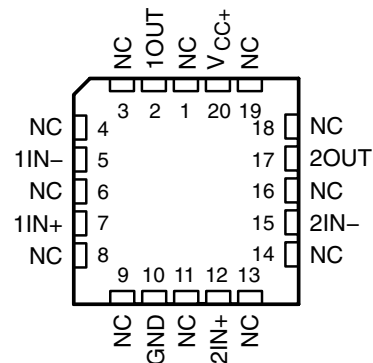
- **Wide Supply Range:**
  - Single Supply . . . 3 V to 32 V  
(26 V for LM2904)
  - or Dual Supplies . . .  $\pm 1.5$  V to  $\pm 16$  V  
( $\pm 13$  V for LM2904)
- **Low Supply-Current Drain, Independent of Supply Voltage . . . 0.7 mA Typ**
- **Common-Mode Input Voltage Range Includes Ground, Allowing Direct Sensing Near Ground**
- **Low Input Bias and Offset Parameters:**
  - Input Offset Voltage . . . 3 mV Typ  
A Versions . . . 2 mV Typ
  - Input Offset Current . . . 2 nA Typ
  - Input Bias Current . . . 20 nA Typ  
A Versions . . . 15 nA Typ
- **Differential Input Voltage Range Equal to Maximum-Rated Supply Voltage . . . 32 V  
(26 V for LM2904)**
- **Open-Loop Differential Voltage Amplification . . . 100 V/mV Typ**
- **Internal Frequency Compensation**

LM158, LM158A . . . JG PACKAGE  
LM258, LM258A . . . D, DGK, OR P PACKAGE  
LM358 . . . D, DGK, P, PS, OR PW PACKAGE  
LM358A . . . D, DGK, P, OR PW PACKAGE  
LM2904 . . . D, DGK, P, PS, OR PW PACKAGE

(TOP VIEW)



LM158, LM158A . . . FK PACKAGE  
(TOP VIEW)



NC – No internal connection

## description/ordering information

These devices consist of two independent, high-gain frequency-compensated operational amplifiers designed to operate from a single supply over a wide range of voltages. Operation from split supplies also is possible if the difference between the two supplies is 3 V to 32 V (3 V to 26 V for the LM2904), and  $V_{CC}$  is at least 1.5 V more positive than the input common-mode voltage. The low supply-current drain is independent of the magnitude of the supply voltage.

Applications include transducer amplifiers, dc amplification blocks, and all the conventional operational amplifier circuits that now can be implemented more easily in single-supply-voltage systems. For example, these devices can be operated directly from the standard 5-V supply used in digital systems and easily can provide the required interface electronics without additional  $\pm 5$ -V supplies.



Please be aware that an important notice concerning availability, standard warranty, and use in critical applications of Texas Instruments semiconductor products and disclaimers thereto appears at the end of this data sheet.

PRODUCTION DATA information is current as of publication date. Products conform to specifications per the terms of Texas Instruments standard warranty. Production processing does not necessarily include testing of all parameters.

**TEXAS  
INSTRUMENTS**

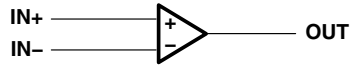
POST OFFICE BOX 655303 • DALLAS, TEXAS 75265

Copyright © 2010, Texas Instruments Incorporated  
On products compliant to MIL-PRF-38535, all parameters are tested unless otherwise noted. On all other products, production processing does not necessarily include testing of all parameters.

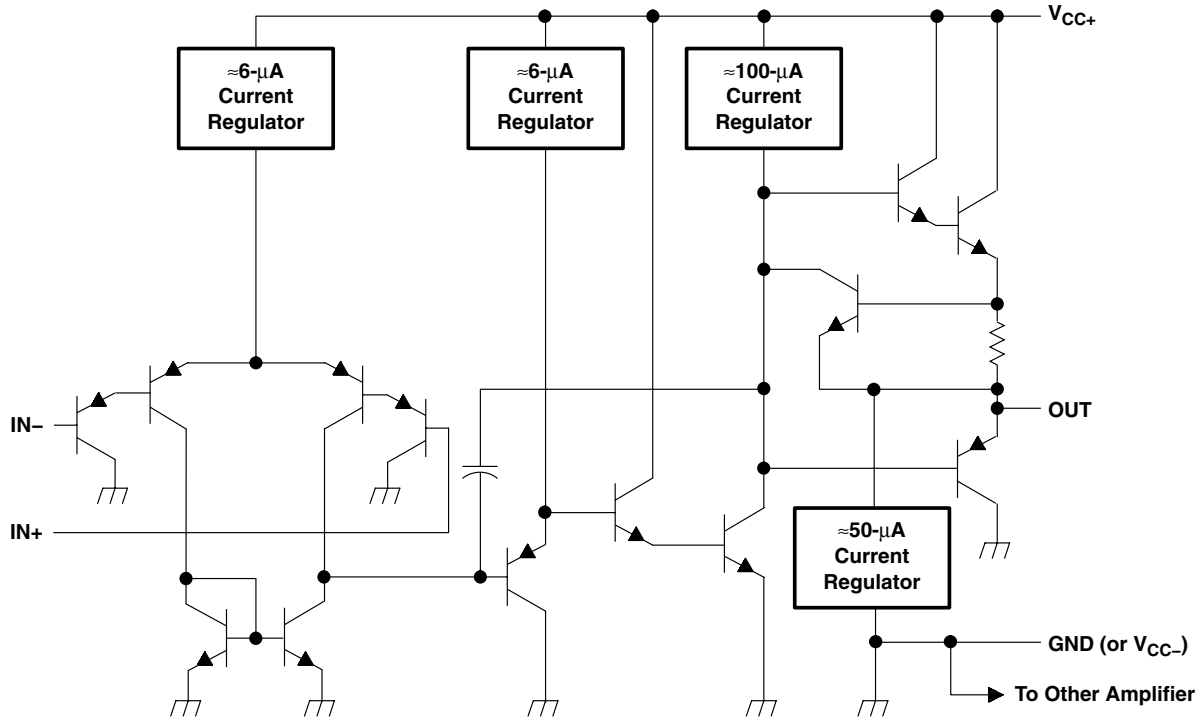
**LM158, LM158A, LM258, LM258A  
LM358, LM358A, LM2904, LM2904V  
DUAL OPERATIONAL AMPLIFIERS**

SLOS068R – JUNE 1976 – REVISED JULY 2010

**symbol (each amplifier)**



**schematic (each amplifier)**



COMPONENT COUNT	
Epi-FET	1
Diodes	2
Resistors	7
Transistors	51
Capacitors	2

# LM158, LM158A, LM258, LM258A LM358, LM358A, LM2904, LM2904V DUAL OPERATIONAL AMPLIFIERS

SLOS068R – JUNE 1976 – REVISED JULY 2010

## absolute maximum ratings over operating free-air temperature range (unless otherwise noted)<sup>†</sup>

		LM158, LM158A LM258, LM258A LM358, LM358A LM2904V	LM2904	UNIT
Supply voltage, $V_{CC}$ (see Note 1)		±16 or 32	±13 or 26	V
Differential input voltage, $V_{ID}$ (see Note 2)		±32	±26	V
Input voltage, $V_I$ (either input)		-0.3 to 32	-0.3 to 26	V
Duration of output short circuit (one amplifier) to ground at (or below) 25°C free-air temperature ( $V_{CC} \leq 15$ V) (see Note 3)		Unlimited	Unlimited	
Package thermal impedance, $\theta_{JA}$ (see Notes 4 and 5)	D package	97	97	°C/W
	DGK package	172	172	
	P package	85	85	
	PS package	95	95	
	PW package	149	149	
Package thermal impedance, $\theta_{JC}$ (see Notes 6 and 7)	FK package	5.61		°C/W
	JG package	14.5		
Operating free-air temperature range, $T_A$	LM158, LM158A	-55 to 125		°C
	LM258, LM258A	-25 to 85		
	LM358, LM358A	0 to 70		
	LM2904	-40 to 125	-40 to 125	
Operating virtual junction temperature, $T_J$		150	150	°C
Case temperature for 60 seconds	FK package	260		°C
Lead temperature 1,6 mm (1/16 inch) from case for 60 seconds	JG package	300	300	°C
Storage temperature range, $T_{stg}$		-65 to 150	-65 to 150	°C

<sup>†</sup> Stresses beyond those listed under “absolute maximum ratings” may cause permanent damage to the device. These are stress ratings only, and functional operation of the device at these or any other conditions beyond those indicated under “recommended operating conditions” is not implied. Exposure to absolute-maximum-rated conditions for extended periods may affect device reliability.

- NOTES:
- All voltage values, except differential voltages and  $V_{CC}$  specified for measurement of  $I_{OS}$ , are with respect to the network ground terminal.
  - Differential voltages are at  $IN+$  with respect to  $IN-$ .
  - Short circuits from outputs to  $V_{CC}$  can cause excessive heating and eventual destruction.
  - Maximum power dissipation is a function of  $T_J(\max)$ ,  $\theta_{JA}$ , and  $T_A$ . The maximum allowable power dissipation at any allowable ambient temperature is  $P_D = (T_J(\max) - T_A)/\theta_{JA}$ . Operating at the absolute maximum  $T_J$  of 150°C can affect reliability.
  - The package thermal impedance is calculated in accordance with JESD 51-7.
  - Maximum power dissipation is a function of  $T_J(\max)$ ,  $\theta_{JC}$ , and  $T_C$ . The maximum allowable power dissipation at any allowable case temperature is  $P_D = (T_J(\max) - T_C)/\theta_{JC}$ . Operating at the absolute maximum  $T_J$  of 150°C can affect reliability.
  - The package thermal impedance is calculated in accordance with MIL-STD-883.



**LM158, LM158A, LM258, LM258A  
LM358, LM358A, LM2904, LM2904V  
DUAL OPERATIONAL AMPLIFIERS**

SLOS068R – JUNE 1976 – REVISED JULY 2010

**electrical characteristics at specified free-air temperature,  $V_{CC} = 5\text{ V}$  (unless otherwise noted)**

PARAMETER	TEST CONDITIONS†	$T_A$ ‡	LM158 LM258			LM358			UNIT	
			MIN	TYP§	MAX	MIN	TYP§	MAX		
$V_{IO}$ Input offset voltage	$V_{CC} = 5\text{ V to MAX}$ , $V_{IC} = V_{ICR(min)}$ , $V_O = 1.4\text{ V}$	25°C		3	5		3	7	mV	
		Full range			7			9		
$\alpha_{V_{IO}}$ Average temperature coefficient of input offset voltage		Full range		7			7	$\mu\text{V}/^\circ\text{C}$		
$I_{IO}$ Input offset current	$V_O = 1.4\text{ V}$	25°C		2	30		2	50	nA	
		Full range			100			150		
$\alpha_{I_{IO}}$ Average temperature coefficient of input offset current		Full range		10			10	$\text{pA}/^\circ\text{C}$		
$I_{IB}$ Input bias current	$V_O = 1.4\text{ V}$	25°C		-20	-150		-20	-250	nA	
		Full range			-300			-500		
$V_{ICR}$ Common-mode input voltage range	$V_{CC} = 5\text{ V to MAX}$	25°C		0 to $V_{CC} - 1.5$			0 to $V_{CC} - 1.5$	V		
		Full range		0 to $V_{CC} - 2$			0 to $V_{CC} - 2$			
$V_{OH}$ High-level output voltage	$R_L \geq 2\text{ k}\Omega$	25°C		$V_{CC} - 1.5$			$V_{CC} - 1.5$		V	
		25°C								
	$V_{CC} = \text{MAX}$	$R_L = 2\text{ k}\Omega$	Full range		26		26			
		$R_L \geq 10\text{ k}\Omega$	Full range		27	28	27	28		
$V_{OL}$ Low-level output voltage	$R_L \leq 10\text{ k}\Omega$	Full range		5	20		5	20	mV	
$A_{VD}$ Large-signal differential voltage amplification	$V_{CC} = 15\text{ V}$ , $V_O = 1\text{ V to }11\text{ V}$ , $R_L \geq 2\text{ k}\Omega$	25°C		50	100		25	100	V/mV	
		Full range		25			15			
CMRR Common-mode rejection ratio	$V_{CC} = 5\text{ V to MAX}$ , $V_{IC} = V_{ICR(min)}$	25°C		70	80		65	80	dB	
$k_{SVR}$ Supply-voltage rejection ratio ( $\Delta V_{DD}/\Delta V_{IO}$ )	$V_{CC} = 5\text{ V to MAX}$	25°C		65	100		65	100	dB	
$V_{O1}/V_{O2}$ Crosstalk attenuation	$f = 1\text{ kHz to }20\text{ kHz}$	25°C		120			120		dB	
$I_O$ Output current	$V_{CC} = 15\text{ V}$ , $V_{ID} = 1\text{ V}$ , $V_O = 0$	Source	25°C		-20	-30		-20	-30	mA
			Full range			-10		-10		
	Sink	25°C		10	20		10	20		
		Full range		5			5			
$I_O$ Output current	$V_{ID} = -1\text{ V}$ , $V_O = 200\text{ mV}$	25°C		12	30		12	30	$\mu\text{A}$	
$I_{OS}$ Short-circuit output current	$V_{CC}$ at 5 V, GND at -5 V, $V_O = 0$	25°C		$\pm 40$	$\pm 60$		$\pm 40$	$\pm 60$	mA	
$I_{CC}$ Supply current (two amplifiers)	$V_O = 2.5\text{ V}$ , No load	Full range		0.7	1.2		0.7	1.2	mA	
	$V_{CC} = \text{MAX}$ , $V_O = 0.5\text{ V}$ , No load	Full range		1	2		1	2		

† All characteristics are measured under open-loop conditions, with zero common-mode input voltage, unless otherwise specified. MAX  $V_{CC}$  for testing purposes is 26 V for the LM2904 and 30 V for others.

‡ Full range is  $-55^\circ\text{C}$  to  $125^\circ\text{C}$  for LM158,  $-25^\circ\text{C}$  to  $85^\circ\text{C}$  for LM258,  $0^\circ\text{C}$  to  $70^\circ\text{C}$  for LM358, and  $-40^\circ\text{C}$  to  $125^\circ\text{C}$  for LM2904.

§ All typical values are at  $T_A = 25^\circ\text{C}$ .



**LM158, LM158A, LM258, LM258A**  
**LM358, LM358A, LM2904, LM2904V**  
**DUAL OPERATIONAL AMPLIFIERS**  
 SLOS068R – JUNE 1976 – REVISED JULY 2010

**electrical characteristics at specified free-air temperature,  $V_{CC} = 5\text{ V}$  (unless otherwise noted)**

PARAMETER	TEST CONDITIONS†		$T_A$ ‡	LM2904			UNIT
				MIN	TYP§	MAX	
$V_{IO}$ Input offset voltage	$V_{CC} = 5\text{ V to MAX}$ , $V_{IC} = V_{ICR(min)}$ , $V_O = 1.4\text{ V}$	Non-A devices	25°C	3	7	mV	
			Full range	10			
		A-suffix devices	25°C	1	2		
			Full range	4			
$\alpha_{V_{IO}}$ Average temperature coefficient of input offset voltage		Full range	7		$\mu\text{V}/^\circ\text{C}$		
$I_{IO}$ Input offset current	$V_O = 1.4\text{ V}$	Non-V device	25°C	2	50	nA	
			Full range	300			
		V-suffix device	25°C	2	50		
			Full range	150			
$\alpha_{I_{IO}}$ Average temperature coefficient of input offset current		Full range	10		$\text{pA}/^\circ\text{C}$		
$I_{IB}$ Input bias current	$V_O = 1.4\text{ V}$		25°C	-20	-250	nA	
			Full range	-500			
$V_{ICR}$ Common-mode input voltage range	$V_{CC} = 5\text{ V to MAX}$		25°C	0 to $V_{CC} - 1.5$		V	
			Full range	0 to $V_{CC} - 2$			
$V_{OH}$ High-level output voltage	$R_L \geq 10\text{ k}\Omega$	$V_{CC} = \text{MAX}$ , Non-V device	25°C	$V_{CC} - 1.5$		V	
			Full range	$R_L = 2\text{ k}\Omega$	22		
				$R_L \geq 10\text{ k}\Omega$	23		24
			Full range	$R_L = 2\text{ k}\Omega$	26		
$R_L \geq 10\text{ k}\Omega$	27 28						
$V_{OL}$ Low-level output voltage	$R_L \leq 10\text{ k}\Omega$		Full range	5	20	mV	
$A_{VD}$ Large-signal differential voltage amplification	$V_{CC} = 15\text{ V}$ , $V_O = 1\text{ V to }11\text{ V}$ , $R_L \geq 2\text{ k}\Omega$		25°C	25	100	V/mV	
			Full range	15			
CMRR Common-mode rejection ratio	$V_{CC} = 5\text{ V to MAX}$ , $V_{IC} = V_{ICR(min)}$	Non-V device	25°C	50	80	dB	
		V-suffix device	25°C	65	80		
$k_{SVR}$ Supply-voltage rejection ratio ( $\Delta V_{DD}/\Delta V_{IO}$ )	$V_{CC} = 5\text{ V to MAX}$		25°C	65	100	dB	
$V_{O1}/V_{O2}$ Crosstalk attenuation	$f = 1\text{ kHz to }20\text{ kHz}$		25°C	120		dB	
$I_O$ Output current	$V_{CC} = 15\text{ V}$ , $V_{ID} = 1\text{ V}$ , $V_O = 0$	Source	25°C	-20	-30	mA	
			Full range	-10			
	$V_{CC} = 15\text{ V}$ , $V_{ID} = -1\text{ V}$ , $V_O = 15\text{ V}$	Sink	25°C	10	20	mA	
			Full range	5			
	$V_{ID} = -1\text{ V}$ , $V_O = 200\text{ mV}$	Non-V device	25°C	30		$\mu\text{A}$	
		V-suffix device	25°C	12	40		
$I_{OS}$ Short-circuit output current	$V_{CC}$ at 5 V, GND at -5 V, $V_O = 0$		25°C	$\pm 40$	$\pm 60$	mA	
$I_{CC}$ Supply current (two amplifiers)	$V_O = 2.5\text{ V}$ , No load		Full range	0.7	1.2	mA	
	$V_{CC} = \text{MAX}$ , $V_O = 0.5\text{ V}$ , No load		Full range	1	2		

† All characteristics are measured under open-loop conditions, with zero common-mode input voltage, unless otherwise specified. MAX  $V_{CC}$  for testing purposes is 26 V for the LM2904, 32 V for the LM2904V, and 30 V for others.

‡ Full range is -55°C to 125°C for LM158, -25°C to 85°C for LM258, 0°C to 70°C for LM358, and -40°C to 125°C for LM2904.

§ All typical values are at  $T_A = 25^\circ\text{C}$ .



**LM158, LM158A, LM258, LM258A  
LM358, LM358A, LM2904, LM2904V  
DUAL OPERATIONAL AMPLIFIERS**

SLOS068R – JUNE 1976 – REVISED JULY 2010

**electrical characteristics at specified free-air temperature,  $V_{CC} = 5\text{ V}$  (unless otherwise noted)**

PARAMETER	TEST CONDITIONST	$T_A$ †	LM158A			LM258A			UNIT	
			MIN	TYP§	MAX	MIN	TYP§	MAX		
$V_{IO}$ Input offset voltage	$V_{CC} = 5\text{ V to }30\text{ V}$ , $V_{IC} = V_{ICR(\text{min})}$ , $V_O = 1.4\text{ V}$	25°C			2		2	3	mV	
		Full range			4			4		
$\alpha_{V_{IO}}$ Average temperature coefficient of input offset voltage		Full range		7	15*		7	15	$\mu\text{V}/^\circ\text{C}$	
$I_{IO}$ Input offset current	$V_O = 1.4\text{ V}$	25°C		2	10		2	15	nA	
		Full range			30			30		
$\alpha_{I_{IO}}$ Average temperature coefficient of input offset current		Full range		10	200		10	200	$\text{pA}/^\circ\text{C}$	
$I_{IB}$ Input bias current	$V_O = 1.4\text{ V}$	25°C		-15	-50		-15	-80	nA	
		Full range			-100			-100		
$V_{ICR}$ Common-mode input voltage range	$V_{CC} = 30\text{ V}$	25°C		0 to $V_{CC} - 1.5$		0 to $V_{CC} - 1.5$			V	
		Full range		0 to $V_{CC} - 2$		0 to $V_{CC} - 2$				
$V_{OH}$ High-level output voltage	$R_L \geq 2\text{ k}\Omega$ $V_{CC} = 30\text{ V}$	25°C		$V_{CC} - 1.5$		$V_{CC} - 1.5$			V	
		Full range	$R_L = 2\text{ k}\Omega$	26		26				
			$R_L \geq 10\text{ k}\Omega$	27	28	27	28			
$V_{OL}$ Low-level output voltage	$R_L \leq 10\text{ k}\Omega$	Full range		5	20		5	20	mV	
$A_{VD}$ Large-signal differential voltage amplification	$V_{CC} = 15\text{ V}$ , $V_O = 1\text{ V to }11\text{ V}$ , $R_L \geq 2\text{ k}\Omega$	25°C		50	100		50	100	V/mV	
		Full range		25			25			
CMRR Common-mode rejection ratio		25°C		70	80		70	80	dB	
$k_{SVR}$ Supply-voltage rejection ratio ( $\Delta V_{DD}/\Delta V_{IO}$ )		25°C		65	100		65	100	dB	
$V_{O1}/V_{O2}$ Crosstalk attenuation	$f = 1\text{ kHz to }20\text{ kHz}$	25°C		120			120			dB
$I_O$ Output current	$V_{CC} = 15\text{ V}$ , $V_{ID} = 1\text{ V}$ , $V_O = 0$	Source	25°C	-20	-30	-60	-20	-30	-60	mA
		Full range		-10			-10			
	Sink	25°C		10	20		10	20		
		Full range		5			5			
	$V_{ID} = -1\text{ V}$ , $V_O = 200\text{ mV}$	25°C		12	30		12	30	$\mu\text{A}$	
$I_{OS}$ Short-circuit output current	$V_{CC}$ at 5 V, GND at -5 V, $V_O = 0$	25°C		$\pm 40$	$\pm 60$		$\pm 40$	$\pm 60$	mA	
$I_{CC}$ Supply current (two amplifiers)	$V_O = 2.5\text{ V}$ , No load	Full range		0.7	1.2		0.7	1.2	mA	
	$V_{CC} = \text{MAX}$ , $V_O = 0.5\text{ V}$ , No load	Full range		1	2		1	2		

\*On products compliant to MIL-PRF-38535, this parameter is not production tested.

† All characteristics are measured under open-loop conditions, with zero common-mode input voltage, unless otherwise specified. MAX  $V_{CC}$  for testing purposes is 26 V for LM2904 and 30 V for others.

‡ Full range is  $-55^\circ\text{C}$  to  $125^\circ\text{C}$  for LM158A,  $-25^\circ\text{C}$  to  $85^\circ\text{C}$  for LM258A, and  $0^\circ\text{C}$  to  $70^\circ\text{C}$  for LM358A.

§ All typical values are at  $T_A = 25^\circ\text{C}$ .



**LM158, LM158A, LM258, LM258A**  
**LM358, LM358A, LM2904, LM2904V**  
**DUAL OPERATIONAL AMPLIFIERS**

SLOS068R – JUNE 1976 – REVISED JULY 2010

**electrical characteristics at specified free-air temperature,  $V_{CC} = 5\text{ V}$  (unless otherwise noted)**

PARAMETER	TEST CONDITIONS†	$T_A$ ‡	LM358A			UNIT	
			MIN	TYP§	MAX		
$V_{IO}$ Input offset voltage	$V_{CC} = 5\text{ V to }30\text{ V}$ , $V_{IC} = V_{ICR(min)}$ , $V_O = 1.4\text{ V}$	25°C		2	3	mV	
		Full range			5		
$\alpha_{V_{IO}}$ Average temperature coefficient of input offset voltage		Full range		7	20	$\mu\text{V}/^\circ\text{C}$	
$I_{IO}$ Input offset current	$V_O = 1.4\text{ V}$	25°C		2	30	nA	
		Full range			75		
$\alpha_{I_{IO}}$ Average temperature coefficient of input offset current		Full range		10	300	$\text{pA}/^\circ\text{C}$	
$I_{IB}$ Input bias current	$V_O = 1.4\text{ V}$	25°C		-15	-100	nA	
		Full range			-200		
$V_{ICR}$ Common-mode input voltage range	$V_{CC} = 30\text{ V}$	25°C		0 to $V_{CC} - 1.5$		V	
		Full range		0 to $V_{CC} - 2$			
$V_{OH}$ High-level output voltage	$R_L \geq 2\text{ k}\Omega$ $V_{CC} = 30\text{ V}$	25°C		$V_{CC} - 1.5$		V	
		Full range	$R_L = 2\text{ k}\Omega$	26			
			$R_L \geq 10\text{ k}\Omega$	27 28			
$V_{OL}$ Low-level output voltage	$R_L \leq 10\text{ k}\Omega$	Full range		5	20	mV	
$A_{VD}$ Large-signal differential voltage amplification	$V_{CC} = 15\text{ V}$ , $V_O = 1\text{ V to }11\text{ V}$ , $R_L \geq 2\text{ k}\Omega$	25°C		25	100	V/mV	
		Full range		15			
CMRR Common-mode rejection ratio		25°C		65	80	dB	
$k_{SVR}$ Supply-voltage rejection ratio ( $\Delta V_{DD}/\Delta V_{IO}$ )		25°C		65	100	dB	
$V_{O1}/V_{O2}$ Crosstalk attenuation	$f = 1\text{ kHz to }20\text{ kHz}$	25°C		120		dB	
$I_O$ Output current	$V_{CC} = 15\text{ V}$ , $V_{ID} = 1\text{ V}$ , $V_O = 0$	Source	25°C	-20	-30	-60	mA
			Full range	-10			
	$V_{CC} = 15\text{ V}$ , $V_{ID} = -1\text{ V}$ , $V_O = 15\text{ V}$	Sink	25°C	10	20		
			Full range	5			
	$V_{ID} = -1\text{ V}$ , $V_O = 200\text{ mV}$	25°C		30		$\mu\text{A}$	
$I_{OS}$ Short-circuit output current	$V_{CC}$ at 5 V, GND at -5 V, $V_O = 0$	25°C		$\pm 40$	$\pm 60$	mA	
$I_{CC}$ Supply current (two amplifiers)	$V_O = 2.5\text{ V}$ , No load	Full range		0.7	1.2	mA	
	$V_{CC} = \text{MAX}$ , $V_O = 0.5\text{ V}$ , No load	Full range		1	2		

† All characteristics are measured under open-loop conditions, with zero common-mode input voltage, unless otherwise specified. MAX  $V_{CC}$  for testing purposes is 26 V for LM2904 and 30 V for others.

‡ Full range is -55°C to 125°C for LM158A, -25°C to 85°C for LM258A, and 0°C to 70°C for LM358A.

§ All typical values are at  $T_A = 25^\circ\text{C}$ .





**LM158, LM158A, LM258, LM258A  
LM358, LM358A, LM2904, LM2904V  
DUAL OPERATIONAL AMPLIFIERS**

SLOS068R – JUNE 1976 – REVISED JULY 2010

operating conditions,  $V_{CC} = \pm 15\text{ V}$ ,  $T_A = 25^\circ\text{C}$

PARAMETER		TEST CONDITIONS	TYP	UNIT
SR	Slew rate at unity gain	$R_L = 1\text{ M}\Omega$ , $C_L = 30\text{ pF}$ , $V_I = \pm 10\text{ V}$ (see Figure 1)	0.3	$\text{V}/\mu\text{s}$
$B_1$	Unity-gain bandwidth	$R_L = 1\text{ M}\Omega$ , $C_L = 20\text{ pF}$ (see Figure 1)	0.7	MHz
$V_n$	Equivalent input noise voltage	$R_S = 100\ \Omega$ , $V_I = 0\text{ V}$ , $f = 1\text{ kHz}$ (see Figure 2)	40	$\text{nV}/\sqrt{\text{Hz}}$

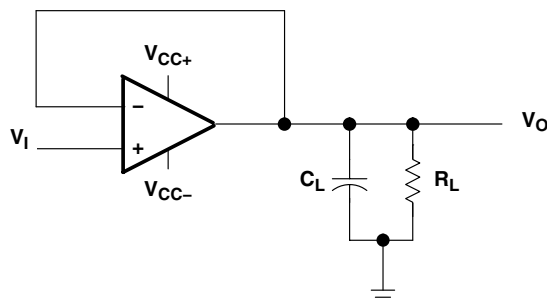


Figure 1. Unity-Gain Amplifier

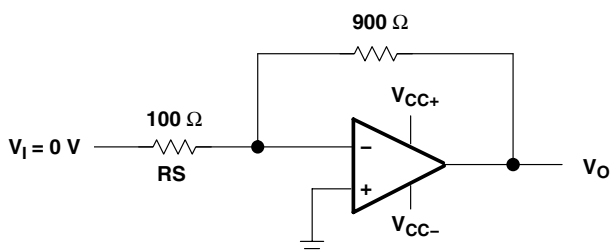


Figure 2. Noise-Test Circuit



# Bibliography

- [1] AMERICAN HEART ASSOCIATION. *AHA Statistical Update, Executive Summary: Heart Disease and Stroke Statistics-2012 Update*. <http://circ.ahajournals.org/search?tocsectionid=AHA+Statistical+Update&sortspec=date&submit=Submit>. [consulted on 16/08/2012].
- [2] ASTIN, A. D. *Finger force capability: measurement and prediction using anthropometric and myoelectric measures*. PhD thesis, Faculty of the Virginia Polytechnic Institute and State University, 1999. Master of Science in Industrial System Engineering.
- [3] BERG, V., CLAY, D. J., FATHALLAH, F. A., AND HIGGINBOTHAM, V. L. *Trends in Ergonomics/Human Factors V*. Aghazadeh, F. - Elsevier Publishers, Amsterdam, 1988. Chap: The effects of instruction on finger strength measurements: applicability of the Caldwell Regimen.
- [4] BOISSY, P., BOURBONNAIS, D., CARLOTTI, M., GRAVEL, D., AND ARSENAULT, B. A. Maximal grip force in chronic stroke subjects and its relationship to global upper extremity function. *Journal of Clinical Rehabilitation* (1999).
- [5] CALDWELL, L. S., CHAFFIN, D. B., DOBOS, F. N., KROEMER, K. H., LAUBACH, L. L., SNOOK, S., AND WASSERMAN, D. A proposed standard procedure for static muscle strength testing. *American Industrial Hygiene Association Journal* (1974), 201–206.
- [6] CHANG, L. *Foundations of MEMS*. Pearson Prentice Hall, 2006. Chap: 6 Piezoresistive Sensors.

## BIBLIOGRAPHY

---

- [7] CROWDER, R. M. University of Southampton: Course notes. <http://www.southampton.ac.uk/~rmc1/robotics/artactile.htm>. [consulted on 02/10/2012].
- [8] CRUZ, E. G., WALDINGER, H. C., AND KAMPER, D. G. Kinetic and kinematic workspaces of the index finger following stroke. *Oxford Journal: Brain (A journal of neurology)* 128, 5 (2005), 1112–1121.
- [9] DEMPSEY, P. G., AND AYOUB, M. M. The influence of gender, grasp type, pinch width and wrist position on sustained pinch strength. *International Journal of Industrial Ergonomics* (1996), 259–273.
- [10] DIETZ, V., NEF, T., AND ZEV RYMER, W., Eds. *Neurorehabilitation Technology*. Springer, 2012.
- [11] DONOGHUE, J. P., NURMIKKO, A., BLACK, M., AND HOCHBERG, L. R. Assistive technology and robotic control using motor cortex ensemble-based neural interface systems in humans with tetraplegia. *The Journal of Physiology* 579 (2007), 603–611.
- [12] DOVAT, L., LAMBERCY, O., GASSERT, R., MAEDER, T., MILNER, T., LEONG, T. C., AND BURDET, E. Handcare: a cable-actuated rehabilitation system to train hand function after stroke. *IEEE Transactions on neural systems and rehabilitation engineering* 16, 6 (2008).
- [13] ELLIOTT, J. M., AND CONNOLLY, K. J. A classification of manipulative hand movements. *Developmental Medicine and Child Neurology* 26 (1984), 283–296.
- [14] FESS, E. E., AND MORAN, C. American society of hand therapists: Clinical assessment recommendations. *Garner: the Society* (1981).
- [15] FOLEY N, R. TEASELL, S., AND SPEECHLEY, M. The efficacy of stroke rehabilitation. *The Evidence-Based Review of Stroke Rehabilitation (EBRSR)* (2008). <http://www.ebrsr.com>, [consulted on 23/08/2012].
- [16] GOBLE, D. J. Proprioceptive acuity assessment via joint position matching: from basic science to general practice. *Journal of the American Physical Therapy Association* (2010).

- 
- [17] HILLMAN, M., Ed. *Rehabilitation robotics from past to present - a historical perspective* (2003), Bath Institute of Medical Engineering, The Eighth International Conference on Rehabilitation Robotics.
- [18] IMRHAN. Trends in finger pinch strength in children, adults, and the elderly. *Human Factors* (1989), 689–701.
- [19] JUNG, J., SONG, W., LEE, H., KIM, J., AND BIEN, Z. A study on the enhancement of manipulation performance of wheelchair-mounted rehabilitation service robot.
- [20] KAMAKURA, N., MATSUO, M., ISHII, H., FUMIKE, M., AND YORIKO, M. Patterns of static prehension in normal hands. *The American Journal of Occupational Therapy* 34, 7 (1980), 437–445.
- [21] KEEN, D., AND FUGLEVAND, A. Common input to motor neurons innervating the same and different compartments of the human extensor digitorum muscle. *Journal of Neurophysiology* 91, 1 (2004), 57–92.
- [22] KINETIC MUSCLES INC. Improving life after-stroke. <http://www.kineticmuscles.com/hand-physical-therapy-hand-mentor.html>. [consulted on 13/10/2012].
- [23] KINOSHITA, KAWAI, IKUTA, AND TERAOKA. Individual finger forces acting on a grasped object during shaking actions. *Ergonomics* (1996), 243–256.
- [24] KUTNER, N. G., ZHANG, R., BUTLER, A. J., WOLF, L. S., AND ALBERTS, J. L. Quality-of-life change associated with robotic-assisted therapy to improve hand motor function in patients with subacute stroke: a randomized clinical trial. *Journal of physical Therapy* 90 (2010), 493–504.
- [25] LANDSMEER, J. M. Power grip and precision handling. *Annals of the Rheumatic Diseases* 21 (1962), 164–170.
- [26] LUCAS, L., DICICCO, M., AND MATSUOKA, Y. An emg-controlled hand exoskeleton for natural pinching. *Journal of Robotics and Mechatronics* 16, 5 (2004), 482–488.
- [27] MATHIOWETZ, RENNELLS, AND DONAHOE. Effect of elbow position on grip and key pinch strength. *Journal of Hand Surgery* (1985), 694–697.
-

## BIBLIOGRAPHY

---

- [28] MATHIOWETZ, WEBER, VOLLAND, AND KASHMAN. Reliability and validity of grip and pinch strength evaluations. *Journal of Hand Surgery* (1984), 222–226.
- [29] MATHIOWETZ, V., KASHMAN, N., VOLLAND, WEBER, G., DOWE, K., AND ROGERS, S. Grip and pinch strength: normative data for adults. *Archives of Physical Medicine and Rehabilitation*, (1985), 69–74.
- [30] NAPIER, J. The prehensile movements of the human hand. *Journal of Bone and Joint Surgery* (1956).
- [31] NATIONAL SPINAL CORD INJURY STATISTICAL CENTER (NSCISC). *The 2011 annual statistical report for the spinal cord injury model systems*. <https://www.nscisc.uab.edu>. [consulted on 22/08/2012].
- [32] OUNJIAN, M., ROY, R., ELDRED, E., GARFINKEL, A., PAYNE, J. R., ARMSTRONG, A., TOGA, A., AND EDGERTON, V. R. Physiological and developmental implications of motor unit anatomy. *Journal of Neurobiology* 22 (1991), 547–559.
- [33] PATTEN, C., LEXEL, J., AND BROWN, H. E. Weakness and strength training in persons with poststroke hemiplegia: rationale, method and efficacy. *Journal of Rehabilitation Research and Development* 41, 3A (2004), 293–312.
- [34] PENFIELD, W., AND RASMUSSEN, T. *The cerebral cortex of man: a clinical study of localization of function*. The Macmillan Company, 1950.
- [35] PFURTSCHELLER, G., GUGER, C., MÜLLER, G., KRAUSZ, G., AND NEUPER, C. Brain oscillations control hand orthosis in a tetraplegic. *Neuroscience Letters* 292 (2000), 211–214.
- [36] PLAUTZ, E. J., MILLIKEN, G. W., AND NUDO, R. J. Effects of repetitive motor training on movement representations in adult squirrel monkeys: role of use versus learning. *Journal of Neurobiology of Learning and Memory* 74 (2000), 27–55.
- [37] PORTER, R., AND LEMON, R. *Corticospinal function and voluntary movement*. Oxford:Clarendon Press, 1993.

- 
- [38] RADWIN, OH, JENSEN, AND WEBSTER. External finger forces in submaximal five-finger static pinch prehension. *Ergonomics* (1992), 275–288.
- [39] SCHMIDT, R. T., AND TOEWS, J. V. Grip strength as measured by the jamar dynamometer. *Archives of Physical Medicine and Rehabilitation* (1970), 321–327.
- [40] SITO DEL MINISTERO DELLA SALUTE. *Stroke Units*. <http://www.quadernidellasalute.it/download/press-area/cartella-stampa/2-marzo-aprile-2010/2-marzo-aprile-2010-Sintesi-dei-contributi.pdf>. [consulted on 16/08/2012].
- [41] SOLLERMAN, C. *Handens greppfunktion*. PhD thesis, Goteborg University, 1980. Chapters: Assessment of grip function. Evaluation of a new test method. The use of eight main hand grips in activities of daily living.
- [42] SOLLERMAN, C., AND EJESKÄR, A. Sollerman hand function test: A standardised method and its use in tetraplegic patient. *Scandinavian Journal of Plastic and Reconstructive Surgery and Hand Surgery* 29, 1 (1956), 167–176.
- [43] SUNNERHAGEN, K. S., SVANTESSON, U., LONN, L., KROTKIEWSKI, M., AND GRIMBY, G. Upper motor neuron lesions: their effect on muscle performance and appearance in stroke patients with minor motor impairment. *Archives of Physical Medicine and Rehabilitation* (1999), 155–161.
- [44] SWANSON, A. B., MATEV, I. B., AND DE GROOT, G. The strength of the hand. *Bulletin of Prosthetics Research* (1970), 145–153.
- [45] TAYLOR, D. M., TILLERY, S. I. H., AND SCHWARTZ, A. B. Information conveyed through brain-control: cursor versus robot. *IEEE Transactions on neural systems and rehabilitation engineering* 11 (2003), 195–199.
- [46] TEASELL, R., BAYONA, N., AND BITENSKY, J. Background concepts in stroke rehabilitation. *The Evidence-Based Review of Stroke Rehabilitation (EBRSR)* (2008). <http://www.ebrsr.com>, [consulted on 23/08/2012].
- [47] TORRE, G. R. D. L., AND HAYWARD, V. Force can overcome object geometry in the perception of shape through active touch, 2001.
-

## BIBLIOGRAPHY

---

- [48] TROMBLY, C. A., AND WU, C. Y. Effect of rehabilitation tasks on organization of movement after stroke. *American Journal of Occupational Therapy* 53 (1999), 333–344.
- [49] VALERO, F., CUEVAS, J., JOHANSON, M., AND TOWLES, J. D. Towards a realistic biomechanical model of the thumb: the choice of kinematic description may be more critical than the solution method or the variability/uncertainty of musculoskeletal parameters. *Journal of Biomechanics* (2003).
- [50] WILLIAMSON, T. L., AND RICE, V. J. *Advances in Industrial Ergonomics and Safety IV*. Kumar S - New York: Taylor and Francis, 1992.
- [51] WINSTEIN, C., ROSE, D., SYLVIA, M., TAN, M., LEWTHWAITE, M., CHUI, H., STANLEY, M., AND AZEN, P. A randomized controlled comparison of upper-extremity rehabilitation strategies in acute stroke: a pilot study of immediate and long-term outcomes. *Archives of Physical Medicine and Rehabilitation* 85 (2004), 620–628.
- [52] XIE, J., GEORGE, M. G., AND ET AL., C. A. Outpatient rehabilitation among stroke survivors - 21 states and the district of columbia, 2005. *Morbidity and Mortality Weekly Report (MMWR)* 56, 20 (2007), 504–507.